

**EPA Radiogenic Cancer Risk Models and
Projections for the U.S. Population**

Draft

**U.S. Environmental Protection Agency
Office of Radiation and Indoor Air**

December 2008

CONTENTS

Acronyms and Abbreviations	6
Executive Summary	7
1. Introduction	10
2. Scientific Basis for Cancer Risk Models	11
2.1 Biological Mechanisms	11
2.1.1 Biophysical Interactions	11
2.1.2 Carcinogenesis	12
2.1.3 Radiogenic Carcinogenesis	13
2.1.4 Extrapolation of Low-LET Risks to Low Doses and Low Dose Rates	15
2.1.5 Low Dose Phenomena	16
2.2 Epidemiology	18
3. EPA Risk Projections for Low-LET Radiation	21
3.1 Introduction	21
3.2 BEIR VII Risk Models	21
3.3 Residual Site Cancers	29
3.4 Calculating Lifetime Attributable Risk	32
3.5 Dose and Dose Rate Adjustment Factor	34
3.6 EAR and ERR LAR Projections for Cancer Incidence	34
3.7 ERR and EAR Projections for Cancer Mortality	37
3.8 U.S. Baseline and Census Data	39
3.9 Combining Results from ERR and EAR Models	40
3.9.1 BEIR VII Approach	40
3.9.2 EPA Approach	41
3.9.3 Should Risk Models be Combined Using a Weighted GM?	43
3.10 Calculating Radiogenic Breast Cancer Mortality Risk	47
3.11 LAR by Age at Exposure	50
3.12 Summary of Main Results	54
4. Uncertainties in Projections of LAR for Low-LET Radiation	59
4.1 Introduction	59
4.2 Uncertainty from Sampling Variability	60
4.2.1 Bayesian Approach for Most Solid Cancers.....	60
4.2.2 Approach for Other Cancers	63
4.3 Non-sampling Sources of Uncertainty	64
4.3.1 Risk Transport	65
4.3.2 DDREF	66
4.3.3 Other Non-sampling Sources of Uncertainty	67
4.4 Results	73
4.5 Comparison with BEIR VII	78

4.5.1	Quantitative Uncertainty Analysis in BEIR VII	78
4.5.2	Comparison of Results	80
4.6	Conclusions	80
5.	Risks from Higher LET Radiation	82
5.1	Alpha Particles	82
5.1.1	Laboratory Studies	82
5.1.2	Human Data	83
5.1.3	Nominal Risk Estimates for Alpha Radiation	91
5.1.4	Uncertainties in Risk Estimates for Alpha Radiation	91
5.2	Lower Energy Beta Particles and Photons	92
6.	Risks from Prenatal Exposure	96
7.	Radionuclide Risk Coefficients	98
	References	99
	Glossary	112

LIST OF FIGURES

Figure 2-1	Dose response curves	14
Figure 3-1	Age-time patterns in radiation-associated risks	26
Figure 3-2	ERR for Leukemia for age-at-exposure = 20 and time-since-exposure = 10	28
Figure 3-3	ERR and EAR by time-since-exposure for three different ages	29
Figure 3-4	Examples of uniform $U(0,1)$ and trapezoidal distributions	44
Figure 3-5	Sex-averaged LAR for incidence by age at exposure for selected cancers	51
Figure 3-6	Sex-averaged LAR for cancer mortality by age at exposure for selected cancers	52
Figure 4-1	Uniform and log-uniform distributions for values of LAR intermediate between the ERR and EAR projections for stomach and colon cancer	66
Figure 4-2	Subjective probability density function for DDREF	67
Figure 5-1	Cumulative fraction of total dose as a function of secondary electron kinetic energies for a variety of low-LET radiations	94
Figure 5-2	Cumulative fraction of total dose as a function of secondary electron kinetic energies for a variety of slow and fast initial electron energies.....	95

LIST OF TABLES

Table 3-1	BEIR VII Risk Model Cancer Sites	23
Table 3-2	Summary of BEIR VII Preferred Risk Models	25
Table 3-3	Parameter Values for Preferred Risk Models in BEIR VII	27
Table 3-4	EAR and ERR model projections of LAR Projections for a stationary population	36
Table 3-5	Age-averaged LAR for solid cancer mortality based on a stationary population	38
Table 3-6	Baseline lifetime risk estimates of cancer incidence and mortality	40
Table 3-7	EPA and BEIR VII methods for combining EAR and ERR LAR incidence projections for selected sites	42
Table 3-8	Comparison of EPA and weighted arithmetic mean method for combining EAR and ERR LAR projections for incidence	46
Table 3-9	Female breast cancer cases and 5-y relative survival rates by age for 12 SEER areas	49
Table 3-10	LAR for Cancer incidence for exposures to a stationary U.S. population	53
Table 3-11	LAR projections for incidence	54
Table 3-12	LAR projections for mortality	56
Table 3-13	Sex-averaged LAR projections for incidence and mortality	57
Table 3-14	Comparisons of EPA and BEIR VIII LAR calculations	58
Table 4-1	Prior distributions for ERR model parameters	63
Table 4-2	Non-sampling sources of uncertainty	65
Table 4-3a	EPA projection and uncertainty distribution for the LAR for male cancer incidence	73
Table 4-3b	EPA projection and uncertainty distribution for the LAR for female cancer incidence	74
Table 4-3c	EPA projection and uncertainty distribution for the sex-averaged LAR for cancer incidence	75
Table 4-4a	EPA projection and uncertainty distributions for male cancer incidence in a stationary population exposed to uniform whole-body radiation	76
Table 4-4b	EPA projection and uncertainty distributions for female cancer incidence in a stationary population exposed to uniform whole-body radiation	77
Table 4-5	95% EPA and BEIR VII 95% uncertainty intervals for LAR of solid cancer incidence	80
Table 5-1	Lung cancer mortality and RBE	89

LIST OF ACRONYMS AND ABBREVIATIONS

BCC	Basal Cell Carcinoma
BEIR VII	<i>Health Risks from Exposure to Low Levels of Ionizing Radiation BEIR VII Phase 2</i>
CI	Confidence Interval
DDREF	Dose and Dose Rate Effectiveness Factor
DEF	Dose Effectiveness Factor
DREF	Dose Rate Effectiveness Factor
DSB	Double Strand Break
EAR	Excess Absolute Risk
EPA	Environmental Protection Agency
ERR	Excess Relative Risk
eV	Electron Volt
FGR-13	Federal Guidance Report 13
GM	Geometric Mean
GSD	Geometric Standard Deviation
Gy	Gray
ICRP	International Commission on Radiological Protection
IR	Ionizing Radiation
IREP	Interactive RadioEpidemiological Program
LAR	Lifetime Attributable Risk
LET	Linear Energy Transfer
LNT	Linear No -Threshold
LQ	Linear-Quadratic
LSS	Life Span Study
NAS	National Academy of Sciences
NCHS	National Center for Health Statistics
NCI	National Cancer Institute
NCRP	National Council on Radiation Protection and Measurements
NIOSH	National Institute for Occupational Safety and Health
NRC	National Research Council
ORIA	Office of Radiation and Indoor Air
RBE	Relative Biological Effectiveness
REF	Radiation Effectiveness Factor
RR	Relative Risk
SCC	Squamous Cell Carcinoma
SEER	Surveillance, Epidemiology, and End Results
Sv	Sievert
UNSCEAR	United Nations Scientific Committee on the Effects of Atomic Radiation
WLM	Working Level Months

EXECUTIVE SUMMARY

This document presents new EPA estimates of cancer incidence and mortality risks due to low doses of ionizing radiation (IR) for the U.S. population, as well as their scientific basis. For the most part, these estimates are calculated using models recommended in the National Research Council's BEIR VII Report (NRC 2006), which was sponsored by EPA and several other federal agencies.

As in BEIR VII, models are provided for estimating risk as a function of age at exposure, age at risk, gender, and cancer site, but a number of extensions and modifications to the BEIR VII approach have been implemented. First, BEIR VII focused on the risk from low-LET radiation only, whereas risks from higher LET radiations are also addressed here. Second, this document goes beyond BEIR VII in providing estimates of risk for basal cell carcinomas and bone sarcomas, and cancers from prenatal exposures. Third, a modified method is employed for estimating breast cancer mortality risk, which corrects for temporal changes in breast cancer incidence and survival. Finally, this report provides a somewhat altered and expanded analysis of the uncertainties in the cancer risk estimates, focusing especially on estimates of risk for whole-body irradiation and for some specific target organs.

Underlying the risk models is a large body of epidemiological and radiobiological data. In general, results from both lines of research are consistent with a linear, no-threshold dose (LNT) response model in which the risk of inducing a cancer in an irradiated tissue by low doses of IR is proportional to the dose to that tissue.

The most important source of epidemiological data is the Life Span Study (LSS) of the Japanese atomic bomb survivors, who received an acute dose of IR, mostly in the form of gamma rays, with a small admixture of neutrons. The LSS study has important strengths, including: a nearly instantaneous exposure, which can be pin-pointed in time; a large, relatively healthy exposed population encompassing both genders and all ages; a wide range of radiation doses to all organs of the body, which can be estimated reasonably accurately; and detailed epidemiological follow-up for about 50 years. Nevertheless, precision is limited by errors in dosimetry and sampling errors. The sampling errors are often quite large for specific cancer types, and the uncertainties are even larger if one focuses on a specific gender, age at exposure, or time after exposure. Another important uncertainty is the transfer of site-specific cancer risk estimates to the U.S. population, based on results obtained on the LSS population, for sites with substantially different baseline incidence rates.

Summary risk coefficients are calculated for a stationary population defined by 2000 U.S. Vital Statistics. Numerically, the same coefficients apply for

a cohort exposed throughout life to a constant dose rate. For uniform whole-body exposures of low-dose gamma radiation to the entire population, the cancer incidence risk coefficient is $1.01 \times 10^{-1} \text{ Gy}^{-1}$ (7.0×10^{-2} to 2.4×10^{-1}), where the numbers in parentheses represent an estimated 90% confidence interval. The corresponding coefficient for cancer mortality is about one-half that for incidence: $5.18 \times 10^{-2} \text{ Gy}^{-1}$ ($3.5 \times 10^{-2} \text{ Gy}^{-1}$ to $1.2 \times 10^{-1} \text{ Gy}^{-1}$). For perspective, the average individual receives about 1 mGy each year from low-LET background radiation, or (≈ 75 mGy, lifetime). The average cancer incidence and mortality risks from background radiation are then estimated to be about 0.76% and 0.39%, respectively. The risks are significantly higher for females than for males: $1.23 \times 10^{-1} \text{ Gy}^{-1}$ vs. $7.85 \times 10^{-2} \text{ Gy}^{-1}$ (incidence) and $6.28 \times 10^{-2} \text{ Gy}^{-1}$ vs. $4.06 \times 10^{-2} \text{ Gy}^{-1}$ (mortality), respectively.

Radiogenic risks for childhood exposures are often of special interest. Doses received from ingestion or inhalation are often larger for children than adults, and the risks per unit dose are substantially larger for exposures during childhood (here defined as the time period ending at the 15th birthday) than from exposures later in life. For children, the estimated risks from uniform whole-body radiation for cancer incidence are $1.6 \times 10^{-1} \text{ Gy}^{-1}$ (males) and $3.0 \times 10^{-1} \text{ Gy}^{-1}$ (females) with 90% uncertainty intervals: 1.0×10^{-1} to $4.2 \times 10^{-1} \text{ Gy}^{-1}$ (males) and 2.0×10^{-1} to $7.1 \times 10^{-1} \text{ Gy}^{-1}$ (females). The corresponding estimated risks for mortality are $7.2 \times 10^{-2} \text{ Gy}^{-1}$ (males) and $1.4 \times 10^{-1} \text{ Gy}^{-1}$ (females). There is generally much more uncertainty about the estimated risks from childhood exposures than for risks for the entire population. One oft-cited reason for this (EPA 1994, 1999) is that A-bomb survivors who were children at the time of the bombings (ATB) still have substantial years of life remaining in which cancers are to be expressed. At the present, there are too few cancer cases for precise estimate of risks from childhood exposures.

For ingestion or inhalation of many radionuclides that concentrate in individual organs risks for specific sites are important. For most cancer sites, the new EPA risk projections for incidence are not very different from the risk projections in the current version of FGR 13. Exceptions include female lung, female bladder, thyroid, and kidney (increased); and female colon cancer (decreased). For both males and females, the LAR for all cancer combined increased by about 20%. For mortality, there was a notable decrease in estimated risk for cancers of the stomach and female colon. Estimated mortality risks increased for cancers of the female lung, female thyroid, and female kidney. In general, the new EPA mortality estimates are remarkably consistent with those in FGR 13; e.g., for all sites combined, the estimates decreased by about 10% for both males and females. Not surprisingly, uncertainties for site-specific cancer risks are greater than for uniform whole-body radiation. This is largely due to the smaller number of cancers for specific sites in the LSS and to uncertainties in how radiogenic risks for specific cancer sites in the U.S. might differ from those in a Japanese population of A-bomb survivors.

The most contentious issue in radiation risk assessment is the extrapolation of risk estimates derived from relatively high acute exposures in case of the LSS cohort to low dose, or chronic exposure situations, which are of greatest interest to EPA. Many subjects in the LSS cohort did receive very low doses, but there is inadequate statistical power to quantify risk below about 0.1 Gy. This is about 100 times the annual whole-body, low-LET dose to an average individual from natural background. Thus, the question is how to extrapolate from an observed risk due to an instantaneous dose of 0.1 Gy or more to an extrapolated risk from a chronic exposure of ≈ 1 mGy/y.

Efforts have been made to integrate information gathered from radiation biology and epidemiology into a theoretical framework that would allow reliable risk projections at dose rates approaching natural background. IR is known to induce mutagenic damage to the cell's DNA. Due to clustering of ionizations produced by low-LET as well as high-LET radiation, this damage is often complex, involving two or more breaks with concomitant base damage all within a few nanometers in the DNA molecule. This argues against a threshold for radiation-induced carcinogenesis and in favor of a linear dose-response relationship at low doses. However, experimental studies have uncovered novel low-dose phenomena, raising doubts about the reliability of the LNT model. In view of these findings, some have contended that very low doses of IR may be much less harmful than estimated based on LNT, and may even be beneficial. But the relevance of these findings to human carcinogenesis remains unclear, and epidemiological studies of cancer induction in cohorts receiving fractionated or chronic exposures have so far been broadly consistent with LNT predictions. The BEIR VII Committee unequivocally recommended continuing adherence to the LNT approach. EPA also finds strong scientific support for LNT, while acknowledging that new research might conceivably force a revision to this approach in the future.

1. Introduction

The 1994 report, *Estimating Radiogenic Cancer Risks*, presented EPA estimates of site-specific risks cancer incidence and mortality associated with low doses of ionizing radiation (IR) (EPA 1994). Primarily, the calculated risks were derived from models recommended by the International Commission on Radiological Protection (Land and Sinclair 1991), based on analysis of epidemiological data on Japanese atomic bomb survivors. While focusing mainly on a quantitative assessment of uncertainties in these estimates, a subsequent report also made minor adjustments in EPA's cancer risk estimates, reflecting changes in U.S. vital statistics (EPA 1999a). Finally, the methodology developed in the above reports was used in Federal Guidance Report No. 13 (FGR-13) to derive cancer risk coefficients for low level internal and external exposures to a set of over 800 radionuclides (EPA 1999b).

In 2006, the National Research Council of the National Academy of Sciences (NAS) released the BEIR VII report (NRC 2006), which reviewed recent evidence pertaining to the health risks from low-level, low linear energy transfer (LET) ionizing radiation (IR). The BEIR VII Committee developed models for calculating the risks of radiogenic cancers, based on updated information on the A-bomb survivors, as well as other data. In this report, we employ the BEIR VII models to arrive at revised estimates of radiogenic risks for most cancer sites. BEIR VII risk estimates were derived for low doses of gamma rays with typical energies between about 0.1 and 10 MeV, with a brief discussion of possible enhancement of risk for more densely ionizing electrons and photons. Although the main focus here is, like BEIR VII, on low-LET risks, we extend the evaluation of cancer risks to high-LET radiation (alpha-particles) and to lower energy photons and electrons, which may convey a higher risk than the higher energy gamma rays irradiating the LSS cohort. We also present risk models and estimates for bone cancers and non-melanoma skin cancers, which are not covered in BEIR VII. Finally, we derive uncertainty bounds on our risk estimates, based on information on BEIR VII and other relevant sources.

This report is not intended to provide an exhaustive review of the scientific basis for our risk models. For the most part, the reader is referred to BEIR VII and other sources in the literature. We have attempted to highlight major sources of uncertainty and, where pertinent, to include recently published information not considered by the BEIR VII Committee.

2. Scientific Basis for Cancer Risk Models

2.1 Biological Mechanisms

2.1.1 Biophysical Interactions. By definition, IR passing through matter has sufficient energy to break chemical bonds and to remove electrons from molecules. When this chemical damage occurs in the DNA of a somatic cell, a mutation in the genetic material can result, ultimately leading to a malignancy. The damage can be produced directly, when an ionizing particle impacts the DNA, or indirectly, through the creation of free radicals in the cellular medium, which diffuse and interact with the genetic material.

Only a tiny fraction of the free radicals produced in cells each day arise from IR; nevertheless, DNA damage by low-level IR is not negligible. This is because energy deposition events are often produced in clusters, which can, in turn, produce double strand breaks (DSBs) and more complex damage in DNA, involving multiple breaks and chemical modifications within a very restricted portion of the double helix. Cellular repair processes are less capable of repairing DSBs and complex damage than the simpler types of damage almost always induced by isolated free radicals. This makes IR unique among environmental carcinogens. Even a single track of IR is capable of producing complex damage sites, which, if misrepaired, can leave the cell with a mutated gene that can be passed on to the cell's progeny. Depending on the nature of the mutation, this may be one step in the formation of a malignancy. At reasonably low doses of IR the number of DSBs and sites of complex damage is expected to be strictly proportional to dose (UNSCEAR 2000b, NCRP 2001, NRC 2006); this is the primary basis for the linear no-threshold (LNT) theory in which the probability of inducing a cancer by IR is proportional to dose with no threshold below which there is no risk.

Some recent research has cast doubt on the LNT assumption, but the BEIR VII Report concluded that these results in no way constituted compelling evidence against LNT. Additional discussion of the issue will be found in sections below.

The degree of clustering of ionizations, and therefore of the DNA damage, depends on the type of radiation and its energy. This is reflected in the linear energy transfer of charged particle radiation (LET), which is a measure of the amount of energy deposited, per unit path length, as the particle passes through a medium. Alpha-particles emitted by the decay of unstable atomic nuclei have a relatively high LET ($\approx 100\text{-}200$ keV/ μm) in aqueous media, producing a high density of ionizations, leading to a high frequency of DSBs and clustered damage sites in the DNA. Since this type of damage is more likely to be misrepaired, high-LET radiation is more effective at causing mutations, cell transformation, and cell death (NCRP 2001). This higher effectiveness per unit dose, relative to some standard radiation (e.g., ^{60}Co gamma rays), is expressed in terms of a

factor called the Relative Biological Effectiveness¹ (RBE) (see Section 5). Initially, 200 kVp x rays were used as the reference; however, since current radiogenic cancer risk estimates largely rest on studies of the Japanese atomic bomb survivors, whose predominant exposure was from gamma rays, it is now common to use ⁶⁰Co gamma rays as the reference radiation. That convention will be adopted here.

Compared to alpha-particles, beta-particles and the secondary electrons produced by incident gamma rays or medical x rays typically have much lower linear energy transfer (0.1 -10 keV/μm). The ionizations produced by energetic electrons are more widely spaced, on average, but their production is a stochastic process in which several ionizations can be created separated by a distance no greater than the characteristic distance between adjacent DNA bases or between DNA strands. Moreover, as electrons lose energy, the LET increases and closely spaced ionizations become more frequent. Hence, clustered DNA damage is more likely to be produced near the ends of the electron tracks.

X rays and gamma rays can travel appreciable distances through matter without producing ionizations; however, they interact with atoms to produce energetic secondary electrons, which behave identically to incident electrons of the same energy. In aqueous media, over the incident photon energy range 0.1-10 MeV, the predominant photon interaction is Compton scattering, a process in which an incident photon transfers part of its energy to an atomic electron, creating a free electron and a lower energy photon. The energy of a Compton electron is positively correlated with the incident photon energy. Consequently, as the incident photon energy is reduced within this energy range, a higher fraction of the energy is dissipated in the form of lower energy (higher LET) electrons, resulting in more complex DNA damage and, therefore, perhaps an increased RBE. As the incident photon energy is reduced further, below 0.1 MeV, photoelectric absorption becomes increasingly important compared to Compton scattering, and the variation of LET with the photon energy is no longer monotonic.

2.1.2 Carcinogenesis. Carcinogenesis is thought to be a multi-staged process “initiated” by a mutation in a single cell. Before a malignancy can result, however, additional mutations must accumulate. This process may be enhanced by enlarging the pool of initiated cells (clonal expansion), which might be

¹ Kocher et al. (2005) have introduced a quantity called the “radiation effectiveness factor” (REF) to compare the cancer causing potency in humans of a specified type of radiation relative to some standard. According to their definition, the REF is to be distinguished from measured RBEs that may be used as a basis for estimating the REF, although the RBEs themselves may have been measured for a different end-point or in a different species. Although it is important to keep in mind that RBEs used for human risk estimation are generally extrapolated, and not directly measured, we follow common practice here in applying the term RBE more broadly to include the estimation of human radiogenic cancer risk.

triggered by the presence of a “promoter”. After clonal expansion, more initiated cells are available to undergo additional mutations, a process referred to as “cancer progression”. Particularly important may be those mutations that increase the probability of further mutations – e.g., those impairing DNA repair processes. Eventually, a set of mutations may remove the essential controls over cell division, resulting in a malignancy.

2.1.3 Radiogenic Carcinogenesis. Over a period of decades, a conceptual model of radiation carcinogenesis was built up from numerous studies conducted at the molecular, cellular, tissue, and whole organism levels. In this picture an ionizing track produces DNA damage through direct interaction with the double helix or through the interaction of free radicals diffusing to the DNA damage site, after being produced nearby. Misrepair of the DNA damage can then lead an initiated cell and, eventually, to a malignancy as outlined above. The dose response for radiation carcinogenesis is then expected to have the same mathematical form as that for radiation-induced mutations.

As shown in Figure 2-1, the dose response for the induction of mutations, cell transformation, or carcinogenesis by low-LET IR appeared to be linear at low doses, curvilinear upward at higher doses until eventually becoming concave downward at still higher doses. Mathematically, the initial portions of the curve is expressed as a “linear-quadratic” (LQ) function of effect (E) vs dose (D).

$$E = \alpha_1 D + \alpha_2 D^2 \quad (2-1)$$

At low dose rates, the effect was found to increase linearly, with the same slope, α_1 , observed initially at high dose rates. The expected response at high doses is therefore reduced by lowering the dose rate, which effectively removes the quadratic term in Eq. 2-1.

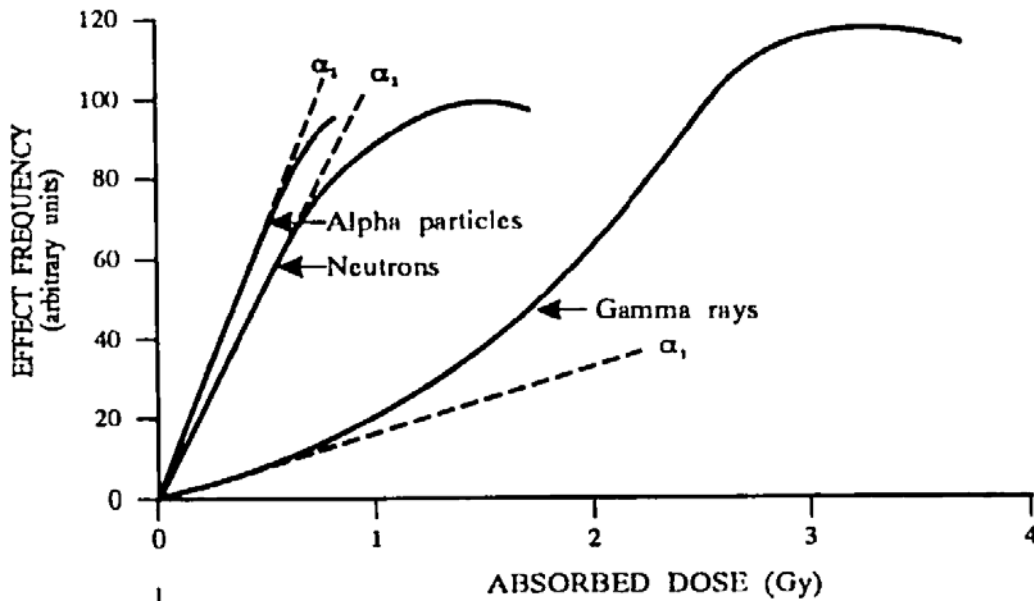


Figure 2-1: Solid curves depict the classical dose-response curves for low-LET gamma rays and high-LET neutrons or alpha-particles. The dashed lines show the expected response at low dose rates for each type of radiation. From UNSCEAR 1993, p. 698.

As also shown in Figure 2-1, the dose-response for high-LET radiation, appeared to be linear and independent of dose rate, except at rather high doses, where the function flattens or even turns over. At the high doses, moreover, an “inverse dose rate effect” may be observed in which the response is increased when the dose rate is reduced.

Thus, at low doses and dose rates the dose-response for either low- or high-LET radiation appears to be linear with no evidence of a threshold.

In the case of low-LET radiation, it was inferred that the passage of two tracks close together in space and time increases the probability of misrepaired damage, either because the damage produced is more complex or because the repair machinery becomes partially saturated, reducing its effectiveness. It was presumed that, at either low doses or low dose rates, only the damage produced by single tracks is significant, and the response is simply proportional to dose. At high dose rates, however, repair efficiency will decrease with increasing dose, leading to the quadratic term in Eq. 2-1.

At low or moderate doses of high-LET radiation, the production of multiply-damaged sites in DNA is dominated by single track events. The flattening or downturn observed at high acute doses may reflect cell killing (NCRP 1980). An alternative explanation has been proposed in which at any given time a subpopulation of cells exists in a sensitive time window; spreading the dose out more in time allows more cells to be hit while they are in that time window, resulting in an enhanced response (Rossi and Kellerer 1986, Elkind 1994).

Downward curvature and an inverse dose rate effect can also result from the “bystander effect” (Brenner and Sachs 2003), which will be discussed below.

Conclusions: Traversal of a cell nucleus by IR can induce damage to the cell’s DNA, initiating the carcinogenic process. Since the damage produced by even a single track of IR can sometimes be misrepaired, a threshold for cancer induction would appear improbable unless there is a mechanism for eliminating essentially all dividing cells with damaged DNA (e.g., through some kind of immune surveillance). A nearly foolproof screening mechanism of this sort would seem to be ruled out, however, by the significant rate of cancer incidence among people not exposed to high levels of IR.

Under conditions of low doses or low dose rates, the effect of multiple tracks is expected to be negligible, so the probability of a cell becoming initiated is simply proportional to dose. This provides a mechanistic basis for the linear no-threshold (LNT) model of carcinogenesis in which the probability of IR causing a cancer is proportional to dose, even at very low doses for which there is insufficient statistical power to detect any excess incidence of the disease in a human population.

2.1.4 Extrapolation of Low-LET Risks to Low Doses and Dose Rates.

As discussed above, radiobiological data suggest that the probability of mutational damage in a cell’s DNA from an *acute* exposure to low-LET IR can be expressed as a linear-quadratic (LQ) function of dose (D):

$$E = \alpha_1 D + \alpha_2 D^2 \tag{2-1}$$

The linear term is assumed to reflect the effect of single tracks, the quadratic term the added effect of two tracks traversing the cell close together in space and time, or perhaps the saturation of repair mechanisms at higher doses. If doses are delivered in a widely spaced temporal series of acute dose fractions, it is expected that each dose fraction, D_f , will produce an incremental effect,

$$E_f = \alpha_1 D_f + \alpha_2 D_f^2 \tag{2-2}$$

If each fraction is made very small, the quadratic terms will be negligible, and the overall summed effect will be linear with dose; i.e., $E = \alpha_1 D$, where $D = \sum D_f$. A chronic exposure can be thought of as a sequence of very small fractionated exposures. It follows that if the dose rate from a chronic exposure is low enough so that the interaction of multiple tracks can be neglected, then the effect will again be simply given by $E = \alpha_1 D$, where D is the total dose.

The effect per unit dose will be reduced in going from a large acute dose, D , where the quadratic term is significant, to a low dose, where only the linear term contributes. Overall the effect will be reduced by a Dose Effectiveness

Factor (DEF) = $(\alpha_1 + \alpha_2 D) / \alpha_1 = 1 + \theta D$, where $\theta = \alpha_2 / \alpha_1$. Likewise the estimated effect per unit dose will be reduced by a Dose Rate Effectiveness Factor (DREF), when a large acute dose is delivered chronically. Since the slope is the same (α_1) at low doses or dose rates, the DREF and the DEF are equal. Thus, according to the LQ model, the extrapolation from a high acute dose to either a low dose or to a low dose rate can be embodied into a single correction factor, the Dose/Dose Rate Effectiveness Factor (DDREF).

It is presumed that the probability of carcinogenesis induced in an organism from an exposure to IR is proportional to the number of induced mutations remaining after repair is complete. This has led scientists to model the excess risk as a LQ function of dose for a relatively high acute dose, with a reduction by a DDREF factor for low doses and dose rates. The DDREF for carcinogenesis would be equal to that for the underlying process of radiation-induced mutagenesis.

Based on its review of radiobiological and epidemiological data, the UNSCEAR Committee (UNSCEAR 1993; 2000b) concluded that any dose below 200 mGy, or any dose rate below 0.1 mGy/min (when averaged over about an hour), should be regarded as low. Thus, according to the linear-quadratic model, for these doses and dose rates, the risk per unit dose would be approximately equal to the linear coefficient, α_1 .

2.1.5 Low Dose Phenomena. Much recent research in radiobiology has focused on several new phenomena relating to the effects of low dose IR, including: (1) the adaptive response, (2) genomic instability, and (3) bystander effects. These phenomena have raised questions about the reliability of the LNT model for radiation carcinogenesis. They indicate that, at least under some conditions, IR may induce DNA damage, *indirectly*, by affecting non-targeted cells, and that the processing of DNA damage by cells may be strongly dependent on dose, even at very low doses.

Adaptive Response. Under some conditions, it has been found that pre-irradiating cells with an “adapting dose” of low-LET radiation (~10 mGy) reduces the effects (e.g., chromosome damage, mutations, or cell transformation) of a subsequent “challenge dose” of ~1 Gy. This has provided some support for the suggestion that low-dose radiation may stimulate defense mechanisms, which could be beneficial in preventing cancer or other diseases. Supporting this view also have been studies in which the spontaneous transformation rates of certain cells in culture have been reduced by exposure to very low level IR (Azzam et al. 1996, Redpath and Antoniono 1998). A subsequent study, however, has shown a threshold for this “beneficial effect”; suppression of transformation disappeared when the dose rate was reduced below 1 mGy/day (Elmore et al. 2008). Thus, even if this phenomenon occurs *in vivo*, it may not be operative at environmental exposure levels.

Genomic Instability. It has been found that irradiation of a cell can produce some kind of change in that cell, not yet characterized, which increases the probability of a mutation one or more cell divisions later (Morgan et al. 1996). The relatively high frequency of inducing genomic instability implies that the relevant target is much larger than a single gene, and there is evidence that, at least in some cases, the phenomenon is mediated by IR-induced epigenetic changes rather than DNA damage (Kadhim et al. 1992, Morgan et al. 1996). The delayed mutations are typically simple point mutations, unlike other mutations caused by IR, which are typically deletions or other types of chromosomal changes resulting from DSBs and more complex DNA damage (Little et al. 1997).

Bystander Effects. Contrary to the conventional picture, DNA damage in a (bystander) cell can be induced by passage of an ionizing track through a neighboring cell. The bystander effect can apparently be triggered by passage of a signal through gap junctions (Azzam et al. 1998). Media transfer experiments have demonstrated that it can also be induced – although probably less effectively (Mitchell et al. 2004) – by molecules leaking out into the extracellular fluid (Mothersill and Seymour 1998, Lehnert and Goodwin 1998). It also appears that the adaptive response and genomic instability may be induced in bystander cells under some conditions (Coates et al. 2004, Kadhim et al. 2004, Tapio and Jacob 2007). Recent evidence has also been found of bystander signals from irradiated cells inducing apoptosis in neighboring transformed cells (Portess et al. 2007).

The preponderance of data regarding these effects has been obtained from experiments on isolated cells. There is limited information on the occurrence of these effects *in vivo*, and no understanding of how they might modulate risks at low doses. At first sight, it would appear that the adaptive response should be protective, whereas bystander effects and genomic instability might increase risk. Interpretation may be complicated, however, by the possibility for triggering protective mechanisms in bystander cells, such as an adaptive response or apoptosis of precancerous cells (Lyng et al. 2000, Portess et al. 2007, Tapio and Jacob 2007).

The BEIR VII Committee was not convinced that these effects would operate *in vivo* in such a way as to significantly modify risks at low doses. It was a consensus of the Committee that:

the balance of evidence from epidemiologic, animal and mechanistic studies tend to favor a simple proportionate relationship at low doses between radiation dose and cancer risk. (BEIR VII, p. 14)

A similar conclusion was reached by another group of experts assembled by the International Commission on Radiological Protection (ICRP 2005).

In contrast, the French Academy of Sciences issued a report that strongly questioned the validity of the LNT hypothesis (Tubiana *et al.* 2005). The French Academy report cited a paper by Rothkamm and Löbrich (2003) showing that repair of DSBs, as measured by the disappearance of γ -H2AX foci, was absent or minimal at low doses, presumably leading to apoptosis of cells with DSBs. The French Academy report claimed that this finding indicated that risks were greatly overestimated at low doses. Recent studies have cast doubt on the significance of this finding, however (Löbrich *et al.* 2005, Marková *et al.* 2007).

Conclusion. EPA accepts the recommendations in the BEIR VII and ICRP Reports to the effect that there is strong scientific support for LNT and that there is no plausible alternative at this point. However, research on low dose effects continues and the issue of low dose extrapolation remains unsettled.

2.2 Epidemiology

There is overwhelming evidence from epidemiological studies of irradiated human populations that IR increases the risk of cancer. Most important from the standpoint of quantifying radiation risks is the Lifespan Study (LSS) of atomic bomb survivors in Hiroshima and Nagasaki, Japan. The survivors constitute a relatively healthy population at the time of exposure, including both genders and all ages, with detailed medical follow-up for about half a century. Extremely significant, also, is the wide range of fairly accurately known individual radiation doses.

The LSS cohort shows an excess in various types of cancer, with the rates increasing with increasing dose to the target organ. The data from the LSS are adequate to serve as a basis for developing detailed mathematical models for estimating risk as a function of cancer site, dose, age, and gender. However, due to limitations in statistical power, it has not been possible to demonstrate and quantify risk in the LSS at doses below about 100 mGy.

Epidemiological studies of medically irradiated cohorts provide strong confirmation for the carcinogenic effects of IR and some additional information for generating risk estimates – in particular, for the bone, thyroid, liver, and breast. Radiation risks have also been extensively studied in occupationally exposed cohorts, but so far such studies – aside from those on radon-induced lung cancers in underground miners – have not proved very useful for actually quantifying risk. Major reasons for this failure have been: poor dosimetry; low doses, leading to low statistical power; and potential confounding by life-style factors or other occupational exposures. As discussed in a later section, however, recent data on workers at the Mayak plutonium production plant in the former Soviet Union may provide an improved basis for estimating risks from inhaled alpha-emitters.

Although the epidemiological data on radiation-induced carcinogenesis are extensive, calculated risks to members of the U.S. population from doses of IR typically received environmentally, occupationally, or from diagnostic medical procedures suffer from significant sources of uncertainty. Among these sources are: (1) errors in the epidemiological data underlying the risk models, including sampling errors, errors in dosimetry, and errors in disease ascertainment; (2) uncertainties in how risks vary over times longer than the period of epidemiological follow-up; (3) uncertainties in “transporting” risk estimates to the U.S. population from a study population (e.g., the LSS cohort), which may differ in its sensitivity to IR; (4) differences in the type of radiation or its energy between the epidemiological cohort and the target U.S. population; and (5) uncertainty in how to extrapolate from moderate doses (>0.1 Gy), for which there are good data upon which to quantify risk, to lower doses, and from acute to chronic exposure conditions.

Especially contentious is the extrapolation to low doses and dose rates. Generally speaking, epidemiology cannot be used to detect and quantify the carcinogenic effects of radiation at doses below about 100 mGy of low-LET radiation because of limitations on statistical power (Land 1980, Brenner et al. 2003). Most cells in the body receive a radiation dose of about 1 mGy/y – predominantly gamma rays from cosmic, terrestrial and internal sources. Given the typical energies of these background gamma rays (0.1-3 MeV) this corresponds to roughly 1 ionizing track traversing each cell nucleus, on average, annually. Thus, during the estimated typical time for DNA repair to be completed (a few hours), roughly 1 out of 1,000 cell nuclei will be hit, and the probability of multiple hits to the same nucleus will be very low. By way of comparison, at the lowest doses for which risk can be quantified in the A-bomb survivors, each nucleus was instantaneously impacted by ~100 tracks.

A notable exception to this 100 mGy limit on the sensitivity of epidemiological studies appears to be for studies of childhood cancers induced by prenatal exposure to diagnostic x rays, where an excess risk has been observed at a dose level of about 6-10 mGy (see Section 6). In this case, statistical power is magnified by the apparent heightened sensitivity of the fetus, combined with a low background rate of childhood cancers. Typically, the x rays employed in these examinations were 80 kVp, and the estimated mean dose was 6 mGy; this corresponds to only about 1 incident photon per cell nucleus (Brenner and Sachs 2006). Thus, this finding argues against a threshold for radiation carcinogenesis.

Although epidemiology otherwise lacks the power to detect risks from acute doses of radiation below about 100 mGy, it can provide information on risks from smaller doses through studies of populations receiving fractionated or chronic IR doses that cumulatively add up to about 100 mGy or more. For example, it was found that multiple fluoroscopic examinations, each delivering an average dose of approximately 8 mGy, produced a similar increase in breast

cancer, per unit dose, as a single acute dose to the breast (Howe and McLaughlin 1996). Likewise, female scoliosis patients under 20 years of age, who received repeated x-ray examinations, each with a mean breast dose of approximately 4 mGy, had a higher breast cancer mortality compared to controls and an increasing mortality with an increasing number of examinations (Doody et al. 2000). In both these studies, breast cell nuclei received at most a few nuclear hits from each dose fraction. Finally, children irradiated for ringworm (mean total thyroid dose 84 mGy in 5 fractions) had a statistically significant increase in thyroid cancer compared to unirradiated controls (Ron et al. 1989)

In addition, epidemiological studies have been conducted on cohorts of individuals who received cumulative doses of 100 mGy or more, but where the dose is spread out over months or years. Radiologists (Lewis 1963, Smith and Doll 1981) and radiological technicians (Wang et al. 1988, Doody et al. 2006), working before modern radiation protection standards had been implemented, show increased risks of leukemia and breast cancer, respectively. However, individual dose estimates are generally lacking in these studies, and they are not very useful for obtaining quantitative risk estimates. A number of cohort studies are underway, however, which may better demonstrate and quantify risks from protracted doses of low-LET IR.

Among the most important of these studies are: nuclear workers in various countries (Cardis et al. 2005, 2007); Chernobyl cleanup workers ("liquidators") (Hatch et al. 2005); residents downriver from the Mayak nuclear plant in Russia (Ostroumova et al. 2006, Krestinina et al. 2005); residents downwind from the Semipalatinsk nuclear test site in Kazakhstan (Bauer et al. 2005); and inhabitants of Taiwanese apartments constructed with steel beams contaminated with ^{60}Co (Hwang et al. 2008). Studies on these populations are ongoing and suffer from various shortcomings, including incomplete follow-up and dosimetric uncertainties. Nevertheless, results from several of them suggest that radiation risks can be detected and quantified, even in cases where the average dose rate is well below 1 mGy/day, corresponding to less than 1 ionizing track per cell nucleus per day (Puskin 2008).

3. EPA Risk Projections for Low-LET Radiation

3.1 Introduction

For cancer sites other than bone and skin cancer, the new EPA risk projections for low-LET radiation are based on the risk models recommended in BEIR VII and are described in the next section. As in BEIR VII, the risk models form the basis for calculating estimates of lifetime attributable risk (LAR), which approximate the premature probability of a cancer or cancer death which can be attributed to radiation exposure. Relatively minor modifications were made to the approach used in BEIR VII to the methodology for calculating LAR; details are given in Section 3.2 and subsequent sections. Although the main results are the new EPA estimates of LAR associated with a constant lifetime dose rate, we also provide estimates to indicate how radiogenic risks might depend on age at exposure. A detailed discussion of the uncertainties associated with these risks is given in Section 4.

The main focus of the BEIR VII Report was to develop estimates of risk for low-dose, low-LET radiation. However, the BEIR VII models are predominantly based on analyses of the A-bomb survivor data, where the exposure included high-LET neutrons, as well as gamma rays. A recently completed reappraisal of the A-bomb dosimetry, referred to as DS02, was used as a basis for the BEIR VII analysis. In BEIR VII, it was assumed that neutrons had a constant RBE of 10 compared to gamma rays, implying a “dose equivalent”, d , to each survivor (in Sv) given by:

$$d = d_{\gamma} + 10 d_n,$$

where d_{γ} and d_n are, respectively, the gamma ray and neutron absorbed doses (in Gy). The BEIR VII approach then yields models for calculating the risk per Sv, which can be directly applied to estimate the risk per Gy from a gamma-ray exposure.

With a constant RBE of 10, the estimated contribution of neutrons is relatively minor, although not negligible. A recent publication (Sasaki et al. 2008) presented radiobiological data supporting an RBE for neutrons that was highly dose dependent, approaching a value of nearly 100 in the limit of low doses. The authors found that applying their estimates for the RBE brought about better agreement between Hiroshima and Nagasaki chromosome aberration data and reduced the estimate of gamma-ray risk by about 30%. <BEIR VII, p. 146>

3.2 BEIR VII Risk Models

The BEIR VII Committee used excess relative risk (ERR) and excess absolute risk (EAR) to project radiogenic cancer risks to the U.S. population for each of the cancer sites given in Table 3-1. ERR represents the ratio of the age-

specific increase in cancer rate attributable to a radiation dose divided by the baseline rate, i.e. the rate associated with the background radiation level, whereas EAR is simply the difference in rates attributable to radiation. In the models preferred by the BEIR VII Committee for solid cancer sites, ERR and EAR are functions of age-at-exposure, attained age (the age at which a cancer might occur), and sex. For leukemia, the “BEIR VII models” also explicitly allow for dependence of ERR or EAR on time-since-exposure.

For all cancer sites, the BEIR VII risk models were based, at least partially, on analyses of data from atomic bomb survivors. ERR and EAR models of the form given in Eq. 3-1 and 3-2 were fit to LSS data on incidence and mortality:

$$\begin{aligned} \text{ERR model: } \lambda(c, s, a, b, d) &= \lambda_0(c, s, a, b)[1 + ERR(s, e, a, d)] \\ &= \lambda_0(c, s, a, b)[1 + d \overline{ERR}(s, e, a, d)] \end{aligned} \quad (3-1)$$

$$\begin{aligned} \text{EAR model: } \lambda(c, s, a, b, d) &= \lambda_0(c, s, a, b) + EAR(s, e, a, d) \\ &= \lambda_0(c, s, a, b) + d \overline{EAR}(s, e, a, d) \end{aligned} \quad (3-2)$$

Here, $ERR(s, e, a, d)$ and $EAR(s, e, a, d)$ are, respectively, the ERR and EAR for a given sex (s), age at exposure (e), attained age (a), and absorbed dose (d). $\overline{ERR}(s, e, a, d)$ and $\overline{EAR}(s, e, a, d)$ denote the ERR and EAR per unit of dose expressed in Gy (for low-LET radiation), and $\lambda_0(c, s, a, b)$ is the baseline rate, which depends on city (c , Hiroshima or Nagasaki), sex, attained age, and year of birth (b). For all solid cancer sites, an LNT model was fit to the LSS data. In other words, increases in solid cancer rates were assumed to be approximately equal to the product of a linear-dose parameter that depends on sex, the absorbed dose, and a function that depends on age-at-exposure and attained-age, so that \overline{ERR} and \overline{EAR} does not depend on dose.

Table 3-1: BEIR VII risk model cancer sites

Cancer site(s)	ICD-O-2 codes
Stomach	C16 / 3
Colon	C18 / 3
Liver	C22 / 3
Lung	C33, 34 / 3
Breast (female only)	C50 / 3
Prostate	C61 / 3
Uterus	C53-54, C559 / 3
Ovary	C 56, C57 (0,1,2,3,4,8) / 3
Bladder	C67 / 3
Thyroid	C739 / 3
“Remainder category”. Solid cancers of the oral cavity, esophagus, small intestine, rectum, gall bladder, pancreas, digestive system*, nasal cavity, larynx, other respiratory system*, thymus, kidney, and central nervous system. Also includes renal pelvis, ureter cancers, melanoma, bone, connective tissue, other genital cancers*, and other solid cancers*	C00-C15 / 3, C17 / 3, C19-21 / 3, C 23-25 / 3, C26 / 3, C422 / 3, C37-39 / 3, C379 / 3, C649 / 3, C70-72/ (2,3), C40 / 3, C41 / 3, C47 / 3, C49 / 3, C44 / 3, M8270-8279, C659 / 3, C 669 / 3, C51/3, C52/3, C57 (7,8,9)/3, C58 / 3, C60 / 3, C63 / 3, C42 (0,1,3,4) / 3, C69 / 3, C74-76 / 3, C 77 / 3, C809 / 3.
Leukemia	Revised ICD 9: 204-208

* Refers to sites not specified elsewhere in this table.

The BEIR VII committee used very similar models to project risks to the U.S. population. Their ERR and EAR preferred risk models are of the form,

$$\lambda(s, a, d) = \lambda_0(s, a)[1 + d \overline{ERR}(s, e, a, d)] \quad (3-3)$$

$$\lambda(s, a, d) = \lambda_0(s, a) + d \overline{EAR}(s, e, a, d) \quad (3-4)$$

The only difference in the BEIR VII models for projecting risk to the U.S. compared to the models fit to the LSS data is that in Eq. 3-3 and 3-4, $\lambda_0(s, a)$ represents the baseline rate for the U.S. population, which depends only on sex and attained age. Otherwise, the two set of models are identical, i.e., $\overline{ERR}(s, e, a, d)$ and $\overline{EAR}(s, e, a, d)$ represent the same function in Eq. 3-3 and 3-4 as in Eq. 3-1 and 3-2. For example, the BEIR VII committee found that the ERR decreased by about 25% per decade in the model that “best” fit the LSS data for

most cancer sites; consequently, the ERR decreases by the same 25% per decade in their models used to project risk to the U.S.

Of the two types of risk models, ERR models are more appropriate for cancer sites for which age-specific excess in cancer incidence rates attributable to radiation might be roughly proportional to the baseline rate – independent of the population. In contrast, EAR models are appropriate when the excess in cancer rates is independent of the baseline risks. The BEIR VII Committee used each type of risk model (EAR and ERR) to calculate site-specific risk projections for a U.S. population. For cancers for which the baseline rates are higher in the U.S. than in the LSS, the ERR models tend to yield larger projections of radiogenic risk than the projections from EAR models. For other cancer sites, the projections from EAR models tend to be larger.

A compromise between the two approaches was used for most cancer sites. If, as seems likely, radiogenic risks for most cancer sites for the U.S. population are within the ranges defined by the ERR and EAR projections, a reasonable approach would be to calculate an “average” the projections based on the two types of risk models, e.g., a weighted arithmetic or geometric mean. This is the approach used by BEIR VII and other comprehensive reports on radiation risks and is described in more detail in Section 3.9.

Table 3-2 provides a summary of the BEIR VII ERR and EAR risk models. For all solid cancer sites except breast and thyroid, the BEIR VII models were based exclusively on analyses of the A-bomb survivor incidence data. This differs from EPA’s current risk models (EPA 1994), which for most cancer sites were derived from LSS mortality data. In general, the LSS incidence data is preferred as a basis for the risk models because “site-specific cancer incidence data are based on diagnostic information that is more detailed and accurate than death certificate data and because, for several sites, the number of incident cases is larger than the number of deaths (NRC 2006).” For breast and thyroid cancers, the BEIR VII models were based on pooled analyses of both A-bomb survivor and medical cohort data. The risk model for leukemia was based on an analysis of mortality within the LSS cohort. In contrast to some other cancer types, “the quality of diagnostic information for the non-type-specific leukemia mortality used in these analyses is thought to be high (NRC 2006).”

Table 3-2: Summary of BEIR VII preferred risk models

Cancer site	Description	Data sources
Solid cancers except breast, thyroid	ERR and EAR increase linearly with dose; depends also on sex (s), age at exposure (e), attained age (a)	1958-1998 LSS cancer incidence
Breast	EAR increases linearly with dose. ERR model not used. Effect modifiers: (e, a).	1958-1993 LSS breast cancer incidence; Massachusetts TB fluoroscopy cohorts (Boice et al. 1991); Rochester infant thymic irradiation cohort (Hildreth et al. 1989)
Thyroid	ERR increases linearly with dose. EAR model not used. Effect modifiers (s, e, a).	1958-1987 LSS thyroid cancer incidence (Thompson et al. 1994); Medical cohort studies: Rochester thymus (Shore et al. 1993), Israel tinea capitis (Ron et al. 1989), Chicago tonsils (Schneider et al. 1993), Boston tonsils (Pottern et al. 1990). Medical case-control studies: Cervical cancer (Boice et al. 1988), Childhood cancer (Tucker et al. 1991).
Leukemia	ERR and EAR are quadratic functions of dose. Effect modifiers: (s, e, a) and time since exposure (t).	1950-2000 LSS cancer mortality (Preston et al. 2004).

Solid cancer sites other than breast and thyroid. For most solid cancer sites, the preferred BEIR VII EAR and ERR models are functions of sex, age at exposure, and attained age, and are of the following form:

$$EAR(d, s, e, a) \text{ or } ERR(d, s, e, a) = \beta_s d \exp(\gamma e^*) (a/60)^\eta, \quad (3-5)$$

$$\text{where } e^* = \frac{\min(e, 30) - 30}{10}. \quad (3-6)$$

As seen in Table 3-3, the values for the parameters β_s , γ , and η depend on the type of model (EAR or ERR). For ERR models for most sites:

β , the ERR per Sv at age-at-exposure 30 and attained age 60, tends to be larger for females than males;

$\gamma = -0.3$ implies the radiogenic risk of cancer at age e falls by about 25% for every decade increase in age-at-exposure up to age 30; and

$\eta = -1.4$ implies the ERR is almost 20% smaller at attained age 70 than at age 60.

As a consequence, *ERR* decreases with age-at-exposure (up to age 30) and attained age. In contrast, for EAR models, $\gamma = -0.41$ and $\eta = 2.8$ for most sites. Thus *EAR* decreases with age-at-exposure, but *increases* with attained age. These patterns are illustrated in Figure 3-1.

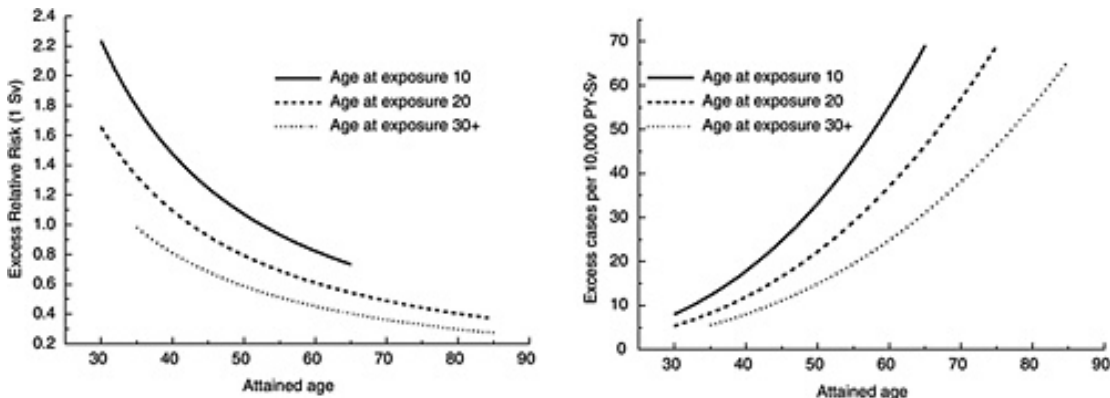


Figure 3-1: Age-time patterns in radiation-associated risks for solid cancer incidence excluding thyroid and nonmelanoma skin cancer. Curves are sex-averaged estimates of the risk at 1 Sv for people exposed at age 10 (solid lines), age 20 (dashed lines), and age 30 or more (dotted lines). (BEIR VII: Figure 12-1A, p. 270).

Thyroid. For thyroid cancer, the BEIR VII Committee used only an ERR model to quantify risk. It was of slightly different form than for other solid cancers

in that ERR continues to decrease exponentially with age-at-exposure for ages greater than 30 y, and ERR is independent of attained age. ERR for thyroid cancer is given in Eq. 3-7:

$$ERR(d, s, e) = \beta_s d \exp[\gamma(e - 30)/10](a/60)^\eta, \quad (3-7)$$

Table 3-3: Parameter values for preferred risk models in BEIR VII¹

Cancer	ERR model				EAR model			
	β_M	β_F	γ	η	β_M	β_F	γ	H
Stomach	0.21	0.48	-0.3	-1.4	4.9	4.9	-0.41	2.8
Colon	0.63	0.43	-0.3	-1.4	3.2	1.6	-0.41	2.8
Liver	0.32	0.32	-0.3	-1.4	2.2	1	-0.41	4.1
Lung	0.32	1.4	-0.3	-1.4	2.3	3.4	-0.41	5.2
Breast	Not used				See text			
Prostate	0.12		-0.3	-1.4	0.11		-0.41	2.8
Uterus		0.055	-0.3	-1.4		1.2	-0.41	2.8
Ovary		0.38	-0.3	-1.4		0.7	-0.41	2.8
Bladder	0.5	1.65	-0.3	-1.4	1.2	0.75	-0.41	6
Other solid	0.27	0.45	-0.3	-2.8	6.2	4.8	-0.41	2.8
Thyroid ²	0.53	1.05	-0.83	0	Not used			
Leukemia	1.1	1.2	-0.4	None	1.62	0.93	0.29	None
	$\delta = -0.48,$ $\theta = 0.87 \text{ Sv}^{-1}, \phi = 0.42$				$\theta = 0.88 \text{ Sv}^{-1}, \phi = 0.56$			

¹ Adapted from Tables 12-2 and 12-3 of BEIR VII.

² Unlike for other sites, the dependence of ERR on age-at-exposure is not limited to ages < 30.

Breast. For breast cancer, the BEIR VII Committee used only an EAR model to quantify risk. In the BEIR VII model, EAR depends on both age at exposure and attained age (Eq. 3.8). Unlike other cancers, the EAR continues to decrease exponentially with age-at-exposure throughout one's lifetime, and the EAR increases with attained age less rapidly after age 50 (about the time of menopause).

$$EAR(d, s, e, a) = \beta d \exp[\gamma(e - 25)/10](a/60)^\eta \quad (3-8)$$

where $\eta = 3.5$ for $a < 50$ and 1 for $a \geq 50$.

Leukemia. BEIR VII provided both EAR and ERR risk models for leukemia (see Eq. 3-9). These differ from models for most other cancer sites. In the leukemia models, both ERR and EAR depend on time since exposure (t), and

risk is a linear-quadratic function of dose. As shown in Figure 3-2, the EAR and ERR per unit dose both increase with dose (the fitted value for θ in Eq. 3-9 is positive).

$$EAR(d, e, t) \text{ or } ERR(d, e, t) = \beta_s (1 + \theta d) \exp[\gamma e^* + \delta \log(t/25) + \phi e^* \log(t/25)],$$

for $t \geq 5$, and

$$EAR(d, e, t) = EAR(d, e, 5), \text{ for } 2 < t \leq 5,$$

$$ERR(d, e, t) = ERR(d, e, 5) \frac{\lambda_0(s, e+5)}{\lambda_0(s, e+2)}, \text{ for } 2 < t \leq 5, \text{ and}$$

$$EAR(d, e, t) = ERR(d, e, t) = 0 \text{ for } t \leq 2. \tag{3-9a,b}$$

The dependence of *EAR* and *ERR* on age and time-since-exposure is illustrated in Figure 3-3. Both *EAR* and *ERR* decrease with time-since-exposure for $t > 5$, and the rate of decrease is larger for younger ages at exposure. For the time period 2 to 5 y after exposure, the EAR is constant. The EAR that would be calculated using the ERR model (note that excess absolute risk is equal to the product of the ERR and the baseline cancer rate) is also constant for this time period ($2 < t \leq 5$).

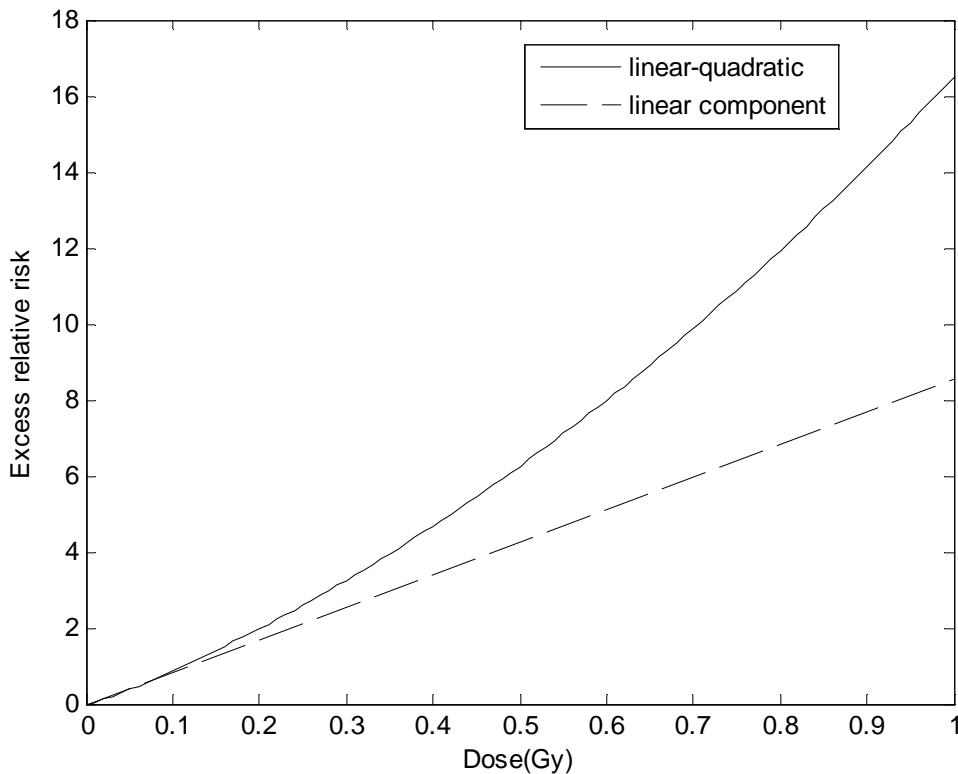


Figure 3-2: ERR for leukemia for age-at-exposure = 20 and time-since-exposure = 10. The linear component of the dose-response is also shown.

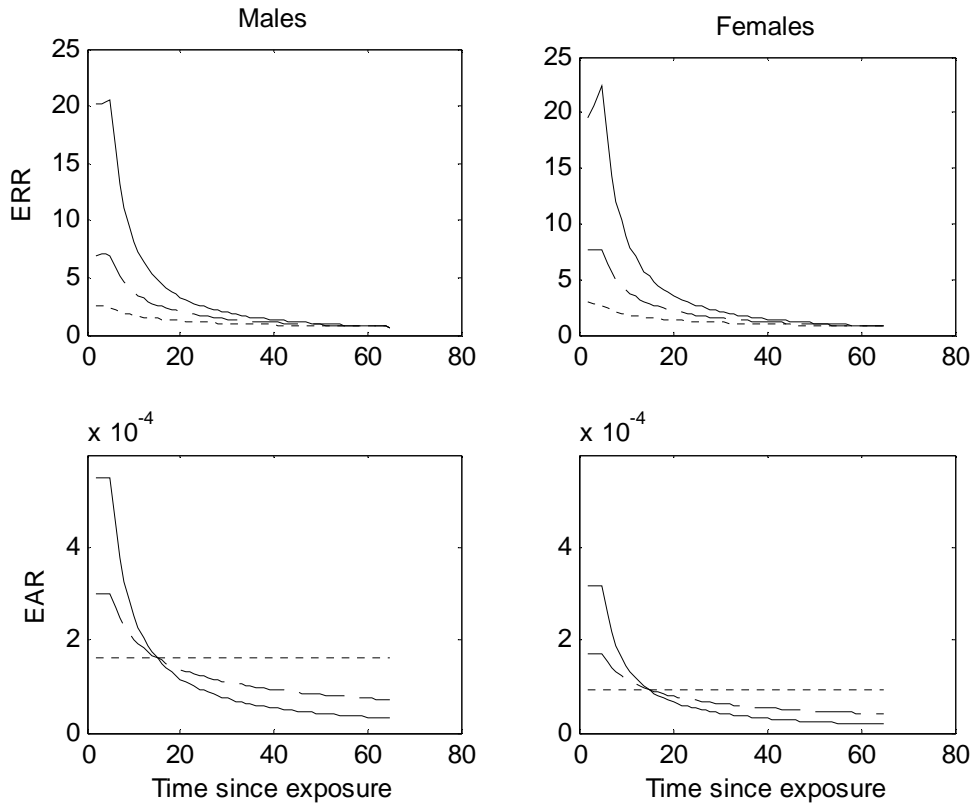


Figure 3-3: ERR and EAR by time-since-exposure for three different ages at exposure: 10 (solid), 20 (dashed), and 30 (dotted).

3.3. Residual Sites and Skin Cancer

BEIR VII's risk model for what are often termed "residual site" cancers deserves special mention. The residual category generally includes cancers for which there were insufficient data from the LSS cohort or other epidemiological studies to reliably quantify radiogenic site-specific risks. For these sites, results from the LSS cohort were pooled to obtain stable estimates of risk. With five exceptions (cancers of the esophagus, bone, kidney, prostate and uterus) the BEIR VII Report included the same cancers in this category as EPA did in its previous risk assessment (EPA 1994, 1999).

Esophagus. EPA (1999) employed a separate risk model for esophageal cancer, whereas in BEIR VII the esophagus is one of the "residual" sites. In part, this is because the risk models for the previous assessment were based on LSS mortality data, for which there was a significant dose-response for esophageal cancer. In contrast, the BEIR VII models are based on LSS incidence data, for which there was insufficient evidence of a dose-response. Consistent with BEIR VII, we include esophageal cancer as one of the residual sites. This decision is expected to have only a minor impact on EPA's risk coefficients for intake of radionuclides.

Kidney. EPA (1999) uses a separate model for cancer of the kidney, but BEIR VII includes kidney as one of the residual sites. In contrast to esophageal cancer, a separate risk model is needed for this cancer site because the kidney is an important target for several radionuclides, including isotopes of uranium. There is little direct evidence upon which to base an estimate for kidney cancer LAR. In a recent analysis of LSS incidence data (Preston et al. 2007), there were only 115 kidney cancers, 70% of which were renal cell cancers. The authors estimated only 6 excess renal cell cancers from radiation exposure. Furthermore, whatever the association might be between kidney cancer and radiation, it is complicated by the fact that the etiology for the various kidney cancer types differ. The estimated dose-response in the LSS appears to be sensitive to the type of model being fit. Within the LSS cohort, no indication of a positive dose response was found ($p > 0.5$) when a constant ERR model was fit, but results were significant when fit to a constant EAR model. Confidence intervals for linear dose response parameters are wide for both models, and there is insufficient evidence to conclude that the dose response in LSS is substantially different for kidney cancers than other residual site cancers. It was therefore concluded that a reasonable approach would be to use the BEIR VII residual site ERR model for kidney cancers. For the kidney EAR model, an adjustment factor was applied, equal to the ratio of the age-specific kidney cancer baseline rates divided by the rates for the residual site cancers. EPA's new kidney cancer EAR model is given in Eq. 3-10:

$$\overline{EAR}_{kidney}(s, e, a) = \frac{\lambda_{I, kidney}(s, a)}{\lambda_{I, residual}(s, a)} \overline{EAR}_{residual}(s, e, a) \quad (3-10)$$

Bone. A new EPA model for alpha-particle-induced bone cancer risks is based on an analysis of data on radium dial painters exposed to ^{226}Ra and ^{228}Ra and patients injected with the shorter-lived isotope ^{224}Ra (Nekolla et al. 2000). The risk per Gy for low-LET radiation is assumed to be 1/10 that estimated for alpha-particle radiation. Details about the EPA bone cancer risk model and its derivation are provided in Section 5.1.2 (on human data on risks from higher-LET radiation).

The new risk projections for bone cancer incidence from low-LET radiation are $2.04 \times 10^{-4} \text{ Gy}^{-1}$ (males), $1.95 \times 10^{-4} \text{ Gy}^{-1}$ (females), and $1.99 \times 10^{-4} \text{ Gy}^{-1}$ (sex-averaged). About 35% of all bone cancers are fatal, and it is assumed here that the same lethality holds for radiogenic cases. The mortality risk projections are $7.13 \times 10^{-5} \text{ Gy}^{-1}$ (males), $6.82 \times 10^{-5} \text{ Gy}^{-1}$ (females), and $6.96 \times 10^{-5} \text{ Gy}^{-1}$ (sex-averaged).

Prostate and Uterus. In contrast to EPA (1999), BEIR VII provides separate risk models for these two cancer sites, and these BEIR VII models form the basis for new EPA projections. This is in contrast to EPA (1999), in which

these two cancer sites were included in the residual category. The A-bomb survivor data now provides sufficient information for radiogenic uterine cancer to formulate a risk projection of reasonable precision. BEIR VII cited the vastly differing baseline rates for the U.S. compared to Japan as a reason for providing a separate prostate estimate.

Skin. Previously, EPA risk estimates for radiation-induced skin cancer mortality (EPA 1994) were taken from ICRP Publication 59 (ICRP 1991). The one modification made by EPA was to apply a DDREF of 2 at low doses and dose rates. Recognizing that the great majority of nonmelanoma skin cancers are not life threatening or seriously disfiguring, EPA included only the fatal cases in its estimates of radiogenic skin cancer incidence. The contribution of skin cancers to the risk from whole-body irradiation was then minor: about 0.2% and 0.13% of the total mortality and incidence, respectively.

ICRP's calculation of skin cancer incidence risk employed an ERR of 55% per Sv, along with U.S. baseline skin cancer incidence rates from the 1970's. The ICRP mortality estimate was also based on conservative assumptions that: (1) 1/6 of radiogenic skin cancers would be squamous cell carcinomas (SCC), the remainder basal cell carcinomas (BCC); and (2) essentially all of the BCC would be curable, whereas about 1% of SCC would be fatal. Predicated on these considerations, ICRP Publication 59 estimated that 0.2% of the cases would be fatal.

The ICRP risk estimates closely mirror those previously published by Shore (1990), who also served as a member of the committee that drafted ICRP Publication 59. Shore (2001) reviewed the subject again in light of additional information and concluded that essentially all of the radiation-induced skin cancers at low to moderate doses would be BCC. He maintained that the fatality rate for BCC is "virtually nil" but cites a study indicating a rate of 0.05% Weinstock (1994). Shore also notes that there is no persuasive evidence that radiation-induced BCC would be more fatal than sporadic cases.

At the same time, there is evidence that the baseline rates for BCC have increased dramatically since the 1970's, which might also result in a higher (absolute) risk per unit dose of inducing a radiogenic skin cancer.

For our new skin risk model, we applied results from a recent analysis of LSS incidence data (Preston et al. 2007). Of these, the most appropriate for our purposes is the estimated ERR of 48% per Gy (90% CI 0.12 to 1.3) for BCC among survivors with doses < 1 Gy. We note that for doses above 1 Gy, the ERR per Gy was significantly greater: 2.64, CI = (2.2, 3). The authors found no evidence for an association between dose and SCC. As for most other cancer sites, we employ a DDREF of 1.5.

For lifetable calculations, baseline incidence rates are needed, but SEER does not include nonmelanoma skin cancers in its database. BCC incidence rates have increased dramatically over the last 3 decades (Karagas et al. 1999), and it has been estimated that there are 900,000 incident cases of BCC annually in the U.S. (550,000 in men, 350,000 in women), the great majority of these in whites (Ramsey 2006). The estimated lifetime risk of BCC in the white population is very high: 33-39% in men and 23-28% in women. Overall, the age-adjusted incidence per 100,000 white individuals is 475 cases in men and 250 cases in women. To calculate age-specific baseline incidence rates, we applied these age-adjusted numbers and assumed that the rates increase with age to the power of 4.5, which is the roughly the pattern observed for many cancers (Breslow and Day 1987).

The age-adjusted fatality rate has recently been estimated to be 0.08 per 100,000 individuals, based on only 12 BCC deaths in the state of Rhode Island between 1988 and 2000 (Lewis and Weinstock 2004). The case fatality rate for BCC can then be roughly estimated to be: $0.08 / 0.5(475+250) \approx 0.03\%$, which is what we used for our mortality projections.

The new risk projections for skin cancer incidence are $1.10 \times 10^{-1} \text{ Gy}^{-1}$ (males), $6.37 \times 10^{-2} \text{ Gy}^{-1}$ (females), and $8.67 \times 10^{-2} \text{ Gy}^{-1}$ (sex-averaged). The mortality risk projections are $3.31 \times 10^{-5} \text{ Gy}^{-1}$ (males), $1.91 \times 10^{-5} \text{ Gy}^{-1}$ (females), and $2.60 \times 10^{-5} \text{ Gy}^{-1}$ (sex-averaged).

3.4 Calculating Lifetime Attributable Risk

As in BEIR VII, lifetime attributable risk (LAR) is our primary risk measure. As discussed in Section 3.2, separate evaluations of LAR were made for most cancer sites using both an excess absolute risk (EAR) model and an excess relative risk (ERR) model. For a person exposed to dose (d) at age (e), the LAR is:

$$LAR(d, e) = \int_{e+L}^{110} M(d, e, a) \cdot S(a) / S(e) da, \quad (3-11)$$

where $M(d, e, a)$ is the excess absolute risk at attained age a from an exposure at age e , $S(a)$ is the probability of surviving to age a , and L is the latency period (2 y for leukemia, 5 y for solid cancers). (Note: In Eq. 3-11 and subsequent equations, dependence of these quantities on gender is to be understood). The LAR approximates the probability of a premature cancer death from radiation exposure and can be most easily thought of as weighted sums (over attained ages a up to 110) of the age specific excess probabilities of radiation-induced cancer incidence or death, $M(d, e, a)$.

For any set of LAR calculations (Eq. 3-11), the quantities $M(d, e, a)$ were obtained using either an EAR or ERR model. For cancer incidence, these were calculated using either:

$$M_I(d, e, a) = EAR_I(d, e, a) \quad (\text{EAR model}) \quad (3-12)$$

or
$$M_I(d, e, a) = ERR_I(d, e, a) \cdot \lambda_I(a) \quad (\text{ERR model}) \quad (3-13)$$

where $\lambda_I(a)$ is the U.S. baseline cancer incidence rate at age a . Datasets used for the baseline incidence rates are described in Section 3.8.

For mortality, the approach is very similar, but adjustments needed to be made to the equations since both ERR and EAR models were derived using incidence data. In BEIR VII, it was assumed that the age-specific ERR is the same for both incidence and mortality, and the ERR model-based excess risks were calculated using:

$$M_M(d, e, a) = ERR_I(d, e, a) \cdot \lambda_M(a). \quad (3-14)$$

Here, the subscripts M and I denote mortality and incidence. For EAR models, BEIR VII used essentially the same approach by assuming:

$$M_M(d, e, a) = \frac{EAR_I(d, e, a)}{\lambda_I(a)} \lambda_M(a). \quad (3-15)$$

Note that in Eq. 3-15, the ratio of the age-specific EAR to the incidence rate is the ERR for incidence that would be derived from the EAR model. Eq. 3-14 was used for all cancer sites and Eq. 3-15 for all sites except breast cancer. A description of the approach for estimating breast cancer mortality risk, and its rationale, is given in Section 3.10.

The LAR for a population is calculated as a weighted average of the age-at-exposure specific LAR. The weights are proportional to the number of people, $N(e)$, who would be exposed at age e . The population-averaged LAR is given by:

$$LAR(d, pop) = \frac{1}{N^*} \int_0^{110-L} N(e) \cdot LAR(d, e) \cdot de. \quad (3-16)$$

For the BEIR VII approach, $N(e)$ is the number of people, based on census data, in the U.S. population at age e for a reference year (1999 in BEIR VII), and N^* is the total number summed over all ages. In contrast, for our primary projection, we used a hypothetical stationary population for which $N(e)$ is proportional to $S(e)$, based on observed 2000 mortality rates. In this case,

$$LAR(d, stationary) = \frac{\int_0^{110-L} S(e) \cdot LAR(d, e) \cdot de}{\int_0^{110-L} S(e) de} \quad (3-17)$$

Eq. 3-17 represents the radiogenic risk per person-Gy from a lifetime chronic exposure. For stationary populations, Eq. 3-17 is equivalent to Eq. 3-16, so it also represents the (average) radiogenic risk for a stationary population for an acute exposure. Equation 3-16 is only valid for projecting risks from chronic exposures if one can assume no appreciable changes in future mortality rates.

3.5 Dose and Dose Rate Adjustment Factor

To project risk at low or chronic doses of low-LET IR, the BEIR VII Committee recommended the application of a Dose and Dose Rate Effectiveness Factor (DDREF), as described in Section 2.1.4. Effectively, this assumes that at high acute doses, the risk is given by a linear-quadratic (LQ) expression, $\alpha_1 D + \alpha_2 D^2$, whereas at low doses and dose rates, the risk is simply $\alpha_1 D$.

In the case of leukemia, LSS data shows upward curvature with increasing dose. The BEIR VII fit to the LQ model yielded a value of $\theta = \alpha_2 / \alpha_1 = 0.88 \text{ Sv}^{-1}$.

For solid tumors, the upward curvature in the LSS data appears to be lower and is not statistically significant (i.e., θ is not significantly different from 0). While BEIR VII did not explicitly recommend a LQ model for solid cancer risk, it nevertheless concluded that some reduction in risk at low doses and dose rates was warranted. It adopted a Bayesian approach, developing separate estimates of the DDREF from radiobiological data and a statistical analysis of the LSS data. The estimate for the DDREF obtained in this way was 1.5, somewhat lower than values that had been commonly cited in the past. The BEIR VII Report notes that the discrepancy can largely be attributed to the fact that the DDREF is dependent on the reference acute dose from which one is extrapolating. According to BEIR VII, the appropriate dose should be about 1 Sv because data centered at about this value drives the LSS analysis. In contrast, much of the radiobiological data refers to effects observed at somewhat higher doses, for which the DDREF would be higher. Assuming that the extrapolation is indeed from an acute dose of 1 Sv, the DDREF of 1.5 corresponds to a LQ model in which $\theta = 0.5 \text{ Sv}^{-1}$.

3.6 EAR and ERR LAR Projections for Cancer Incidence

EAR and ERR model-based LAR projections for a stationary population based on 2000 mortality data are given in bold typeface in Table 3-4. These are compared to EAR and ERR projections based on census data, with weights

proportional to the number of people of each age in the year 2000. The results indicate that our primary risk projections are about 5-10% lower than they would be if based on a census population. Results in Table 3-4 reflect the DDREF adjustment of 1.5 for all cancer sites except leukemia.

Table 3-4: EAR and ERR model projections of LAR¹ for a stationary population derived from 2000 decennial lifetables (Arias 2008) or a population based on 2000 census data (NCHS 2004)

		Risk Model Population Weighting			
Cancer site	Sex	ERR Projection		EAR Projection	
		Stationary	Census	Stationary	Census
Stomach	M	15	16	171	184
	F	20	21	204	217
Colon	M	160	171	112	120
	F	104	110	67	71
Liver	M	17	19	92	98
	F	7	8	53	56
Lung	M	154	165	120	126
	F	482	517	233	244
Breast	F	Not used	Not used	281	308
Prostate	M	125	135	4	4
Uterus	F	11	12	50	53
Ovary	F	34	37	29	31
Bladder	M	107	114	75	79
	F	105	111	63	66
Thyroid	M	22	24	No model	No model
	F	110	120	No model	No model
Residual	M	229	250	191	205
	F	252	272	181	193
Kidney	M	26	28	26	28
	F	24	26	19	20
Bone	M	2	2	2	2
	F	2	2	2	2
Leukemia	M	109	109	53	57
	F	87	88	32	34
Skin	M	1100	1150	No model	No model
	F	637	663	No model	No model

¹ Number of cases per 10,000 person-Gy.

3.7 ERR and EAR Projections for Cancer Mortality

We adopt the BEIR VII approach for ERR and EAR projections of LAR for mortality for all cancer sites except breast cancer. As noted previously, for its ERR model-based projection, BEIR VII used:

$$M_M(d, e, a) = ERR_I(d, e, a) \cdot \lambda_M(a), \quad (3-14)$$

and for its EAR based projections,

$$M_M(d, e, a) = \left[\frac{EAR_I(d, e, a)}{\lambda_I(a)} \right] \lambda_M(a) . \quad (3-15)$$

In Eq. 3-15, the ratio in square brackets is equal to the ERR for incidence that would be calculated using the EAR model. In both Eq. 3-14 and 3-15, the BEIR VII approach assumes that the ERR for incidence and mortality are equal. However, this ignores the “lag” between incidence and mortality, which could lead to bias in the estimate of mortality risk in at least two different ways.

First, there would be a corresponding lag between the ERR for incidence and mortality, which might result in an underestimate of mortality risk. For purposes of illustration, suppose that (a) a particular cancer is either cured without any potential life-shortening effects or results in death exactly 10 y after diagnosis and (b) survival does not depend on whether or not it was radiation-induced. Then,

$$ERR_M(e, a) = ERR_I(e, a - 10) \geq ERR_I(e, a).$$

The relationship would also hold for the EAR if the baseline cancer rate has the same age-dependence for A-bomb survivors as for the U.S. population.

Second, since current cancer deaths often occur because of cancers that developed years ago, application of the EAR-based ERR for incidence can result in a substantial bias due to birth cohort effects. If age-specific incidence rates increase (decrease) over time, the denominator in Eq. 3-15 would be too large (small). This could result in an underestimate (overestimate) of the LAR.

The BEIR VII approach is reasonable for most cancers, because the time between diagnosis and a resulting cancer death is typically short. An exception is breast cancer, for which our approach is presented in Section 3.10.

Results of LAR calculations using the BEIR VII approach are given in Table 3-5. Although not shown, LAR for mortality tends to be about 5% larger for census-based weights than for weights based on a stationary population.

Mortality and incidence data used for the calculations are described in the next section.

Table 3-5: Age-averaged LAR¹ for solid cancer mortality based on a stationary population (Arias 2008). Except for skin and bone cancers, projections are based on BEIR VII risk models.

Cancer Site	Sex	Risk Model	
		ERR	EAR
Stomach	M	8	87
	F	11	111
Colon	M	75	52
	F	46	30
Liver	M	13	75
	F	7	47
Lung	M	142	113
	F	385	199
Breast	F	Not used	121 ²
Prostate	M	20	0.8
Uterus	F	2	15
Ovary	F	22	22
Bladder	M	21	19
	F	28	22
Thyroid	M	3	No model
	F	8	No model
Residual	M	94	104
	F	106	105
Kidney	M	8	10
	F	7	7
Bone	M	No model	0.7
	F	No model	0.7
Leukemia	M	80	32
	F	64	20
Skin	M	0.3	Not used
	F	0.2	Not used

¹ Cases per 10,000 person-Gy

² See Section 3.10

3.8 U.S. Baseline and Census Data

Cancer specific incidence and mortality rates are based on the Surveillance, Epidemiology, and End Results (SEER) program of the National Cancer Institute (NCI). Begun in the early 1970s, SEER collects data from several, mostly statewide and metropolitan, cancer registries within the U.S. Rates for this report are calculated using SEER-Stat and the 1975-2005 SEER public-use data (SEER 2007a,b) available from the SEER website (<http://seer.cancer.gov>). The dataset is structured to represent two notable expansions in the SEER program: from 9 registries to 13 registries (SEER 13) in the early 1990's and most recently to 17 registries (SEER 17). For this report, incidence rates are averages of SEER 13 data for the years 1998-2000 and SEER 17 data for the years 2000-2002. This contrasts with BEIR VII, which used (a previous version) of public-use SEER 13 data for the years 1995-99.

SEER regularly revises its statistics on baseline rates, and the baseline rates used for our final risk assessment will likely be based on SEER statistics for the year 2000 that are not yet available. For example, it is anticipated that the denominator (person years at risk) for future versions of the SEER cancer data will be derived using 2000 decennial census results.

SEER areas currently comprise about 26% of the U.S. population and are not a random sample of areas within the U.S. Nevertheless the cancer rates observed in the combined SEER areas are thought to be reasonably similar to rates for the U.S. population.

Finally, 2000 decennial lifetables (Arias 2008) were used instead of 1999 tables as in BEIR VII. Baseline lifetime risk estimates of cancer incidence and mortality for a stationary population based on these data are given in Table 3-6.

Table 3-6: Baseline lifetime risk estimates of cancer incidence and mortality¹

Cancer Site	Incidence		Mortality	
	Male	Female	Male	Female
Stomach	1160	731	600	406
Colon	4220	4360	2000	1970
Liver	852	416	634	368
Lung	7910	6080	7340	4900
Breast	0	13800	0	2990
Prostate	17100	0	2980	0
Uterus	0	3350	0	772
Ovary	0	1500	0	1040
Bladder	3560	1150	738	319
Thyroid	323	909	43	60
Residual	11500	8580	6060	4760
Kidney	1550	916	576	340
Solid	48200	41800	21000	17900
Leukemia	974	752	732	568
Skin	(38300) ²	(22700) ²	12	7
All	49200	42600	21700	18500

¹ Estimated cancer cases or deaths in population of 100,000

² Not included in all

3.9 Combining Results from ERR and EAR Models

3.9.1 BEIR VII Approach. BEIR VII calculates LAR values separately based on preferred EAR and ERR models and then combines results using a weighted geometric mean. More specifically,

$$LAR^{(B7)} = (LAR^{(R)})^{w^*} (LAR^{(A)})^{1-w^*} \quad (3-16)$$

with weight (w^*) – based on results from the ERR model – depending on cancer site. If the weight (w^*) equals 0.5, a simple GM would be calculated. Instead for most cancer sites, BEIR VII recommended a weight (w^*) equal to 0.7 – placing somewhat more emphasis on results from ERR models. (A notable exception is lung cancer, for which the EAR model is given more weight, reflecting near additivity between smoking and gamma radiation in the A-bomb survivor data.)

A problem with the BEIR VII method for averaging the EAR and ERR projections is that the GM is not additive in the sense that the GM of two risk projections for the combined effect of separate exposures is generally not equal to the sum of the GM projections for the exposures. We circumvent this problem by first calculating the weighted GM of the EAR for the two projection models, for

each age at exposure and attained age. Then, results can be integrated to obtain the risk from chronic lifetime exposure.

3.92 EPA Approach. We calculate the combined age-specific risk (at high dose rates) according to:

$$M^{(EPA)}(d, e, a) = [M^{(A)}(d, e, a)]^{w^*} [M^{(R)}(d, e, a)]^{1-w^*}, \quad (3-17)$$

with the LAR at exposure age e calculated as before:

$$LAR(d, e) = \int_{e+L}^{110} M^{(EPA)}(d, e, a) \cdot S(a) / S(e) da. \quad (3-18)$$

In Eq. 3-17, $M^{(A)}$ and $M^{(R)}$ represent the age-specific EAR derived from the EAR and ERR models, respectively; e.g. for incidence: $M_I^{(A)}(d, e, a) = EAR_I(e, a)d$, and $M_I^{(R)}(d, e, a) = ERR_I(e, a)d \cdot \lambda_I(a)$. The difference from the BEIR VII approach is that the risk models are combined **before** integrating the expression in Eq. 3-18 to obtain the LAR.

Results from the two methods of combining results from EAR and ERR models, BEIR VII and the EPA approach, are compared for selected sites in Table 3-7. Of the two methods, the BEIR VII approach yields larger LAR projections for cancer incidence. However, for all sites except for those in the residual category, results from the two methods differ by less than 10%. For all sites combined other than skin cancer, the difference is 5% for males, and 3% for females.

Table 3-7: EPA and BEIR VII Methods for Combining EAR and ERR LAR incidence projections¹ for selected sites

Cancer Site	Sex	ERR Projection (A)	EAR Projection (B)	EPA Projection (C)	BEIR VII Approach² (D)	Ratio: D/C
Stomach	Male	15	171	31	31	1.00
	Female	20	204	40	40	1.00
Colon	Male	160	112	142	144	1.01
	Female	104	67	90	91	1.01
Lung	Male	154	120	125	129	1.03
	Female	482	233	272	290	1.07
Residual	Male	228	191	194	216	1.11
	Female	252	181	201	228	1.14
Leukemia	Male	109	53	81	88	1.08
	Female	87	32	60	64	1.06
Total ³	Male			785	826	1.05
	Female			1230	1280	1.04

¹ Cases per 10,000 person-Gy.

² Weighted geometric mean of the ERR and EAR projections

³ Sum of projections for all cancer sites. Excludes non-fatal skin cancers.

3.9.3 Should Risk Models Be Combined Using a Weighted GM?

EAR and ERR model excess rates were combined here using a weighted GM. An alternative approach would be to use a weighted arithmetic mean. Under the arithmetic mean approach, the (nominal) combined age specific risk projections are calculated using:

$$M^{(Arith)}(d, e, a) = w^* [M^{(R)}(d, e, a)] + (1 - w^*) [M^{(A)}(d, e, a)]. \quad (3-19)$$

(In subsequent equations, the notation (d, e, a) is dropped). This approach would be appropriate, if for example, the age-specific excess risks for the U.S. can be approximated as a weighted arithmetic average of the relative risk and absolute risk models, a subjective probability distribution might be assigned to the weight (w), and the expected value of the probability distribution is the BEIR VII nominal value ($E[w] = w^*$). The remainder of this section describes how subjective probability distributions might be assigned, and compares our results to what the results would have been using the weighted arithmetic mean approach.

Let us assume there is an (unknown) parameter (w), such that the (true) excess risk $M^{(true)}$ in the U.S. population is given by:

$$M^{(true)} = w M^{(R)} + (1 - w) M^{(A)}. \quad (3-20)$$

It follows from Eq. 3-20 that:

$$w = \frac{M^{(true)} - M^{(A)}}{M^{(R)} - M^{(A)}}, \quad (3-21)$$

and if, $0 \leq w \leq 1$, then $M^{(A)} \leq M^{(true)} \leq M^{(R)}$. A subjective probability distribution might be then assigned to the parameter (w) to reflect one's state of knowledge about the relationship between $M^{(true)}$, $M^{(A)}$ and $M^{(R)}$. For example, if one believes that either the ERR or EAR model is correct **AND** each model is equally likely, then one would assign subjective probabilities of 0.5 to the corresponding values for w :

$$P(w = 0) = 0.5; P(w=1) = 0.5$$

Alternatively, if the ERR model is more likely than the EAR model, a larger probability would be assigned to the former: e.g.,

$$P(w = 0) = 0.3; P(w=1) = 0.7.$$

On the other hand, $M^{(true)}$ may actually be intermediate between the excess rates calculated using the EAR and ERR models. If any such value is "equally likely", then the uniform distribution $U(0,1)$ might be assigned to the parameter w . However, if the excess rates are more likely to be close to the rates predicted by,

say, some type of average of the two risk models, then other choices, such as a trapezoidal distribution, $Tr(a,b,c,d)$, might be more appropriate (see Figure 3-4).

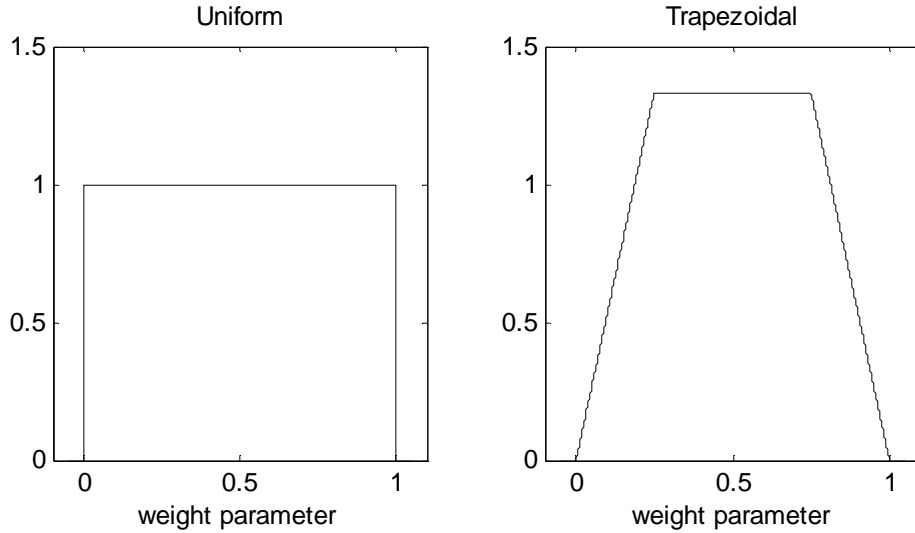


Figure 3-4: Examples of uniform, $U(0,1)$ and trapezoidal distributions, $Tr(0, 0.25, .75, 1.0)$, which might be used for the risk transport weight parameter. Probabilities for the weight parameter are equal to areas under the curve.

A fundamental problem with assigning subjective distributions is that there is very rarely a unique subjective distribution which best describes what might be agreed upon for a parameter. In particular, there is no unique way to define what is meant by statements such as “any value in the interval $(M^{(A)}, M^{(R)})$ is equally likely”. For example, if $M^{(A)} < M^{(R)}$, two possibilities are:

a) $M^{(true)}$ is uniformly distributed:

$$M^{(true)} \sim U(M^{(A)}, M^{(R)}) \quad (3-22)$$

b) $\log(M^{(true)})$ is uniformly distributed:

$$\log(M^{(true)}) \sim U(\log(M^{(A)}), \log(M^{(R)})) \quad (3-23)$$

In the latter case, one might re-parameterize Eq. 3-20 as:

$$M^{(true)} = \exp[w^{(\log)} \log(M^{(R)}) + (1 - w^{(\log)}) \log(M^{(A)})]. \quad (3-24)$$

For this parameterization, note that:

$$w^{(\log)} = \frac{\log(M^{(true)}) - \log(M^{(A)})}{\log(M^{(R)}) - \log(M^{(A)})} \quad (3-25)$$

To illustrate the difference between the two parameterizations, assume that for a hypothetical site $M^{(A)} = 20$, $M^{(R)} = 80$, and $M^{(true)} = 40$. From Eq. 3-21, w

= 1/3, whereas from Eq. 3-25, $w^{(\log)} = 0.5$. The interpretation is that on the original (non-transformed scale, the risk ($M^{(true)}$) lies one-third of the way between the EAR and ERR model risk projections, whereas on the logarithmic scale, $M^{(true)}$ is halfway between the two “extremes”.

The arithmetic mean approach for combining results from the two projection methods (Eq. 3-19) is most easily understood using the parameterization in Eq. 3-20. Note that for any subjective probability distribution for the parameter w ,

$$E[M^{(true)}] = E[w] M^{(R)} + (1 - E[w]) M^{(A)} . \quad (3-26)$$

It follows that, under this parameterization, if the nominal weight parameter is equal to its expected value, $E[w]$, the resulting arithmetic mean is unbiased with respect to the subjective distribution assigned to w . However, this argument does not work for the parameterization in Eq. 3-24.

It is somewhat more difficult to make the same type of argument for the GM approach used in BEIR VII. Even if one accepts the parameterization given in Eq. 3-24 and assigns a subjective distribution to $w^{(\log)}$, it can be easily shown that:

$$E[M^{(true)}] \geq \exp[E(w^{(\log)}) \log(M^{(R)}) + (1 - E(w^{(\log)})) \log(M^{(A)})] \quad (3-27)$$

Thus, if the nominal weights are unbiased “estimates” of the parameters ($w^{(\log)}$), the weighted GM approach will result in projections that tend to underestimate risks to the U.S. population. On the other hand, the weighted GM approach would result in very reasonable projections with respect to subjective distributions for $w^{(\log)}$, for which probabilities are concentrated around the nominal (BEIR VII) weights (w^*). With respect to some of these distributions, the weighted arithmetic mean can result in substantial bias.

In general, the weighted arithmetic mean approach (Eq. 3-19) will always result in larger LAR projections than our approach based on the GM. However, as can be seen in Table 3-8, the difference is substantial only for sites such as stomach, liver, prostate, and uterine cancers, for which the LAR projection is sensitive to the model type (ERR vs. EAR). For all cancers combined (excluding non-fatal skin cancers), use of the weighted arithmetic mean would result in a LAR projection about 11% (females) or 17% (males) greater than our projection.

Table 3-8: Comparison of EPA and weighted arithmetic mean method for combining EAR and ERR LAR projections for incidence¹

Cancer Site	Sex	ERR Projection (A)	EAR Projection (B)	EPA Projection (C)	Weighted Arithmetic Mean of A and B: (D)	Ratio: D/C
Stomach	M	15	171	31	62	2.01
	F	20	204	40	75	1.90
Colon	M	160	112	142	146	1.03
	F	104	67	90	93	1.03
Liver	M	17	92	28	40	1.45
	F	7	53	13	21	1.60
Lung	M	154	120	125	130	1.04
	F	482	233	272	308	1.13
Prostate	M	125	4	42	89	2.10
Uterus	F	11	50	17	23	1.36
Ovary	F	34	29	32	33	1.03
Bladder	M	107	75	94	97	1.04
	F	105	63	87	93	1.06
Residual	M	228	191	194	217	1.12
	F	252	181	201	231	1.15
Kidney	M	26	26	24	26	1.05
	F	24	19	20	22	1.10
Leukemia	M	109	53	81	92	1.13
	F	87	32	60	70	1.16
Total (excluding skin)	M			785	921	1.17
	F			1230	1361	1.11

¹ Cases per 10,000 person-Gy.

It is unclear which of the two commonly used projection methods would be more appropriate. The weighted GM (BEIR VII) approach yields projections which *might* be substantially biased with respect to “preferred” subjective probability distribution for either $w^{(\log)}$ or w for sites such as stomach cancer, yet it is difficult to ascertain how large the bias might be. A crude indication is given by the results in Table 3-8, which suggest that the absolute relative bias of the weighted GM might be as great as 50% for stomach cancer, but much smaller for most other sites. The arithmetic mean approach might also be biased, depending on what type of subjective probability distribution might be appropriate: e.g., whether the distribution is defined with respect to $w^{(\log)}$ or w .

There is no obvious scientific basis for choosing an appropriate parameterization and/or a distribution for the weight parameter. For example, BEIR VII applied the Moolgavkar-Knudson two-stage clonal expansion model to argue that, for many types of cancer, a transportation model should place greater “weight” on the ERR model over one based on absolute risk. However, BEIR VII did not provide any rationale for the type of parameterization to be used or any explicit guidance as to how the weight parameter might be defined or interpreted.

3.10 Calculating Radiogenic Breast Cancer Mortality Risk

This section details our method for calculating radiogenic breast cancer mortality risk and compares results with calculations based on the BEIR VII method.

Let $M_I(d, e, a_I)$ denote the EAR for incidence at attained age a_I from an exposure at age e . The density function for a radiogenic cancer at a_I would be:

$$f_{d,e}(a_I) = M(d, e, a_I) S(a_I) / S(e). \quad (3-28)$$

For the cancer to result in a death at age $a_M > a_I$, the patient would have to survive the interval (a_I, a_M) , and then die from the cancer at age a_I . This and the concept of the relative survival rate form the basis for the method. The relative survival rate for a breast cancer patient would be the ratio of the survival rate for the patient divided by the expected survival rate (without breast cancer). Assume the relative survival depends only on the length of the time interval and the age of diagnosis. Let $t = a_M - a_I$ and $R(t, a_I)$ be the relative survival function. Then the probability of survival with breast cancer for the interval (a_I, a_M) is:

$$S(a) / S(a_I) R(t, a_I). \quad (3-29)$$

Suppose the breast cancer mortality rate (h) among those with breast cancer depends on the age of diagnosis, but does not depend on other factors such as a) whether the cancer is radiogenic, or b) attained age. Then the density function for age of a radiogenic breast cancer death can be shown to equal:

$$f_{d,e}(a_M) = \int_{e+L}^{a_M} h(a_I) M_I(d, e, a_I) S(a) / S(a_I) R(t, a_I) da_I. \quad (3-30)$$

The LAR for breast cancer mortality for an exposure at age e is:

$$LAR(d, e) = \int_{e+L}^{110} f_{d,e}(a_M) da_M, \quad (3-31)$$

and Eq. 3-17 is applied as before to calculate the LAR for the U.S. population.

$$LAR(d, stationary) = \frac{\int_0^{110-L} S(e) \cdot LAR(d, e) \cdot de}{\int_0^{110-L} S(e) de} \quad (3-17)$$

For these calculations, we used the 5-y relative survival rates given in Table 3-9 (Ries and Eisner, 2003) and assumed that breast cancer mortality rates (for those with breast cancer) depend only on age at diagnosis and are equal to:

$$h(a_t) = -(0.2) \log R(5, a_t) \quad (3-32)$$

It should be noted that results from several studies indicate that, for most stages, breast cancer mortality rates are not highly dependent on time since diagnosis – at least for the first 10 years (Bland et al. 1998, Cronin et al., 2003).

Based on the method just outlined, the LAR for breast cancer mortality is $1.21 \times 10^{-2} \text{ Gy}^{-1}$. This is about 30% larger than what would be calculated using the methods in BEIR VII (see Section 3.7).

Much of the discrepancy between the two sets of results seems to be a consequence of observed increases in breast cancer incidence rates and declines in mortality rates. From 1980 to 2000, age-averaged breast cancer incidence rates (per 100,000 women) increased by about 35% (102.2 to 136.0), whereas the mortality rates declined by about 15% (31.7 to 26.6), (Ries, et al. 2008).

Table 3-9: Female breast cancer cases and 5-y relative survival rates by age for 12 SEER areas, 1988-2001, adapted from Table 13.2 in Ries and Eisner (2003)

Age (y)	Cases	5-y RSR (%)
20-34	6,802	77.8
35-39	12,827	83.5
40-44	24,914	88.0
45-49	33,784	89.5
50-54	34,868	89.5
55-59	32,701	89.6
60-64	32,680	90.1
65-69	34,435	91.0
70-74	32,686	91.8
75-79	27,134	91.4
80-84	17,475	90.7
85+	12,457	86.6
Total	302,763	89.3

To understand the effect these trends in incidence and mortality have on the BEIR VII LAR projection for mortality, recall the BEIR VII formula:

$$M(d,e,a) = EAR(d,e,a) \frac{\lambda_M(a)}{\lambda_I(a)} .$$

The underlying assumptions are that a) the absolute risk of radiogenic cancer death from an exposure at age e is equal to the absolute risk of a radiation-induced cancer multiplied by a lethality ratio (that depends on attained age), and b) lethality ratios can be approximated by current mortality to incidence rate ratios. However, since the time between breast cancer diagnosis and death is relatively long, lethality rates might be better approximated by comparing current mortality rates to incidence rates observed for (much) earlier time periods. If, as data indicate, current incidence rates are considerably higher than past incidence rates, the BEIR VII denominator is too large, and the estimated lethality ratio is too small. This would result in a downward bias in the BEIR VII projection for mortality.

Our projection has limitations which must be noted. First, its validity depends on the extent to which estimates of relative survival functions can be used to approximate mortality rates from breast cancer for people with breast cancer. Long-term survival rates for breast cancer patients are desirable for constructing valid estimates for this approach, but since these survival rates can

change rapidly, there is considerable uncertainty for extrapolation of rates for periods beyond 5 to 10 y. Finally, reduced expected survival among breast cancer patients may be partly attributable to causes other than breast cancer. For example, if some breast cancers are smoking-related, breast cancer patients as a group may be at greater risk of dying from lung cancer.

3.11 LAR by Age at Exposure

Sex-averaged LAR for incidence and mortality by age-at-exposure are plotted in Figures 3-6 and 3-7 for selected cancer sites. More specifically, for both males and females, LAR are calculated as described in Section 3.9 according to:

$$LAR(d, e) = \int_{e+L}^{110} M^{(EPA)}(d, e, a) \cdot S(a) / S(e) da, \quad (3-18)$$

where

$$M^{(EPA)}(d, e, a) = [M^{(A)}(d, e, a)]^{w^*} [M^{(R)}(d, e, a)]^{1-w^*}, \quad (3-17)$$

and sex-averaged LAR were calculated using Eq. 3-33:

$$LAR_{AVG}(d, e) = \frac{1.048S_{MALE}(e)LAR_{MALE}(d, e) + S_{FEMALE}(e)LAR_{FEMALE}(d, e)}{1.048S_{MALE} + S_{FEMALE}} \quad (3-33)$$

Figures 3-6 and 3-7 show that, for most cancer sites, the probability of premature cancer (or cancer death) attributable to an acute exposure decreases with age-at-exposure. The notable exception is leukemia mortality, for which the projected LAR increases slightly from birth to about age 60.

For most cancers, the decrease in LAR with age-at-exposure is assumed to be similar to the pattern shown for colon, lung, and bladder cancers: the LAR decreases by a factor of about 2 or more from birth to age 30; it then levels off until about age 50 and then gradually decreases towards 0. During the first 30 y, the decrease in LAR is almost entirely attributable to the exponential decline in modeled age-specific ERR and EAR (in the risk models $\gamma < -0.3$), whereas the decrease in LAR after age 50 is largely attributable to competing risks – as people age, they have an ever-decreasing chance of living long enough to contract a radiation-induced cancer. For breast and thyroid cancers, the modeled age-specific ERR or EAR continue to decrease after age 30, and the LARs do not level off after age 30. In general, the LAR decreases more rapidly for breast, bone, thyroid, and residual cancers than for other sites.

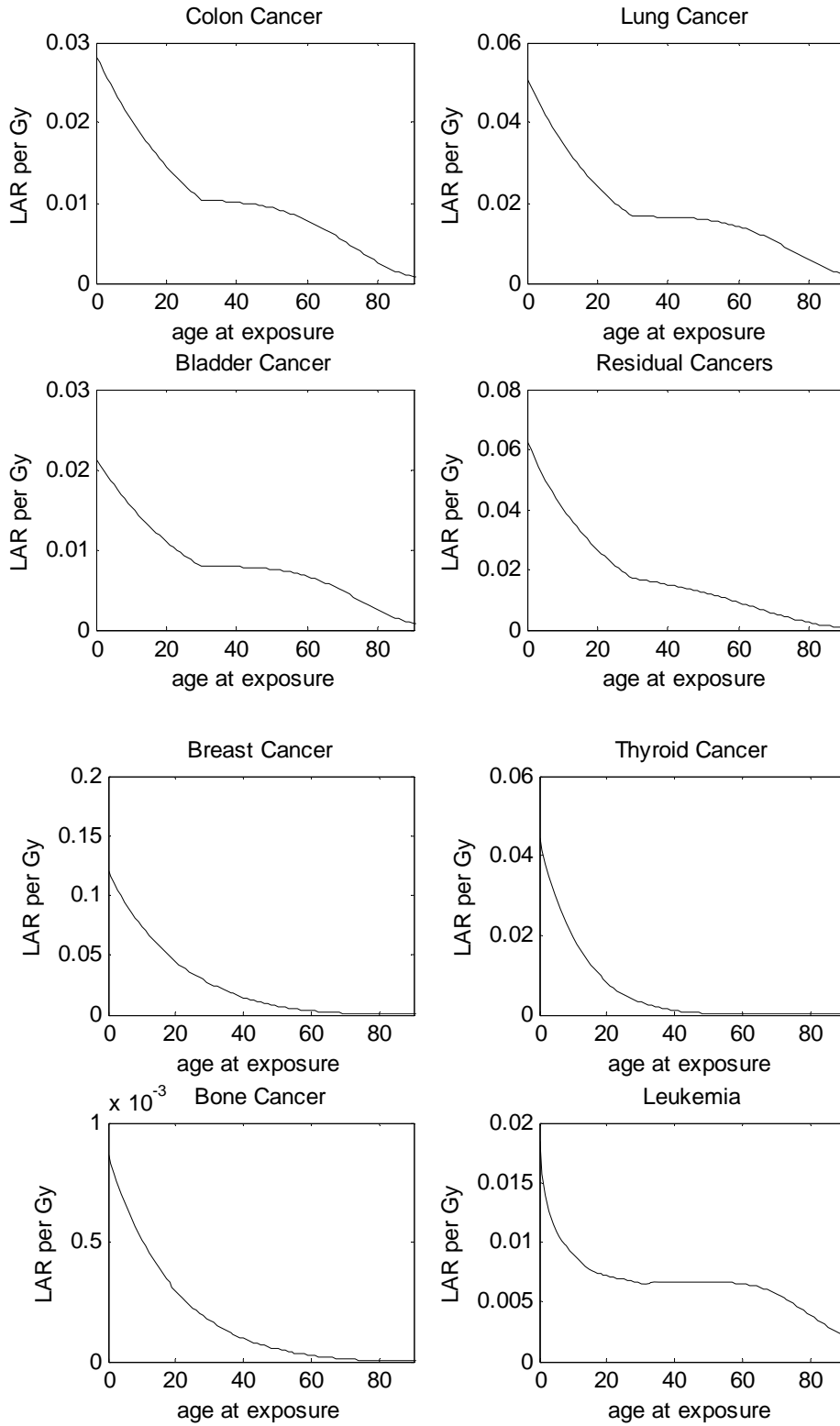


Figure 3-5: Sex-averaged LAR for incidence by age at exposure for selected cancers. A DDREF of 1.5 is used for all solid cancer sites.

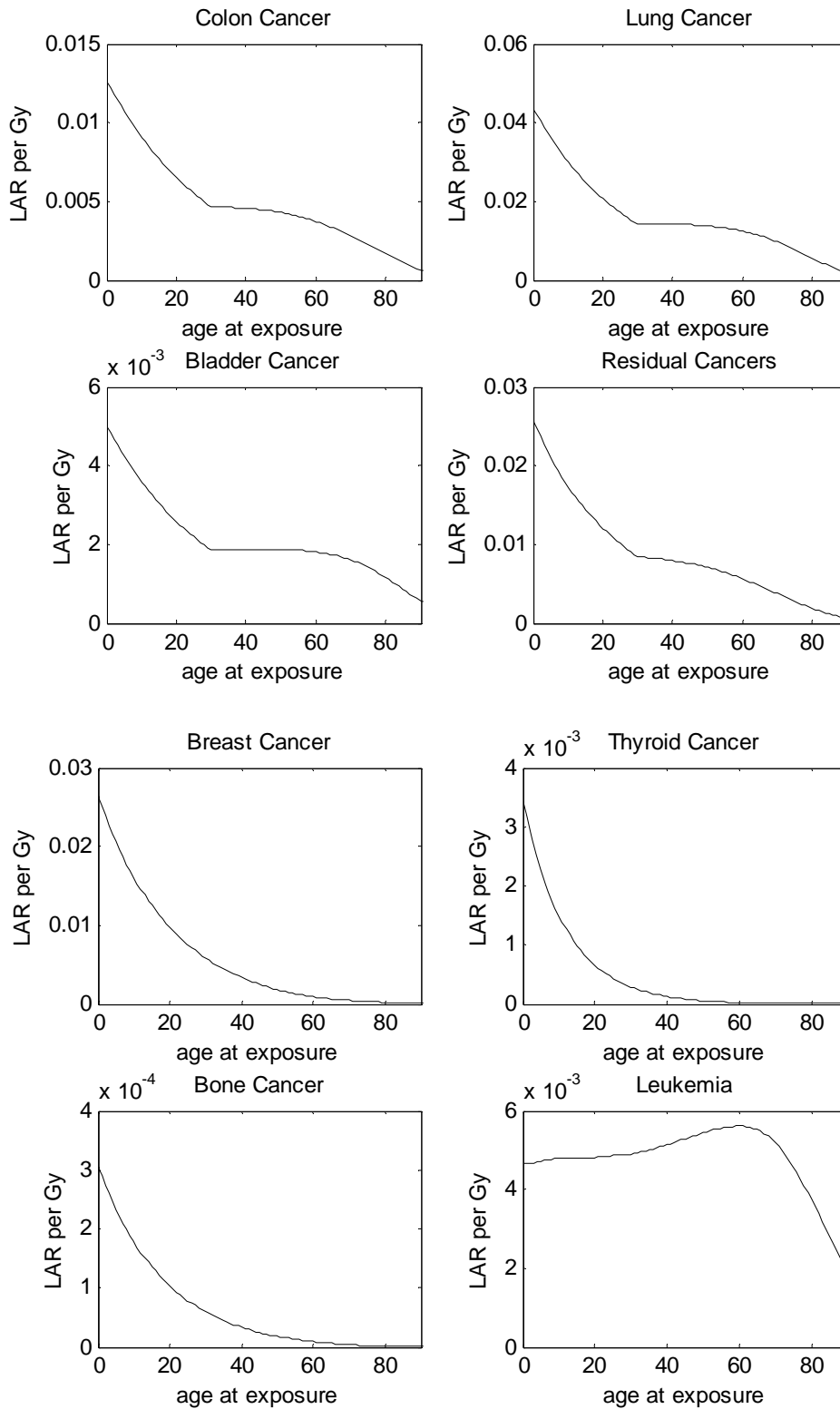


Figure 3-6: Sex-averaged LAR for mortality by age at exposure for selected cancers. A DDREF of 1.5 is used for all solid cancer sites.

Radiogenic risks for childhood exposures are often of special interest. As shown in Figures 3-5 and 3-6, the LAR per unit dose is substantially larger for exposures during childhood (here defined as the time period ending at the 15th birthday) than later on in life. In addition, doses received from ingestion or inhalation are often larger for children than adults. Table 3-10 shows the contribution to the LAR for cancer incidence for exposures before age 15 and compares it to LAR for the entire population (all ages). For uniform, whole body radiation, about 785 radiogenic cancers are expected to occur among U.S. males from a cumulative radiation dose of 10,000 person-Gy. About 313 of the 785 cancers (about 40% of the radiogenic cancers) would occur in males exposed before age 15. For females, about 565 of 1230 cancers (about 45%) would occur among those exposed before age 15. An estimated 145 of 406 cancer deaths (males) and 256 of 628 cancer deaths (females) would be attributable to childhood exposures.

Table 3-10: LAR for cancer incidence¹ for exposures to a stationary U.S. population

Cancer site	LAR		Contribution from exposures for ages < 15	
	Males	Females	Males	Females
Stomach	31	40	12	15
Colon	142	90	54	33
Liver	28	13	11	5
Lung	125	272	48	102
Breast	0	281	0	160
Prostate	42	0	16	0
Uterus	0	17	0	7
Ovary	0	32	0	13
Bladder	94	87	34	31
Thyroid	22	110	16	83
Residual	194	201	89	89
Kidney	24	20	10	8
Bone	2	2	1	1
Solid ²	703	1170	289	547
Leukemia	81	60	24	18
Skin	1100	637	248	137
Total ²	785	1230	313	565

¹ Cases per 10,000 person-Gy.

² Excludes non-fatal skin cancers.

3.12 Summary of Main Results

New EPA LAR projections for incidence are given in Table 3-11. The table also provides 90% uncertainty intervals for the LAR, and – for purposes of comparison – the EPA projections in the current version of FGR 13 (EPA 1999). These intervals were calculated using Bayesian methods, which involved a somewhat complex (Markov Chain) Monte Carlo method for generating site-specific LAR values. This approach allowed for the quantification of uncertainties associated with sources such as: 1) sampling variability, 2) transport of risk estimates from the Japanese A-bomb survivor population, 3) uncertainty associated with the DDREF, and 4) dosimetry errors.

Table 3-11: LAR projections for incidence¹

Cancer Site	New EPA				FGR 13 (1999)	
	Males		Females		Males	Females
	LAR	90% UI	LAR	90% UI		
Stomach	31	(9, 280)	40	(11, 300)	36.1	54.0
Colon	142	(52, 300)	90	(35, 230)	152	225
Liver	28	(9, 150)	13	(5, 120)	19.4	12.3
Lung	125	(47, 310)	272	(120, 710)	81.2	126
Breast	None		281	(160, 490)	None	198
Prostate	42	(0, 520)	—		None	—
Uterus	—		17	(0, 320)	—	None
Ovary	—		32	(12,110)	—	41.7
Bladder	94	(18, 220)	87	(14, 160)	65.5	30.4
Thyroid	22	(6, 73)	110	(32, 370)	20.5	43.8
Residual	194	(100, 600) ²	201	(120, 670) ²	191	229
Kidney	24		20		9.9	6.0
Esophagus	None	None		None	7.7	16.8
Bone	2		2		1.3	1.4
Solid ³	703	(420, 1910)	1170	(770, 2760)	586	983
Leukemia	81	(32, 200)	60	(24, 150)	65.4	47.5
Skin	(1100) ³		(637) ³			
Total ³	785	(510, 2000)	1230	(830, 2830)	651	1030

¹ Cases per 10,000 person-Gy.

² Interval for residual and kidney cancer cases. Residual includes esophageal cancers.

³ Excludes non-fatal skin cancers

For most of the cancer sites, BEIR VII derived parameter estimates for ERR and EAR models based on a statistical analysis of LSS data that was cross-classified by city, sex, dose, and intervals based on age-at-exposure, attained age, and follow-up time. Sampling variability refers to the uncertainty in parameter estimates associated with the variation in the observed numbers of cancer cases or deaths within each of these subgroups. In contrast to BEIR VII, our uncertainty analysis at least partially accounted for the sampling variability associated with risk model parameters for age-at-exposure and attained age. Transport of risk estimate uncertainty refers to uncertainty associated with how to apply the results from the analysis of the Japanese LSS cohort data to the U.S. The ratio of LAR projections based on the EAR model divided by the projection based on the ERR model is a crude indicator of the magnitude of this uncertainty. It follows that “transport” uncertainty is greatest for sites such as stomach and prostate cancer, for which Japanese and U.S. baseline rates are vastly different. A dominant source of uncertainty for all cancers combined is the uncertainty associated with the DDREF. This includes some of the uncertainty associated with the shape of the dose-response function at very low doses. As discussed in Section 4, it does not incorporate uncertainty associated with the validity of the assumption that the linear portion of the dose-response function fitted to the LSS data can be equated to the response that would be observed at lower doses or for chronic exposures. Additional sources of uncertainty, including what is often called model uncertainty, were incorporated by multiplying the randomly generated site-specific LAR values by a random (lognormal) variable. More details are provided in Section 4.

The new EPA risk projection is 785 cancer cases per 10,000 person-Gy for males, and 1230 cancer cases for females. The 90% uncertainty intervals suggest these projections are accurate to within a factor of about 2 or 3. Uncertainties, as measured by the ratio of the upper to lower uncertainty bounds, are greatest for stomach, prostate, uterine, bladder, liver, and thyroid cancers.

For most cancer sites, the new EPA risk projections for incidence are not very different from the risk projections in the current version of FGR 13. Cancer sites for which the relative change from the projected LAR in FGR 13 is greatest include: female colon (↓), female lung (↑), female bladder (↑), female thyroid (↑), and kidney (↑). For both males and females, the LAR for all cancers combined increased by about 20%. The overall increase in LAR is not due to changes in the basic risk models, which in many cases would yield smaller LAR projections than the FGR 13 models if they were applied to comparable mortality and incidence data. Instead the increase is largely attributable to the use of the more recent SEER incidence data as a primary basis for the calculating baseline incidence rates. For FGR 13, probabilities for radiation-induced incidence were derived by applying the inverse of cancer-specific lethality fractions to excess mortality rates. The lifetime probability of getting cancer calculated from the more recent SEER rates is about 40% larger for males and 55% for females than

rates implicit in the FGR 13 calculations. The increase in LAR is also due to a reduction in the nominal DDREF for most cancer sites from 2 to 1.5.

Table 3-12 gives the LAR projections for mortality. The largest relative changes in LAR compared to the projections in FGR 13 were for stomach (↓), female colon (↓), female lung(↑), female thyroid (↑), and female kidney (↑) cancers. In general, the projections were remarkably consistent; e.g., the LAR for all sites combined decreased by about 15% (males) and 10% (females).

Table 3-12: LAR projections for mortality¹

Cancer Site	New EPA		FGR 13	
	Males	Females	Males	Females
Stomach	16	22	32.5	48.6
Colon	66	40	83.8	124
Liver	21	12	18.4	11.7
Lung	117	227	77.1	119
Breast	None	121	None	99.0
Prostate	8	—	None	—
Uterus	—	4	—	None
Ovary	—	22	—	29.2
Bladder	20	25	32.8	15.2
Thyroid	3	8	2.1	4.4
Residual	91	98	135	163
Kidney	8	7	6.4	3.9
Esophagus	None	None	7.3	15.9
Bone	0.7	0.7	0.9	1.0
Solid	350	585	397	636
Leukemia	56	42	64.8	47.1
Skin	0.3	0.2	0.9	1.0
Total	406	628	462	683

¹ Deaths per 10,000 person-Gy

Table 3-13 summarizes the sex-averaged LAR projections for cancer incidence and mortality. Finally, Table 3-14 compares the new EPA LAR projections with projections in BEIR VII. For all cancers combined, the EPA projections are 12% less than the projections in BEIR VII for incidence, 14% less for mortality in males, and 5% less for mortality in females. The difference is

primarily attributable to 1) our use of a stationary population (see Section 3.6) and 2) the age-specific method of combining projections from the ERR and EAR models (see Section 3.9). The decrease in the mortality projection for all female cancer sites is only about 5% because of the larger EPA LAR projection for breast cancer mortality.

Table 3-13: Sex-averaged LAR projections for incidence and mortality¹

Cancer Site	Incidence		Mortality	
	Projection	90% UI	Projection	90% UI
Stomach	35	(11, 290)	19	(6, 150)
Colon	116	(50, 250)	53	(22, 110)
Liver	20	(8, 130)	16	(6, 100)
Lung	199	(93, 490)	172	(78, 430)
Breast ²	142	(80, 250)	61	(34, 110)
Prostate ²	21	(0, 250)	4	(0, 45)
Uterus ²	9	(0, 160)	2	(0, 37)
Ovary ²	16	(6, 54)	11	(4, 38)
Bladder	90	(21, 180)	23	(5, 44)
Thyroid	66	(25, 200)	5	(2, 16)
Residual	197		94	
Kidney	22	(130, 610)	8	(57, 280)
Bone	2		1	
Solid	936	(620, 2270)	468	(290, 1160)
Leukemia	71	(39, 150)	49	(27, 100)
Skin	867	—	0.3	—
Total ³	1010	(700, 2360)	518	(350, 1220)

¹ Deaths per 10,000 person-Gy.

² Sex-averaged results for these cancers are about one-half as large as in Tables 3-11, 3-12.

² Excludes nonfatal skin cancers

Table 3-14: Comparison of EPA and BEIR VII LAR calculations

Site	Sex	Incidence ¹		Mortality ¹	
		EPA	BEIR VII	EPA	BEIR VII
Stomach	M	31	34	16	19
	F	40	43	22	25
Colon	M	142	160	66	76
	F	90	96	40	46
Liver	M	28	27	21	20
	F	13	12	12	11
Lung	M	125	140	117	140
	F	272	300	227	270
Breast	F	281	310	121	73
Prostate	M	42	44	8	9
Uterus	F	17	20	4	5
Ovary	F	32	40	22	24
Bladder	M	94	98	20	22
	F	87	94	25	28
Thyroid	M	22	21	3	None
	F	110	100	8	None
Residual	M	194	290	91	120
	F	201	290	98	132
Kidney	M	24	None	8	None
	F	20	None	7	None
Bone	M	2	None	1	None
	F	2	None	1	None
Solid cancers	M	703	800	350	410
	F	1170	1310	585	610
Leukemia	M	81	100	56	69
	F	60	72	42	52
Total	M	785	900	406	479
	F	1230	1382	628	662

¹ Cases or deaths per 10,000 person-Gy.

4. Uncertainties in Projections of LAR for Low-LET Radiation

4.1 Introduction

This chapter describes a quantitative uncertainty analysis for the LAR projections given in Section 3. As described elsewhere (e.g., Sinclair 1993, EPA 1999), the uncertainty for each site-specific risk estimate can be treated mathematically as the product of several independent sources of uncertainty. A novel feature of this uncertainty analysis is a Bayesian analysis of site-specific risks using the LSS incidence data which – after application of the life-table calculations described in Chapter 3 – results in simulated values for LAR applicable to the Japanese A-bomb survivor cohort. The Bayesian analysis accounts for sampling variability, but does not account for many other important sources of uncertainty such as those associated with DDREF, risk transport, and dosimetry errors. For each of these other sources, a distribution is assigned to an “uncertainty factor” (EPA 1999, Kocher 2008), which defines “the probability that the assumption employed in the model pertaining to the source of uncertainty either underestimates or overestimates the risk by any specified amount” (EPA 1999). Finally, a joint probability distribution for the combined uncertainty due to all sources is obtained through Monte Carlo techniques.

The Bayesian analysis of the LSS data is described in detail in Section 4.2. For most cancer sites, the risk models used for this analysis are the same ERR risk models which BEIR VII fit to the LSS data. That is, we used the same parameters to describe the dependence of ERR on dose, age-at-exposure and attained age as in BEIR VII. However, there were two important differences between the two approaches. First, BEIR VII used classical statistical methods to derive “best” estimates for these parameters, whereas we assigned (prior) probability distributions to these parameters and then applied information gleaned from the LSS to update these distributions. Second, for most sites our Bayesian analysis placed fewer restrictions on parameters, e.g., the parameters for the dependence on age-at-exposure or attained age.

The Bayesian approach allowed for a relatively straightforward method to generate distributions of values for LAR, which account for sampling variability associated with dose, age-at-exposure, and attained age. Rationale for distributions assigned to uncertainty factors for other sources are described in Section 4.3. The next section (4.4) presents the main results of the quantitative uncertainty analysis; distributions for LAR which reflect the combined uncertainties from these sources are summarized.

A comparison with BEIR VII’s uncertainty analysis is given in Section 4.5. Section 4.5 first outlines the BEIR VII uncertainty analysis and some of its more important limitations. We then compare the BEIR VII distributions for site-specific LAR values to ours.

Finally, conclusions are given in Section 4.6. Foremost among them is that results from the EPA uncertainty analysis should not be over-interpreted. The results presented in Section 4.4 are meant solely as guidance as to the (relative) extent to which “true” site-specific risks for a hypothetical stationary U.S. population might differ from the central estimates derived in Section 3. This is because, it was not always possible to satisfactorily evaluate “biases” associated with sources of uncertainty such as risk transport.

4.2 Uncertainty from Sampling Variability

4.2.1 Bayesian Approach for Most Solid Cancers

For most cancer sites, BEIR VII derived parameter estimates for ERR and EAR models based on a statistical analysis of LSS cancer cases and deaths, which were cross-classified by city, sex, dose, and intervals based on age-at-exposure, attained age, and follow-up time. Sampling variability refers to the uncertainty in parameter estimates associated with the variation in the observed numbers of cancer cases or deaths for each of the sub-categories.

This section describes in detail our Bayesian approach for deriving distributions for LAR for uncertainties associated with sampling variability. Such distributions were derived for all solid cancer sites except breast, thyroid, and bone. (Our treatment of sampling variability for the latter three sites and leukemia is given in Section 4.2.2). Section 4.3 describes how results from the Bayesian analysis were then combined to derive the 90% uncertainty intervals for LAR of cancer incidence presented in Section 4.5.

The approach is based on a Bayesian analysis of LSS incidence data for the follow-up period 1958-1998, which in many ways parallels analyses of LSS incidence data by Preston et al. (2007) and the BEIR VII Committee. In particular, essentially the same data and risk models were used.

Data. The dataset we used is a subset of the incidence data analyzed by Preston et al. (2007). This data can be downloaded from the RERF website at <http://www.rerf.or.jp/library/dle/lssinc07.html> (file lssinc07.csv). The dataset incorporates the latest (DS02) dosimetry and is otherwise essentially the same as the one used for the BEIR VII analysis, in that it excludes the “not-in-city” group (see Preston et al. 2007 for details).

Risk models. For most solid cancer sites, we used the same ERR models BEIR VII used in its analysis of the LSS data, which were described in Section 3.2. That is, for a specific cancer site, the ERR for an atomic bomb survivor at attained age a who was exposed at age e is:

$$ERR(d, s, e, a) = \beta_s d \exp(\gamma e^*)(a/60)^\eta, \quad (4-1)$$

where a and e denote attained age and age-at-exposure, and e^* is the age-at-exposure function, which is set to 0 for ages > 30 . The corresponding cancer rate is:

$$\lambda(d, s, a, b, c) = \lambda_0(s, a, b, c)[1 + ERR(d, s, e, a)] \quad (4.2)$$

Here, $\lambda_0(s, a, b, c)$ denotes the baseline rate, which depends on sex (s), attained age (a), year of birth (b), and city (c).

An important feature of our uncertainty analysis is that the age-at-exposure and attained-age parameter values are allowed to depend on site. Separate sets of these two parameters were used for almost all cancer sites; the only exceptions are cancers of the prostate, ovary, and uterus, for which the ERR was assumed to be independent of both age-at-exposure and attained age. This is the approach adopted by Preston et al. because there were insufficient data on these cancers to provide stable estimates for these parameters or their uncertainties. It should be noted that the uncertainty intervals for these three sites are not meant to adequately account for (all) uncertainties relating to age and temporal dependence in risk.

Baseline cancer rate models. For each cancer site, the same sex-specific parametric models as in Preston et al. are used for the baseline rates $\lambda_0(\cdot)$: “In the most general models, for each sex, the log rate was described using city and exposure status effects together with piecewise quadratic functions of log age joining smoothly at ages 40 and 70 and piecewise quadratic functions of birth year joining smoothly at 1915 (age at exposure 30) and 1895 (age at exposure 50). A smooth piecewise quadratic function of x with join points at x_1 and x_2 can be written as $\beta_0 + \beta_1 x + \beta_2 x^2 + \beta_3 \max(x - x_1, 0)^2 + \beta_4 \max(x - x_2, 0)^2$. This parameterization provides flexible but relatively parsimonious descriptions of the rates.”

Bayes method for simulating LAR. The essential difference between our Bayesian analysis and the analyses by Preston et al. and the BEIR VII Committee, is that prior distributions are assigned to each of the unknown parameters used to define ERR (β_s, γ , and η) and to the baseline cancer rates. In theory, these prior distributions would describe what our state of knowledge about baseline rates and ERR would be without the information from the LSS. We then applied a complex Markov Chain Monte Carlo (MCMC) technique using the software WinBUGS (Lunn et al., 2000) to the LSS data to simulate the ERR parameters. This simulation was done with respect to a (posterior) distribution which reflects information implicit in the prior distribution and information that can be gleaned about these parameters from the LSS. The formulas of Section 3.4 were then applied to the sets of ERR parameters to calculate equally likely values for the population LAR. Each of these LAR values were obtained under

the assumption that the ERR method for risk transport is valid. Section 4.2 describes how we quantified uncertainty relating to risk transport.

Prior distributions. For baseline cancer rate parameters, the priors were normal distributions with mean 0 and very large variances (variance = 1000). This is an example of what are sometimes referred to as non-informative priors. Use of non-informative priors will often yield results similar to what would be obtained from more traditional statistical methods, e.g., maximum likelihood. The priors we assigned to the ERR parameters are discussed next and summarized in Table 4-1.

First, independent U(-1,1) distributions were assigned to site-specific, age-at-exposure parameters for most cancers. That is, in Eq. 3-1, γ is defined separately for most cancer sites, and each of these is assumed to follow an independent uniform distribution. This allows the ERR to be up to 20 times larger (or smaller) at birth than at age 30. As we believe is appropriate, the range of possible values (-1, 1) for the site-specific parameters is considerably wider than BEIR VII's 95% confidence interval for the age-at-exposure parameter for all solid cancers: (-0.51, -0.10). The LSS data are insufficient to evaluate uncertainties associated with age-at-exposure or attained age for prostate, uterine, and ovarian cancers (see Preston et al. 2007). Thus, a constant ERR model was assumed for these three cancers, i.e., $\gamma = 0$ and $\eta = 0$.

Second, for cancers other than prostate, uterine or ovarian, an independent normal distribution with mean -1.4 and variance 2 was assigned to the attained age parameter (η). The distribution has a central value equal to the BEIR VII nominal value and assigns a 95% probability to the interval (-4.2, 1.4). For many cancers, the lower limit (-4.2) corresponds roughly to a constant EAR model.

Third, lognormal distributions were assigned to each of the linear dose-response parameters. For males,

$$\log(\beta_M) \sim N(\mu_M, \tau^2). \quad (4-3)$$

That is, the log-transformed parameters for each cancer site were assumed to have prior distributions with a common (unknown) mean (μ_M) and variance (τ^2). For females, the same type of distribution was used but with a different mean (μ_F). The essentially non-informative priors in Eq. 4-4a-c were then assigned to these unknown means and variances. Although this may seem complicated to some, it is a convenient method for allowing the sharing of information on radiogenic risks among cancer sites. The rationale for this type of approach is given in Pawel et al. (2008).

$$\mu_M \sim N(-1.0,10) \quad (4-4a)$$

$$\mu_F \sim N(-0.7,10) \quad (4-4b)$$

$$1/\tau^2 \sim \text{Gamma}(0.001,0.001) \quad (4-4c)$$

Table 4-1: Prior distribution for ERR model parameters

Cancer Site	Parameter			
	$\log(\beta_M)$	$\log(\beta_F)$	γ	η
Stomach				
Colon				
Liver	$N(\mu_M, \tau^2)$	$N(\mu_F, \tau^2)$	U(-1,1)	N(-1.4,2)
Lung				
Bladder				
Prostate	$N(\mu_M, \tau^2)$	—	0	0
Uterus	—	$N(\mu_F, \tau^2)$	0	0
Ovary	—		0	0
Breast	—	$N(\mu_F, \tau^2)$	U(-1,1)	N(-1.4,2)
Other solid	$N(-1,10)$	$N(-0.7,10)$	U(-1,1)	N(-1.4,2)
All sites	$\mu_M \sim N(-1.0,10), \mu_F \sim N(-0.7,10)$			
	$1/\tau^2 \sim \text{Gamma}(0.001,0.001)$			

4.2.2 Approach for Other Cancers

Cancer sites included here are leukemia, breast, thyroid, and bone. EPA risk models for the latter three are not based exclusively on analyses of the LSS data. We also discuss the approach for uniform whole-body radiation.

Leukemia. We applied, with little modification, the BEIR VII uncertainty intervals for LAR from lifetime exposures at 1 mGy per year (Table 12-7). The 95% CI were (33, 300) $\times 10^{-5}$ excess cases for males and (21, 250) $\times 10^{-5}$ cases for females. We assumed lognormal uncertainty distributions for the LAR with GMs equal to the new nominal EPA estimates of 81 $\times 10^{-4}$ person-Gy (males) and 60 $\times 10^{-4}$ person-Gy (females). The GSDs, derived from the 95% CI in BEIR VII are 1.76 (males) and 1.88 (females). Unlike for other cancer sites, we did not treat uncertainties from other sources separately. This lognormal distribution for leukemia accounts for both sampling and risk transport uncertainties. The BEIR VII intervals account for uncertainties relating to a possible quadratic component in the dose response.

Breast and thyroid cancers. The EPA nominal estimates for these two cancer sites were based on risk models derived from a pooled analysis of data from medical cohorts as well as the LSS. It would thus be inappropriate to base uncertainties on sampling variability for estimates derived solely from the LSS (as we did for almost all other cancer sites). For these two sites, the uncertainty from sampling variability was assumed to be lognormal with GMs equal to nominal EPA estimates presented in Section 3. GSDs were derived from the 95% CI in Table 12-2 of BEIR VII for linear dose response parameters. For breast cancer, the 95% CI for EAR is (6.7, 13.3) per 10^4 PY-Sv (GSD = 1.2). For thyroid cancer, the 95% CI for ERR/Gy is (0.14, 2) for males and (0.28, 3.9) for females, and the corresponding GSDs are both about 2.0.

Bone cancer. The nominal EPA risk model was derived from data on radium dial painters exposed to ^{226}Ra and ^{228}Ra and patients injected with the shorter-lived isotope ^{224}Ra . The risk of bone cancer is a relatively small component of the risk for all cancers from uniform whole-body radiation. Uncertainties for bone cancer are not quantified here, but EPA plans to address this issue when it revises FGR 13.

Uniform whole-body radiation. To quantify uncertainties for the LAR for all cancers from uniform whole-body radiation the simulated site-specific LAR values were summed (over all cancer sites) at each iteration.

4.3 Non-sampling Sources of Uncertainty

A combined non-sampling uncertainty factor was obtained as the product of uncertainty factors generated separately for risk transport, DDREF, and several sources of uncertainty not quantified in BEIR VII. The latter include uncertainties about age and temporal dependencies unrelated to sampling variation, dosimetry errors, diagnostic misclassification, and selection bias. It was concluded that some other sources of uncertainty, such as model mis-specification for the dose-response, could not be credibly quantified. A summary of how each source of uncertainty was treated is given in Table 4-2, followed by more detailed discussions in Sections 4.3.1-4.3.3.

Table 4-2: Non-sampling sources of uncertainty

Source	Distribution
Risk Transport	See Section 4.3.1
DDREF	LN(1.0,1.35)
Age and temporal dependence	LN(1.0, 1.2)
Errors in dosimetry	LN(0.9, 1.16)
Random: linear dose response	LN(1.0, 1.05)
Random: DDREF	LN(0.95, 1.1)
Systematic	LN(1.0, 1.1)
Nominal neutron RBE	LN(0.95, 1.05)
Errors in disease detection/diagnosis	LN(1.1, 1.06)
Selection bias	LN(1.1, 1.1)
Relative effectiveness of X-rays	Not quantified
Model misspecification for dose response	Not quantified
Total for all sources not quantified in BEIR VII	LN(1.09, 1.3)

4.3.1 Risk Transport

For sites other than thyroid, breast, bone, lung, and leukemia independent subjective probability distributions were assigned to $LAR^{(true)}$ as follows:

$$P[LAR^{(true)} = LAR^{(R)}] = 0.35 ; P[LAR^{(true)} = LAR^{(A)}] = 0.15 ;$$

$$LAR \sim U(\min(LAR^{(R)}, LAR^{(A)}), \max(LAR^{(R)}, LAR^{(A)})) \text{ with probability } 0.25$$

$$LAR \sim LU(\min(LAR^{(R)}, LAR^{(A)}), \max(LAR^{(R)}, LAR^{(A)})) \text{ with probability } 0.25$$

If the only source of uncertainty is risk transport, then from this distribution either a) the true value for LAR is equal to the ERR or EAR projection, each with probability 0.5, or b) the distribution is uniform or log-uniform for intermediate values. These uniform and log-uniform distributions and the EPA distribution for intermediate values are illustrated in Figure 4-1 for both stomach and colon cancer. For lung cancer, the only difference is that $P[LAR^{(true)} = LAR^{(R)}] = 0.15$ and $P[LAR^{(true)} = LAR^{(A)}] = 0.35$. These distributions appear reasonable, in that it is arguably equally plausible that, for any site, either the ERR or EAR model would yield a much better approximation to the true LAR than the other, or the LAR “could be anywhere in between the two extremes.” Admittedly, for some

sites, the LAR may not be bounded by the ERR and EAR projections. However, there seems to be no good way to determine how far the probability distribution should be extended to account for this.

For bone, thyroid, and breast cancer, no risk transport uncertainty was assumed. For the latter two cancer sites, note that the BEIR VII projections were based on analyses of data from non-Japanese populations, as well as from the LSS cohort.

For leukemia, we applied, with little modification, uncertainty intervals given in BEIR VII (see Sections 4.2.2 and 4.5.1). Probabilities of 0.7 and 0.3 were assigned to ERR and EAR models, respectively.

Since, the Bayesian analysis for sampling variability generated values of LAR from the ERR model, the uncertainty factor is: $\frac{LAR^{(true)}}{LAR^{(R)}}$.

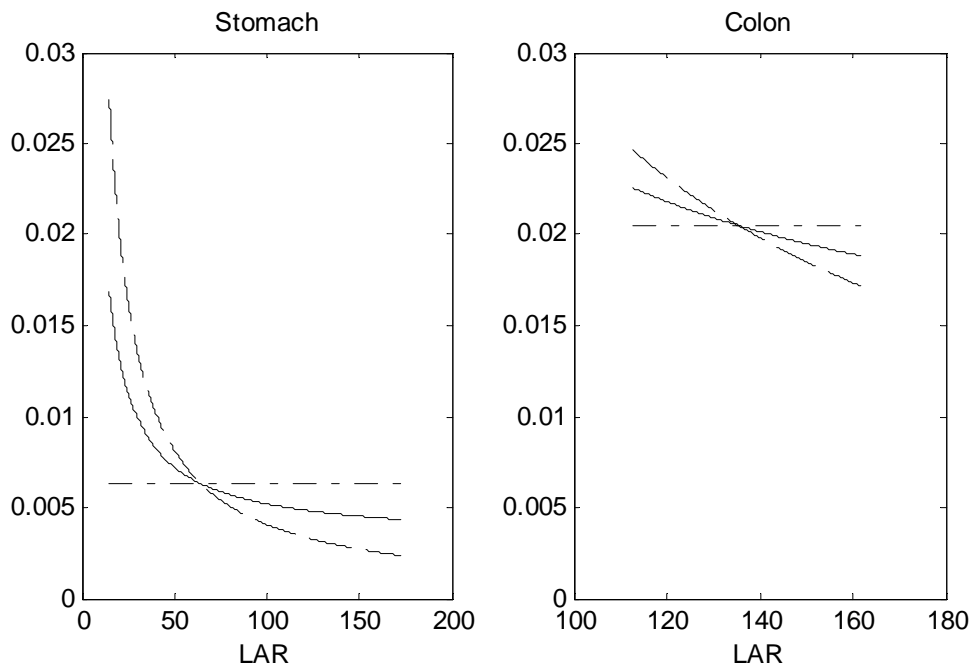


Figure 4-1: Uniform (dash-dot) and log-uniform (dash) distributions for values of LAR intermediate between the ERR and EAR projections for stomach and colon cancer. The EPA distribution for these intermediate values is the average of these two (solid).

4.3.2 DDREF

A lognormal uncertainty factor with GM=1 and GSD=1.35 was assigned to the DDREF for solid cancers (Figure 4-2). This is essentially the same

distribution for DDREF which BEIR VII used for its quantitative uncertainty analysis.

BEIR VII's distribution for uncertainty in DDREF was based, in part, on a Bayesian analysis of the LSS data and animal carcinogenesis studies. The main objective of this analysis was to estimate the curvature of the dose-response, which, as described in Section 2.1.4, translates directly into an estimate for DDREF. The Bayesian analysis resulted in a posterior distribution for the DDREF with GM=1.5 and GSD=1.28. The latter is equivalent to $Var(\log(DDREF)) = 0.06$. However, the BEIR VII Committee opined that: "the [Bayesian] DDREF analysis is necessarily rough and the variance of the uncertainty distribution is ..., if anything, misleadingly small." Accordingly, they inflated the variance representing the $\log(DDREF)$ by 50% and set its variance equal to 0.09.

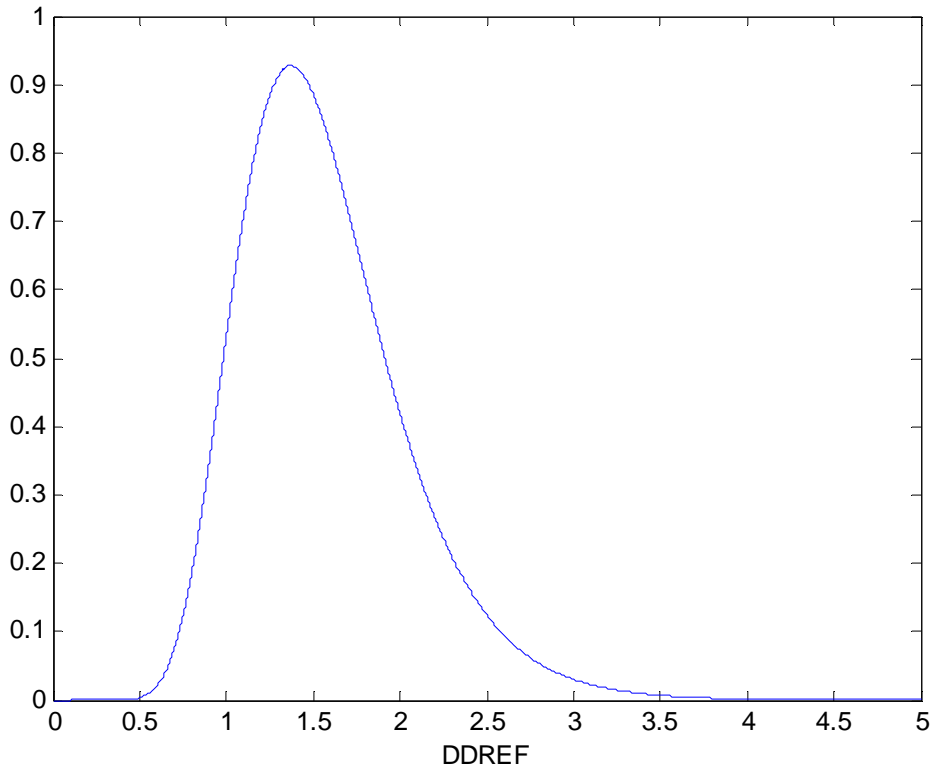


Figure 4-2: Subjective probability density function for DDREF

4.3.3 Other Non-sampling Sources of Uncertainty

Sources of uncertainty considered here include uncertainties from: age and temporal dependence unrelated to sampling variation, dosimetry errors, and

diagnostic misclassification. We assigned a single (encompassing) log normal uncertainty factor with GM=1.09 and GSD = 1.3.

Age and temporal dependence. About 40% to 45% of the projected cancer incidence radiation risk is associated with childhood exposures (see Section 3.11), and there is considerable uncertainty for the estimated risk for children. An oft-cited reason for this (EPA 1994, 1999) is that A-bomb survivors who were children at the time of the bombings (ATB) still have substantial years of life remaining in which cancers are to be expressed. For a crude indication of the relative precision of the LAR for childhood exposures, we note that, for the BEIR VII analysis of the LSS cohort, fewer than 2100 survivors with cancers were exposed at age < 15 compared to more than 3400 for age-at-exposure 15-30. Furthermore, approximately 90% of children < 10 ATB were still alive in the year 2000 (Little et al. 2008). More generally, about 45% of all survivors in the LSS were still alive in 2000, so that uncertainties in LAR projections from the incomplete follow-up, especially for cancers that tend to develop relatively late in life, merit careful consideration.

Both sampling error and modeling uncertainties can lead to uncertainties relating to temporal and age dependence. Here, sampling error uncertainty refers to uncertainty in, say, an LAR associated with the age-at-exposure and attained age parameter (γ , η) sampling errors. Modeling uncertainties refer to possible effects of model misspecification. For example, in models described by Little et al. (2008), ERR and EAR for solid cancer mortality depend on time-since-exposure. The uncertainty of projections based upon the parametric representations in BEIR VII depend on the extent to which ERR and EAR for incidence and mortality depend on time-since-exposure and other factors not accounted for in their risk models.

For EPA's previous assessment of radiogenic cancer risks, based primarily on analysis of the LSS mortality data for follow-up up to 1985, site-specific uniform distributions were assigned to "uncertainty factors" to account for sampling errors and possible model misspecification associated with temporal dependence (1999). For stomach, colon, lung, breast, thyroid and residual site cancers, it was thought that these uncertainties might lead to an overestimate of population risk. For these sites, a relative risk model was used that depended on age-at-exposure but not attained age, and most of the projected risk was associated with exposures before age 20. It was thought that "the contribution of childhood exposures was highly uncertain in view of statistical limitations [i.e., sampling error] and possible decreases in relative risk with time after exposure [i.e, modeling misspecification]". For most of these sites, the distribution, U(0.5, 1), was assigned to the uncertainty factor. In other words, the ratio of the "true" population risks to the EPA projection was thought to range between 0.5 and 1. For other solid cancer sites (except bone), the distribution for the uncertainty factor was 0.8 to 1.5. Due to the longer follow-up period and more flexible and appropriate modeling of age dependence in BEIR VII, uncertainties associated

with both sampling error and modeling misspecification should be greatly reduced. In addition, uncertainties associated with sampling error relating to both the age-at-exposure and attained-age parameters are now explicitly accounted for in the Bayesian analysis already described in Section 4.2.

To update the uncertainty analysis to account for modeling uncertainties, the new EPA risk models (see Section 3) were used to calculate the LAR for time-since-exposure restricted to between 13 and 53 y: the period of follow-up for the LSS incidence data. Slightly more than one-half of the projected LAR is associated with this time period. Thus, unless the temporal dependence differs substantially for time-since-exposure from what has been observed for the period of follow-up in the LSS, it is unlikely to be a major source of uncertainty, with the possible exception of childhood exposures. A common lognormal uncertainty factor with $GM = 1$ and $GSD = 1.2$ was used for solid cancers. Leukemia deserves special mention. To paraphrase Little et al. (2008), uncertainties in risk projections for leukemia would have more to do with risks for times soon after exposure than for times extending beyond the current LSS follow-up. This is because the mortality follow-up in the LSS began in October, 1950, about 5 years after the bombings in Hiroshima and Nagasaki, and there is evidence of risk for time-since-exposures < 5 y from other studies. In particular, a substantial number of leukemia cases reportedly occurred in the LSS before 1951, with an apparent subsequent decline; a significant increase in leukemia within 5 y of radiotherapy was observed in the International Cervical Cancer study; and in an analysis of the Mayak worker study (Shilnikova et al. 2003), the ERR/Gy for leukemia mortality was significantly higher for external doses received 3-5 y prior to death than for doses received more than 5 y earlier. Although the uncertainty associated with time-since-exposures < 5 y might be larger than modeling uncertainties associated with most solid cancers, it is our subjective judgment that it is small compared to the sampling uncertainties described in Section 4.2.2, and we did not quantify this source of uncertainty.

Errors in dosimetry. In 2003, RERF implemented a revised dosimetry system called DS02, which is the culmination of efforts stemming from concerns about the previous (DS86) system for assigning doses to the A-bomb survivors. Chief among these concerns were discrepancies between DS86 calculations and measured thermal neutron activation values (Roesch 1987). These measurements indicated that DS86 might have seriously underestimated neutron doses for Hiroshima survivors, and, as a result, gamma ray risk estimates for solid cancers could possibly be underestimated by more than 20% (Preston et al. 1993, EPA 1999). However, the magnitude of this bias would depend on factors such as the RBE for neutrons. Other factors motivating development of the new system included improved computer models for radiation transport and biodosimetric and cancer data indicating overestimation of doses for Nagasaki factory workers (Preston et al. 2004).

A comprehensive review adequately resolved issues relating to the discrepancies with neutron activation measurements (Preston et al. 2004). As summarized in Preston et al. 2004 and detailed elsewhere (Cullings et al. 2006, Young et al. 2005), major changes in DS02 include: 1) changes in the height burst and yield for the Hiroshima bomb; 2) changes in the gamma radiation released by the Nagasaki bomb; 3) use of new data on neutron scattering, etc., to improve calculations for radiation transport; 4) more detailed information and better methods to account for in-home and terrain shielding; 5) more detailed information for computing free-in-air fluences; and 6) new weighting factors for fluence-to-kerma and fluence-to-dose calculations.

The RERF report on DS02 (Young et al., Chapter 13) divides uncertainties associated with the dosimetry system into two broad categories: systematic and random. "Systematic" refers to "the likelihood that doses to all individuals at a given city will increase or decrease together [from imperfectly or unknown effects]", whereas "random" refers to effects on individual survivor doses that act more or less independently. Examples of systematic uncertainties are those relating to the yields, neutron outputs and burst heights, and the air transport calculation method. Examples of random uncertainties are those relating to survivor location and inputs needed to estimate shielding for individual survivors. In Young et al. (pp. 989, 991), a coefficient of variation (CV) of 12-13% (corresponding to a GSD of about 1.12) was associated with systematic uncertainties.

For assessing the effects of random dose errors on risk projections, we refer to the recent contribution by Pierce et al. (2008). As they note, "RERF has for more than 15 years made adjustments to individual (DS86 and DS02) dose estimates to reduce the effects of imprecision" on estimates of risk. Without adjustment, it is well-established that random dose errors would cause a downward bias in risk estimates if a linear dose-response is assumed. They may also introduce a bias in the estimate of curvature, which is used for evaluating the DDREF. RERF adjustments are currently based on the assumption that the random errors are independent and lognormal with $CV = 0.35$ ($GSD = 1.42$). Pierce et al. argue for adjustments based on more sophisticated treatment of the random errors that account for effects of "the use of smoothing formulae in the DS02 treatment of location and shielding." Results in Pierce et al. (Table 1, p. 123) indicate that the more realistic and sophisticated modeling of random dose errors would result in a change of about 2% in the estimated linear dose-response estimate of ERR and about a 15-20% change in the estimate of curvature, compared to estimates based on current methods and assumptions. The effect on the estimate of DDREF would be somewhat less than this, in part because it depends also on data from animal carcinogenesis studies. Perhaps somewhat conservatively, we assign lognormal uncertainty factors with a GSD equal to 1.05 (effects of random errors on the linear dose parameter estimate) and 1.1 (effects on the estimate for the DDREF). The GM for these factors are set to 1 and 0.95, respectively.

Finally, we quantify uncertainties relating to the use of a nominal neutron RBE of 10. The use of this nominal weight assigned to the neutron component of dose has already been discussed in Section 3.1. Calculations in Preston et al. (2004) indicate that the use of an RBE of 20 would result in a relative decrease in ERR estimates for solid cancers by about 5%. Radiobiological data (Sasaki et al.) indicate an RBE of 20 or greater cannot be ruled out. A lognormal uncertainty factor with GM = 0.95 and GSD of 1.05 is assigned to this source.

Errors in disease detection and diagnosis. The BEIR VII Committee concluded that “this is unlikely a serious source of bias in risk estimates.” Types of diagnostic misclassification that can occur include classification of cancers as non-cancers (detection error) and erroneous classification of non-cancer cases as cancer (confirmation error). The former leads to an underestimate of the EAR, but does not affect the estimated ERR. Conversely, the latter leads to an underestimate of the ERR but does not affect the EAR (EPA 1999).

Analyses of LSS mortality data formed the basis for EPA’s previous risk assessment. For that assessment, results from studies of Sposto et al. (1992) and Pierce et al. (1996) were used to estimate the bias in risk estimates due to diagnostic misclassification in the LSS mortality data. Conclusions from these studies were that the ERR estimate for solid cancers in the LSS should be adjusted upward by about 12% and the EAR estimate should be adjusted upward by about 16%. Based on these results and results from the uncertainty analysis by the NCRP 126 Committee (NCRP 1997), EPA assigned a N(1.15, 0.06) to the uncertainty factor for diagnostic misclassification.

Misdiagnosis is likely to lead to a somewhat smaller bias in the BEIR VII projections than in EPA’s 1994 projections because the former were based on the LSS incidence data. As noted in the BEIR VII report, “cancer incidence data are probably much less subject to bias from underascertainment or from misclassification, and this was an important reason for the committee’s decision to base models for site-specific cancers on incidence data. However, incidence data are not available for survivors who migrated from Hiroshima to Nagasaki. Adjustments are likely to account for this (Sposto et al. 1992), but there is likely to be some uncertainty in the adequacy of these adjustments.” We assign a lognormal uncertainty factor with a GM=1.1 and a GSD = 1.06 for diagnostic misclassification. Admittedly, this understates the uncertainty for some cancers, since the uncertainty factor does not account for misclassification among different cancer types.

Relative effectiveness of medical x rays. For breast and thyroid cancers, the BEIR VII risk models were based on pooled analyses of data from the LSS and several medical studies. Most of the medical studies were based on data from patients who had received X-ray therapy. If the RBE for lower

energy photons is greater than 1, the medical x rays *may* have been more carcinogenic, per unit dose, than gamma rays. In that case, there may be an upward bias in risk estimates derived from the pooled studies, because the higher-energy gamma dose (that would result in the same risk) would be larger for these patients.

However, in many of the medical studies the doses were fractionated. The possibility for an upward (RBE) bias is countered by the possibility that a smaller DDREF than 1.5 should be applied to results derived (in part) from studies involving fractionated doses. If, as seems likely given the evidence presented in Section 4.2, the RBE is typically about 1.5 for x rays at high dose and dose rates, then there would be only a small bias associated with the relative effectiveness of medical x rays.

We did not incorporate any uncertainty associated with the RBE for medical x rays. It should be relatively small compared to the uncertainties associated with sampling variability – especially for thyroid cancer.

Selection bias in the LSS cohort. Here, selection bias refers to the possibility that risk estimates derived from the LSS are biased downward because members of the cohort, by being able to survive the bombings, demonstrated a relative insensitivity to radiation. The question as to whether there is a serious selection bias has been a subject of considerable controversy. For example, Little (2002) cited several papers by Stewart and Kneale from 1973 to 2000 which argued that the selection bias may be substantial. In a recent analysis, Pierce et al. (2007) argue that the magnitude of the bias on the ERR estimate for solid cancer is unlikely to be greater than 15-20%. (The bias might be greater for non-cancer effects). We assign a lognormal distribution with GM 1.1 and GSD 1.1 to the uncertainty factor for selection bias.

Shape of the dose response. As described in Section 3.5, BEIR VII models explicitly (leukemia) or implicitly (solid cancers) assume a linear-quadratic (LQ) dose response for cancer induction by IR. Although epidemiological data are generally consistent with linearity at low doses (Section 2.2), recent mechanistic studies have revealed complex phenomena (Section 2.1) that could conceivably modulate risks at very low doses and dose rates, either up or down, from what would be projected based on a LQ model. The BEIR VII Committee did not attempt a quantification of this source of uncertainty. Attempting to assign a probability distribution to the dose-response model would necessarily be highly speculative and subjective; consequently, EPA does not deem it appropriate to include this source of uncertainty in its quantitative uncertainty analysis. However, it is acknowledged that a breakdown in the model at low doses, leading to substantial errors in our risk projections, cannot be ruled out.

4.4 Results

The mean, median, and 90% uncertainty intervals for male and female cancer incidence LAR are given in Tables 4-3(a, b). Except for prostate and uterine cancers, these were generated using the Monte Carlo methods described above (Section 4.1-4.3). Lower bounds for these two cancers were set to 0, since the analyses of LSS incidence data provide insufficient evidence to indicate a positive dose-response (Preston et al. 2007, NRC 2006). The tables also include the EPA nominal projections described in Section 3. Sex-averaged uncertainty intervals are given in Table 4-3c.

Table 4-3a: EPA projection and uncertainty distribution for the LAR for male cancer incidence¹

Cancer Site	EPA Projection	Uncertainty Distribution				U/L
		Mean	Lower (5%) Limit (L)	Median	Upper (95%) Limit (U)	
Stomach	31	86	9	44	280	32
Colon	142	140	52	130	300	5.8
Liver	28	51	9	34	150	16
Lung	125	150	47	130	310	6.5
Prostate	42	160	0 ²	99	520	∞
Bladder	94	90	18	70	220	13
Thyroid	22	28	6	22	73	11
Residual ³	220	290	100	250	600	5.7
All solid ⁴	703	990	420	890	1910	4.5
Leukemia	81	95	32	82	200	6.3
Total ⁴	785	1090	510	990	2000	3.9

¹ Cases per 10,000 person-Gy

² Set to zero. Dose response for prostate cancer is not significant at 0.05 level.

³ Includes kidney and other cancers not here specified.

⁴ Excludes skin cancer

Table 4-3b: EPA projection and uncertainty distribution for the LAR for female cancer incidence¹

Cancer Site	EPA Projection	Uncertainty Distribution				U/L
		Mean	Lower (5%) Limit (L)	Median	Upper (95%) Limit (U)	
Stomach	40	96	11	51	300	27
Colon	90	110	35	94	230	6.7
Liver	13	37	5	22	120	25
Lung	272	340	120	290	710	6.0
Breast	281	300	160	280	490	3.1
Uterus	17	110	0 ²	76	320	∞
Ovary	32	47	12	40	110	8.6
Bladder	87	64	14	50	160	12
Thyroid	110	140	32	110	370	11
Residual ³	223	330	120	280	670	5.4
All solid ⁴	1170	1570	770	1450	2760	3.6
Leukemia	60	70	24	61	150	6.4
Total ⁴	1230	1640	830	1520	2830	3.4

¹ Cases per 10,000 person-Gy

² Set to zero. Dose response for uterine cancer is not significant at 0.05 level.

³ Includes kidney and other cancers not specified here.

⁴ Excludes skin cancer

Table 4-3c: EPA projection and uncertainty distribution for the sex-averaged LAR for cancer incidence¹

Cancer Site	EPA Projection	Uncertainty Distribution				U/L
		Mean	Lower (5%) Limit (L)	Median	Upper (95%) Limit (U)	
Stomach	35	91	11	49	290	27
Colon	116	130	50	110	250	5.0
Liver	20	44	8	28	130	16
Lung	199	240	93	210	490	5.3
Breast	142	150	80	140	250	3.1
Prostate	21	78	0 ²	49	250	∞
Uterus	9	56	0 ²	39	160	∞
Ovary	16	24	6	20	54	8.6
Bladder	90	77	21	64	180	8.2
Thyroid	66	86	25	69	200	8.2
Residual ³	221	310	130	270	610	4.8
All solid ⁴	936	1280	620	1180	2270	3.7
Leukemia	71	83	39	75	150	3.9
Total ⁴	1010	1365	700	1270	2360	3.4

¹ Cases per 10,000 person-Gy

² Set to zero. Dose response for these cancers are not significant at 0.05 level.

³ Includes kidney and other cancers not specified here.

⁴ Excludes skin cancer

The last column of each of these tables gives the ratio of the upper to lower uncertainty bounds by cancer site. These ratios range from about 25 to ∞ for stomach, liver, prostate and uterine cancers (largest uncertainty) to about 3 for breast cancer (smallest uncertainty). For many sites, the ratio is about 10. For liver and prostate cancers, both risk transport and sampling variability are important sources of uncertainty, whereas for many other sites, the uncertainty for DDREF is most important. For uniform whole-body radiation, the upper-to-lower bound ratio is about 4, and the most important contributor to the uncertainty appears to be DDREF. The sex-averaged 90% uncertainty interval for uniform whole-body radiation is (700, 2360).

Results in Tables 4-3(a-c) were used to calculate uncertainty intervals for radiation-induced cancer mortality. This was accomplished by applying crude estimates of radiogenic cancer fatality rates, equal to the ratio of the nominal EPA projection for mortality divided by the corresponding projection for incidence to the lower and upper bounds for cancer incidence. For uniform whole-body radiation, 90% UIs for cancer mortality are 2.5×10^{-2} to 9.8×10^{-2} for males, 4.1×10^{-2} to 1.5×10^{-1} for females, and 3.5×10^{-2} to 1.2×10^{-1} Gy⁻¹ when sex-averaged. These intervals do not account for uncertainty associated with the cancer fatality ratios.

Tables 4-4(a, b) presents results for childhood exposures. The 90% UI indicate, for a stationary population, ranges for the LAR associated with exposures before age 15. For example, in a stationary population exposed to 10,000 person-Gy of uniform whole-body radiation, the 90% UI for the LAR associated with childhood exposures is (200, 840) for males and (380, 1340) for females. For specific cancer sites, the ratio of upper to lower uncertainty bounds are about 1.5 times larger for childhood exposures than for all ages-at-exposure. The largest uncertainties for childhood exposures are for stomach, bladder, and liver cancers.

Table 4-4a: EPA projection and uncertainty distributions for male cancer incidence in a stationary population exposed to uniform whole-body radiation: LAR associated with exposures < age 15 for selected sites¹

Cancer Site	EPA Projection	Uncertainty Distribution				U/L
		Mean	Lower (5%) Limit (L)	Median	Upper (95%) Limit (U)	
Stomach	12	30	3	15	100	41
Colon	54	58	18	49	130	7.1
Liver	11	20	3	12	62	23
Lung	48	48	9	37	120	14
Bladder	34	31	2	19	100	47
Residual ³	100	170	55	140	380	6.9
All ⁴	313	420	200	370	840	4.2

¹ Cases per 10,000 person-Gy

² Set to zero. Dose response for prostate cancer is not significant at 0.05 level.

³ Includes kidney and other cancers not specified here.

⁴ Excludes skin cancer

Table 4-4b: EPA projection and uncertainty distributions for female cancer incidence in a stationary population exposed to uniform whole-body radiation: LAR associated with exposures < 15 for selected sites¹

Cancer Site	EPA Projection	Uncertainty Distribution				U/L
		Mean	Lower (5%) Limit (L)	Median	Upper (95%) Limit (U)	
Stomach	15	33	3	17	110	35
Colon	33	44	11	36	110	9.3
Liver	5	14	1	8	48	39
Lung	102	110	24	85	270	11
Bladder	31	21	2	12	72	40
Thyroid	83	110	24	82	280	11
Residual ³	99	190	63	160	440	6.9
All ⁴	565	740	380	680	1340	3.5

¹ Cases per 10,000 person-Gy

² Set to zero. Dose response for uterine cancer is not significant at 0.05 level

³ Includes kidney and other cancers not specified here

⁴ Excludes skin cancer

Results suggest that the EPA risk projections for uniform whole-body radiation (total for all cancer sites) are likely to be well within a factor of 3 of the “true” risk for the U.S. population. For individual sites, the projections and actual risks might differ by a factor of about 3 to 5 for most sites to almost 10 for stomach cancer. An important caveat is that the analysis did not account for important uncertainties associated with the shape of the dose response at low doses and dose rates. Another caveat is that it is very difficult to quantify the bias of these risk projections.

If one defines bias as the difference between the means of the uncertainty distributions summarized in this section and the EPA projections presented in Section 3, then bias is dependent on the subjective distributions assigned to sources of uncertainty such as risk transport. For most sites, the means of the uncertainty distributions, based on the subjective distributions EPA assigned to sources of uncertainty, are greater than the nominal EPA projections given in Section 3. (The same is true for the medians, although arguably for most cancer sites, the median and the EPA projection are consistent). For most sites for which there appears to be a large discrepancy. It stems from how the problem of risk transport is handled under the two approaches. For prostate and uterine cancers, the larger mean values also relate to features of the Bayesian analysis outlined in Section 4.2.1. These features include: 1) the use of a lognormal prior distribution for the linear dose response parameter and 2) the sharing of information on radiogenic risks among cancer sites. Details about these (technical) points are given next.

Risk transport. For sites such as stomach, liver, uterine and prostate cancer, the baseline cancer rates are very different in the U.S. compared to Japan, and, as a result, the ERR and EAR model-based projections are also very different. For the uncertainty analysis, we adopted a distribution which assigns with 50% probability one of the two EAR or ERR model-based projections and with 50% probability either a uniform or log-uniform distribution for possibilities between the two “extremes”. The net result is a mean value which for most sites is not much different from a nominal estimate based on a weighted arithmetic mean – with a weight equal to 0.6 for the ERR model. As indicated in Section 3, projections based on arithmetic means would be twice as large as the EPA projection for sites such as stomach cancer, so a much larger mean for the uncertainty distribution is not surprising. If different distributions had been assigned for risk transport, the means for the uncertainty distributions for sites such as stomach cancer could be quite different.

Linear dose response parameter. The prior distribution for the linear dose response parameter was assumed to be lognormal. Taken literally, this rules out the possibility that there is no effect of radiation, which is not appropriate for sites such as prostate or uterine cancer. As already mentioned, the lower bound for these sites is set to 0.

Sharing of information on radiogenic risks. The Bayesian analysis provided a convenient method to share information on radiogenic risks among cancer sites. In essence, the final uncertainty distributions for ERR for a specific solid cancer site represents a compromise between a distribution of ERRs which would have been derived only from data for the specific cancer and a distribution of ERRs derived from data for all solid cancer sites. A consequence is that central values for the uncertainty distributions for the LAR for cancers with small estimated ERRs, such as of the prostate and uterus, are larger than the corresponding ERR estimates given in BEIR VII.

4.5 Comparison with BEIR VII

4.5.1 Quantitative Uncertainty Analysis in BEIR VII

The BEIR VII Report includes a quantitative uncertainty analysis with 95% subjective CIs for each site-specific risk estimate of LAR for low LET radiation. The analysis focused on three sources of uncertainty thought to be most important: sampling variability in the LSS data, the uncertainty in transporting risk from the LSS to the U.S. population, and the uncertainty in the appropriate value of a DDREF for projecting risk at low doses and dose rates from the LSS data. Their treatment of these and other sources of uncertainty are outlined next.

Sampling variability. For most cancer sites, BEIR VII derived parameter estimates for ERR and EAR models based on a statistical analysis of LSS cancer

cases and deaths, which were cross-classified by city, sex, dose, and intervals based on age-at-exposure, attained age, and follow-up time. For all solid cancer sites except breast and thyroid, the BEIR VII uncertainty analysis accounted for only the sampling variability associated with the linear dose parameter (β). The uncertainty analysis made use of an approximation for the variance of the $\log(LAR)$ associated with sampling variability:

$$Var_{SAMPLING}[\log(LAR(d, e))] \approx Var[\log(\hat{\beta})]. \quad (4-5)$$

Risk transport. To quantify uncertainties from risk transport, BEIR VII essentially assumed that either the EAR or ERR model is “correct” for risk transport, and a weight parameter (w) equals the probability the ERR model is correct. BEIR VII approximated $Var[\log(LAR)]$ as follows:

$$Var_{TRANSPORT}[\log(LAR)] \approx \log[LAR^{(R)}(\hat{\mathcal{G}}^{(R)}) / LAR^{(A)}(\hat{\mathcal{G}}^{(A)})]^2 w(1-w). \quad (4-8)$$

Here, $\hat{\mathcal{G}}^{(R)}$ denotes the vector of estimated and nominal parameter values for β , γ , η , and DDREF for the ERR model, and $LAR^{(R)}(\hat{\mathcal{G}}^{(R)})$ represents the corresponding nominal LAR estimate. Likewise, $\hat{\mathcal{G}}^{(A)}$ and $LAR^{(A)}(\hat{\mathcal{G}}^{(A)})$ represent the estimated parameter values and nominal LAR values for the EAR model.

DDREF. BEIR VII’s distribution for uncertainty in DDREF has been given in Section 4.3.2.

Combining sources of uncertainties. To calculate the $\text{var}(\log(LAR))$, the BEIR VII Committee simply summed the variances for $\log(LAR)$ associated with sampling error, risk transport, and DDREF. To calculate 95% subjective confidence intervals, they further assumed that the combined uncertainty for LAR follows a lognormal distribution.

Unquantified sources of uncertainty. BEIR VII noted several other sources of uncertainty but did not quantify them, arguing instead that uncertainties for many of these other sources are relatively small. These other sources of uncertainty include: 1) uncertainty in the age and temporal pattern of risk, especially for individual sites, which was usually taken to be the same as that derived for all solid tumors; 2) errors in dosimetry; 3) errors in disease detection and diagnosis; and 4) unmeasured factors in epidemiological experiments.

4.5.2 Comparison of Results

Results from EPA’s quantitative uncertainty analysis are compared with BEIR VII uncertainty intervals for LAR cancer incidence (Table 4-5). For purposes of comparison, 95% uncertainty intervals were calculated which account for only those uncertainties associated with sampling variability, risk transport, and DDREF. That is, uncertainty factors for other sources of uncertainty, other than those quantified in BEIR VII, were not applied to generate these results. For most sites, results are reasonably consistent. Notable exceptions are prostate cancer, for which the BEIR VII intervals appear to be too wide, and uterine cancer, for which the EPA upper bound is about 2½ times larger (330 compared to 131).

Table 4-5: 95% EPA and BEIR VII 95% uncertainty intervals for LAR of solid cancer incidence, which account for sampling variability, risk transport, and DDREF

Cancer Site	Males		Females	
	EPA	BEIR VII	EPA	BEIR VII
Stomach	(7, 290)	(3, 350)	(10, 300)	(5, 390)
Colon	(45, 280)	(66, 360)	(29, 220)	(34, 270)
Liver	(7, 150)	(4, 180)	(3, 120)	(1, 130)
Lung	(37, 290)	(50, 380)	(100, 670)	(120, 780)
Prostate	(0, 540)	(<0, 1860)		
Breast	None	None	(140, 550)	(160, 610)
Uterus			(0, 330)	(<0, 131)
Ovary			(10, 100)	(9, 170)
Bladder	(12, 230)	(29, 330)	(11, 160)	(30, 290)
Remainder	(89, 570)	(120, 680)	(110, 630)	(120, 680)
Thyroid	(5, 91)	(5, 90)	(26, 450)	(25, 440)
Solid cancers	(390, 1700)	(490, 1920)	(690, 2600)	(740, 2690)

¹ Cases per 10,000 person-Gy

4.6 Conclusions

The main results given in Section 4.4 suggest that the EPA risk projections for uniform whole-body radiation (total for all cancer sites) are likely to be well within a factor of 3 of the “true” risk for the U.S. population. For individual sites, the projections and actual risks might differ by a factor of about 3 to 5 for most sites to about 10 for stomach cancer. For childhood exposures, the uncertainties are somewhat larger. An important caveat is that the analysis did not account for important uncertainties associated with the shape of the dose response at low doses and dose rates.

The quantitative uncertainty analysis did allow for some sources of uncertainty, such as dosimetry errors and cancer misdiagnosis, which were not quantified in BEIR VII. For sources of uncertainty quantified in BEIR VII, results from this analysis and BEIR VII are consistent for most sites.

Results from the EPA uncertainty analysis should not be over-interpreted. The results presented in Section 4.4 are meant solely as guidance as to the (relative) extent to which “true” site-specific risks for a hypothetical stationary U.S. population might differ from the central estimates derived in Section 3. This is because it was not always possible to satisfactorily evaluate “biases” associated with sources of uncertainty such as risk transport.

5. Risks from Higher LET Radiation

5.1 Alpha Particles

Assessing the risks from ingested or inhaled alpha-emitting radionuclides is problematic from two standpoints. First, it is often difficult to accurately estimate the dose to target cells, given the short range of alpha-particles in aqueous media (typically < 100 μm) and what is often a highly non-uniform distribution of a deposited radionuclide within an organ or tissue. Second, for most cancer sites, there are very limited human data on risk from alpha particles. For most tissues, the risk from a given dose of alpha radiation must be calculated based on the estimated risk from an equal absorbed dose of γ rays multiplied by an “RBE” factor that accounts for different carcinogenic potencies of the two types of radiation, derived from what are thought to be relevant comparisons in experimental systems

The high density of ionizations associated with tracks of alpha radiation produces DNA damage which is less likely to be faithfully repaired than damage produced by low-LET tracks. Consequently, for a given absorbed dose, the probability of inducing a mutation is higher for alpha radiation, but so is the probability of cell killing. The effectiveness of alpha radiation relative to some reference low-LET radiation (e.g., 250 kVp x rays or ^{60}Co γ rays) in producing a particular biological end-point is referred to as the alpha-particle relative biological effectiveness (RBE). The RBE may depend not only on the observed end-point (induction of chromosome aberrations, cancer, etc.), but on the species and type of tissue or cell being irradiated, as well as on the dose and dose rate.

In most experimental systems, the RBE increases with decreasing dose and dose rate, apparently approaching a limiting value. This mainly reflects reduced effectiveness of low-LET radiation as dose and dose rate are decreased — presumably because of more effective repair. In contrast, the effectiveness of high-LET radiation in producing residual DNA damage, transformations, cancer, etc. may actually decrease at high doses and dose rates, at least in part due to the competing effects of cell killing. For both low- and high-LET radiations, it is posited that at low enough doses, the probability of a stochastic effect is proportional to dose, and independent of dose rate. Under these conditions, the RBE is maximal and equal to a constant RBE_M . In order to estimate site-specific cancer risks for low dose alpha radiation, we need a low-dose, low-LET risk estimate for that site and an estimate of the RBE_M .

5.1.1. Laboratory Studies

The experimental data on the RBE for alpha particles and other types of high-LET radiation have been reviewed by the NCRP (NCRP 1990) and the ICRP (ICRP 2003). From laboratory studies, the NCRP concluded that: “The effectiveness of alpha emitters is high, relative to beta emitters, being in the

range of 15 to 50 times as effective for the induction of bone sarcomas, liver chromosome aberrations, and lung cancers.” The NCRP made no specific recommendations on a radiation weighting factor for alpha radiation.

The ICRP has reiterated its general recommendation of a radiation weighting factor of 20 for alpha-particles (ICRP 2003, 2005). However, ICRP Publication 92 further states (ICRP 2003):

Internal emitters must be treated as a separate case because their RBE depends not merely on radiation quality, but also, and particularly for α -rays with their short ranges, on their distribution within the tissues or organs. It is, accordingly, unlikely that a single w_R should adequately represent the RBE_M for different α emitters and for different organs...The current w_R of 20 for α -rays can thus serve as a guideline, while for specific situations, such as the exposure to radon and its progeny, or the incorporation of ^{224}Ra , ^{226}Ra , thorium, and uranium, more meaningful weighting factors need to be derived.

Another set of recommendations for α -particle RBE is contained in the NIOSH-Interactive RadioEpidemiological Program (NIOSH-IREP) Technical Documentation meant for use in adjudicating claims for compensation of radiogenic cancers (NIOSH 2002, Kocher et al. 2005). For alpha-particle caused solid cancers (other than radon-progeny-induced lung cancer), IREP posits a lognormal uncertainty distribution for its radiation effectiveness factor (REF, equivalent to RBE_M) with a median of 18 and a 95% CI [3.4, 101]. For leukemia, IREP employs a hybrid distribution: REF=1.0 (25%); =LN(1,15) (50%); =LN(2,60) (25%) where LN(a,b) represents a lognormal distribution with a 95% CI of [a,b].

Studies comparing groups of animals inhaling insoluble particles to which are attached alpha or beta emitters have been performed to assess RBE for lung cancer. In a large long-term study of beagle dogs, Hahn et al. (1999) reported that the RBE was at least 20. In contrast, from an analogous study of lung cancer induction in CBA/Ca mice, Kellington et al. (1997) estimated the RBE to be only 1.9.

5.1.2 Human Data

Results from epidemiological studies of groups exposed to alpha radiation can be used directly to develop risk estimates for alpha radiation; they can also be used in conjunction with low-LET studies to estimate RBE; finally, it is possible to use results from these studies in combination with estimates of RBE to derive low-LET risk estimates where none can be obtained from low-LET studies.

There are four cancer sites for which there are direct epidemiological data on the risks from alpha irradiation: bone, bone marrow, liver, and lung. Not coincidentally, these are sites for which we are particularly interested in obtaining high-LET risk estimates because they are ones which tend to receive higher than average doses of alpha radiation from certain classes of internally deposited

radionuclides. For each of these sites except bone, we also have risk estimates for low-LET radiation derived from the LSS.

Bone cancer. Although there is some new information coming from research on Mayak plutonium workers (Koshurnikova et al. 2000), the most definitive information on bone cancer risk continues to be radium dial painters exposed to ^{226}Ra and ^{228}Ra and patients injected with the shorter-lived isotope ^{224}Ra . The usefulness of the dial painter data for low dose risk estimation suffers from lack of complete epidemiological follow-up and from the possible complicating effects of extensive tissue damage associated with very high doses of radiation in the bone. For this reason, EPA has taken its estimates of risk of alpha-particle-induced bone sarcoma from the BEIR IV analysis of the ^{224}Ra data, which is consistent with a linear, no-threshold dose response (NRC 1988, EPA 1994). The corresponding low-LET risk estimate (per Gy) was assumed to be a factor of 20 lower based on the assumed alpha-particle RBE_M of 20.

Subsequent to BEIR IV, improvements have been made in the dosimetry for the ^{224}Ra patients, especially those treated as children. Some additional epidemiological data have also become available. The updated data set has been analyzed by Nekolla et al. (2000) and found to be well-described by an absolute risk model, which for small acute doses reduces to the form:

$$\Delta r = \alpha D g(e) h(t),$$

where Δr is the increment in bone cancer incidence from an endosteal dose, D , of alpha-radiation; $g(e)$ reflects the variation in risk with age at exposure, e ; and $h(t)$, the variation in with time after exposure, t . A good statistical fit was found for $g(e)$ as an exponentially decreasing function of age at exposure, and $h(t)$ as a lognormal function of time after exposure.

Normalizing the time integral of $h(t)$ to unity, a maximum likelihood calculation yielded:

$$\alpha = 1.782 \times 10^{-3} \text{ Gy}^{-1},$$

$$g(e) = \exp[-0.0532(e - 30)],$$

$$h(t) = (2\pi\sigma)^{-1/2} \times \exp\left[-\frac{(\ln(t) - \ln(t_0))^2}{2\sigma^2}\right] \times \frac{1}{t},$$

where t_0 is 12.72 y and σ is 0.612. Thus, the temporal response, $h(t)$, has a GM=12.72 y and a GSD = $e^\sigma = 1.844$.

For estimates of bone cancer risk from alpha radiation, we adopt the model and calculational methods of Nekolla et al., with one modification. For simplicity, those authors assumed a fixed life-span of 75 y; our lifetime estimates are derived using their derived mathematical models, but, as with our other risk estimates, applied in conjunction with gender-specific survival functions determined from U.S. Vital Statistics. In this way, it is calculated that the average lifetime risk of bone cancer incidence is $2.04 \times 10^{-3} \text{ Gy}^{-1}$ for males and $1.95 \times 10^{-3} \text{ Gy}^{-1}$ for females. The population average of $1.99 \times 10^{-3} \text{ Gy}^{-1}$ is close to the FGR-13 estimate of $2.72 \times 10^{-3} \text{ Gy}^{-1}$ (EPA 1999b). About 35% of all bone cancers are fatal (SEER Fast Stats), and it is assumed here that the same lethality holds for radiogenic cases – half that previously assigned (EPA 1994). Thus the mortality risk projections for alpha-particle-induced bone cancer are $7.13 \times 10^{-4} \text{ Gy}^{-1}$ (males), $6.82 \times 10^{-4} \text{ Gy}^{-1}$ (females), and $6.96 \times 10^{-4} \text{ Gy}^{-1}$ (sex-averaged).

Human data on bone cancer risk from low-LET radiation are very sparse, but an estimate of the RBE for bone cancer induction can be derived from a comparative analysis of data on beagles injected with the alpha-emitter ^{226}Ra or the beta-emitter ^{90}Sr , both of which are distributed fairly uniformly throughout the volume of calcified bone. Employing a two-mutation model for bone cancer induction, Bijwaard et al. (2004), found that the dose-response relationship for both these radionuclides was approximately linear-quadratic at low doses, and that the linear coefficient was approximately 9.4 times higher for radium than for strontium. Based on this finding, EPA is adopting a revised RBE value of 10 for bone cancer; i.e., the risk per Gy for low-LET radiation is assumed to be 1/10 that estimated for alpha-particle radiation.

There has been a great deal of discussion in the scientific literature concerning a possible threshold for induction of bone sarcoma (NRC 1988). Often cited is a plot of bone cancer risk versus dose in radium dial painter data, which appears to show a rather abrupt threshold at about 10 Gy. However, the apparent threshold may simply be an artifact of presenting the data on a semi-log plot (incidence vs. log dose); a conventional plot of incidence vs. dose is consistent with linearity (Mays and Lloyd 1972, NRC 1988). In laboratory studies, Raabe et al. (1983) found that the mean time to tumor increases with decreasing dose rate, suggestive of a “practical threshold” in dose rate below which the latency period would exceed the lifespan of the animal. However, interpretation of this finding remains controversial (NRC 1988). A postulated mechanism for producing a sub-linear dose response relationship, resulting in a practical threshold below which the risk is negligible, is: 1) a requirement for two radiation-induced initiation steps (NRC 1988) or 2) the need for radiation-induced stimulation of cell division (Brenner et al. 2003). It may be hard, however, to reconcile these mechanisms with analyses of the ^{224}Ra injection studies discussed above, which seem indicative of a linear or linear-quadratic dose-response relationship.

Leukemia. Excess leukemia cases have not been observed in studies of radium dial painters or patients injected with high levels of ^{224}Ra , although in some cases there was evidence of blood disorders that may have been undiagnosed leukemias (NRC 1988). It appears from these studies, however, that bone sarcoma is a more common result of internally deposited radium, and that the radium leukemia risk is much lower than that calculated using ICRP dosimetry models together with a leukemia risk coefficient derived from the LSS weighted by an RBE of 20 (Mays et al. 1985, NRC 1988, Harrison and Muirhead 2003, Cerrie 2004).

In part, the anomalously low risk of leukemia from alpha-particles might be attributed to microdosimetry: i.e., target cells may be non-uniformly distributed in the bone marrow in such a way that the dose to these cells is considerably lower than the average marrow dose. Evidence suggests, however, that microdosimetric considerations do not fully account for the lower risk, and that high-LET radiation is only weakly leukemogenic. Thorotrast patients, who are expected to have a more even distribution of alpha-particle energy, do show an excess of leukemia, but only about twice the risk per Gy as seen in the LSS (ICRP 2003). Moreover, an RBE of only about 2.5 has been found for neutron-induced leukemia in mice (Ullrich and Preston 1987), a situation in which the high-LET radiation dose would have been nearly uniform throughout the marrow. The BEIR VII low-LET risk estimate for leukemia incidence is roughly 50% higher than that of UNSCEAR (2000b) or EPA (1994). Using a Bayesian approach, Grogan et al. (2001) estimated the alpha-particle leukemia risk to be 2.3×10^{-2} per Gy. If one adopts the BEIR VII low-LET leukemia (incidence) risk estimate, this would correspond to an RBE of approximately 2.9. Through a comparison of Thorotrast and A-bomb survivor data, Harrison and Muirhead (2003) also estimated the RBE to be 2-3. However, the authors noted that the Thorotrast doses were likely to be underestimated by a factor of 2-3 (Ishikawa et al. 1999), and that the RBE was perhaps very close to 1.

Ankylosing spondylitis patients (mostly young adult males) injected with relatively low amounts of ^{224}Ra had a higher rate of leukemia than that projected from the general population or that observed in a group of unirradiated control patients (Wick et al. 1999, 2008). After 26 y of average follow up, the exposed group of 1471 patients had 19 leukemias compared to 6.8 expected based on age- and gender-specific population rates; after 25 y of average follow up, the 1324 control patients had 12 leukemias (7.5 expected). The average dose to bone surface was estimated at 5 Gy in these patients. According to ICRP dosimetry models, the average marrow dose is about 10% of the bone surface dose for internally deposited ^{224}Ra (ICRP 1993). Thus, the estimated average marrow dose is ≈ 0.5 Gy, and the excess risk, calculated using the population projected rate is $\approx 1.7 \times 10^{-2} \text{ Gy}^{-1}$. This is about twice the leukemia risk projection for 30-y old males derived in BEIR VII from the LSS data (NRC 2006, p. 281). Thus, these radium-injection data are also roughly consistent with an RBE of about 2. Alternatively, if the unirradiated control patients are used as the comparison group, the estimated risk per Gy and RBE are roughly halved.

Hence, these data also support an RBE for leukemia induction of about 1-2. It should be noted, however, that the temporal variation of excess leukemias appeared different in this study from that observed in the LSS (Wick et al. 1999).

EPA has been employing an RBE of 1 for alpha-particle induced leukemia (EPA 1994). Based on the information discussed above, the RBE is being adjusted upward to a value of 2, with a confidence interval of 1-3.

Liver cancer. The LSS shows a statistically significant excess of liver cancer. The uncertainty bounds derived by BEIR VII are wide, both because of the large sampling error and the uncertainty in the population transport (liver cancer rates are about an order of magnitude lower here than in the LSS cohort). The BEIR VII central estimate for gamma radiation is $\approx 2 \times 10^{-3} \text{ Gy}^{-1}$. For comparison, updated analyses of data on Thorotrast patients from Denmark (Andersson et al. 1994) and Germany (van Kaick et al. 1999) yielded estimates of 7×10^{-2} and 8×10^{-2} excess liver cancers per Gy, respectively. Assuming an RBE of 20 for the alpha-particle RBE, these values are about a factor of 2 higher than what would be projected from the BEIR VII liver cancer model – quite reasonable agreement given the large uncertainties and difference in age and temporal distribution. However, Leenhouts et al. (2002) has reanalyzed the Danish Thorotrast data, employing a biologically based, two-mutation model of carcinogenesis, and derived a lifetime liver cancer risk estimate of $2 \times 10^{-2} \text{ Sv}^{-1}$ ($4 \times 10^{-1} \text{ Gy}^{-1}$), an order of magnitude higher than the BEIR VII central estimate, but consistent with the BEIR VII upper bound. One reason given by Leenhouts et al. for the higher risk estimate is that the model projects risk over a whole lifetime, whereas the original analysis by Andersson et al. addressed only the risk over the period of epidemiological follow-up. The increase may also partly stem from a correction for downward curvature in the dose-response function at high doses.

An excess of liver cancer has been found among workers at the Mayak nuclear facility in the Russian Federation, especially among workers with plutonium body burdens and among female workers (Gilbert et al. 2000). Averaged over attained age, the ERR per Gy for plutonium exposures was 2.6 for males and 29 for females. (Sokolnikov et al. 2008). For comparison, the BEIR VII risk model for γ -ray induced liver cancer derived from the LSS yields an ERR per Gy of 0.32 for males and females, calculated for exposure age 30 and attained age 60. Thus, the RBEs that would be derived from the LSS and Mayak worker study would be roughly 8 for males and 90 for females.

In conclusion, the Danish and German Thorotrast results are in good agreement with one another, and the risk projections derived from them are in quite reasonable agreement with what would be projected from the LSS, assuming a plausible RBE of about 40. There is considerable uncertainty in the estimates, relating to uncertainty in the dose estimates, the fraction of the dose “wasted” because it was delivered after the cancer was initiated, and the extrapolation from high doses (several Gy) to low environmental doses. In

addition, as seen from the Leenhouts et al. modeling exercise, there is considerable uncertainty in projecting risk over a whole lifetime, especially the contribution from childhood exposures. The results from the Mayak worker study appear to be in only fair agreement with those from the Thorotrast studies. Based on its review of the available information, EPA adopts a model for calculating α -particle induced liver cancer, which is a scaled version of the BEIR VII model, equivalent to multiplying the corresponding BEIR VII low-LET risk estimates, on an age- and gender-specific basis, by an RBE of 40. The population average risk is then $8 \times 10^{-2} \text{ Gy}^{-1}$.

Lung. Excess lung cancers have been associated with the inhalation of alpha-emitting radionuclides in numerous epidemiological studies. Cohort studies of underground miners have shown a strong association between lung cancer and exposure to airborne radon progeny. This association has also now been found in residential case-control studies. In addition, a cohort study of workers at the Mayak nuclear plant has also shown an association with inhaled plutonium (Gilbert et al. 2004). The miner studies serve as the primary basis for BEIR VI and EPA estimates of risk from radon exposure (NRC 1999, EPA 2003), and results from the residential studies are in reasonable agreement with those risk estimates (Darby et al. 2005, Krewski et al. 2005). The Agency has no plans at this time to reassess its estimates of risk from exposure to radon progeny, but it is the intent here to reassess estimates of risk from inhaled plutonium and other alpha-emitters, along with the lung cancer risk associated with low-LET exposures.

Table 5-1 compares summary measures of risk per unit dose for the U.S. population derived from the LSS in BEIR VII and from the pooled underground miner studies in BEIR VI. For radon, the estimation of lung dose requires a conversion from radon progeny exposure, measured in working level months (WLM). Estimating this conversion factor involves a model calculation of the deposition of radon progeny in the airways, the distribution of alpha particle energy on a microdosimetric scale, and the relative weights attached to different tissues in the lung (NRC 1999, EPA 2003, James et al. 2004). Results are presented for the dose conversion factor of $\approx 12 \text{ mGy/WLM}$ derived by James et al. (2004), or the lower estimate of 6 mGy/WLM recommended in UNSCEAR 2000a, respectively.

Table 5-1: Lung cancer mortality and RBE

Data Source	Gender	Risk per 10⁶ Person-WLM	Risk per 10⁴ Person-Gy		RBE	
A-bomb mortality	Male	—	140		1.0	
	Female	—	270		1.0	
	Combined	—	210		1.0	
EPA radon risk model	Male	640	800 ¹	1600 ²	5.7 ¹	11.4 ²
	Female	440	550 ¹	1100 ²	2.0 ¹	4.1 ²
	Combined	540	675 ¹	1350 ²	3.2 ¹	6.4 ²

¹ Risk per Gy to the whole lung or RBE calculated assuming: (1) 12 mGy/WLM, on average, to sensitive cells in the bronchial epithelium (James et al. 2004) and (2) lung risk partitioned 1/3 (bronchi): 1/3 (bronchioles): 1/3 (alveoli).

² Calculated assuming 6 mGy/WLM, on average, to sensitive cells in the bronchial epithelium (UNSCEAR 2000a).

When compared to results from animal studies, the inferred alpha-particle RBEs in Table 5-1 may appear to be unreasonably low – especially for females. It should be recognized, however, that the risk model used to derive risk estimates for radon are in certain ways incompatible with the models for low-LET lung cancer risk in BEIR VII. They differ not only with respect to their functional dependence on age, gender, and temporal factors, but also with respect to the interaction with smoking. In contrast to the BEIR VII models, the radon risk models do not incorporate a higher risk coefficient for females or for children. The miner cohorts from the radon models were derived consisted essentially entirely of adult males, and it is possible that radon risks are being underestimated for children and females. The radon risk appears to be almost multiplicative with smoking risk (or the baseline lung cancer rate), whereas the LSS data suggests an additive interaction. It is unclear whether these apparent differences with respect to gender and smoking reflect a real mechanistic difference in carcinogenesis by the two types of radiation exposure (chronic alpha versus acute gamma) or unexplained errors inherent in the various studies.

Lung cancer results from the LSS cohort can also be compared with those on Mayak workers, whose lungs were irradiated by alpha particles emitted by inhaled plutonium (Gilbert et al. 2004), but the results of such an analysis must be viewed critically. The dose from inhaled Pu is highly uncertain, as is the relative sensitivity of different target cells to radiation. Information on smoking in both cohorts is limited. The populations are quite different with respect to gender and age profile. Males account for about 75% of the PY and over 90% of the lung cancers among the internally exposed Mayak workers, but for only about

30% and 55% of the PY and lung cancers, respectively, among the LSS cohort. Another issue is that the dependence of the risk on attained age appears to be quite different in the two studies – a monotonically increasing EAR for the LSS but a sharp decrease in the EAR above age 75 for the Mayak workers. There are, however, very few data on these older Mayak workers. Focusing just on lung cancers appearing between ages 55 and 75, one finds that the central estimates of risk per Sv in the two studies are comparable, consistent with an RBE for alpha particles of 10 or more.

A more recent analysis of the Mayak plutonium worker data, based on improved dosimetry, has been published (Sokolnikov et al. 2008). From a statistical modeling of the lung cancer data, it was estimated that the ERRs per Gy at age 60 were 7.1 for males and 15 for females. For comparison, the LSS study yielded an ERR per Gy of 0.32 and 1.4, respectively, for males and females for exposure age 30 and attained age 60. Thus, the two sets of data together would suggest an RBE of roughly 20 for males and 10 for females.

The risk per unit dose estimate from the plutonium exposed Mayak workers appears to be considerably higher than that from the radon studies despite the fact that the lung dose from radon progeny is projected to be almost entirely to the epithelial lining of the airways, whereas the inhaled plutonium dose is expected to be concentrated in the alveoli, which is generally thought to be a much less sensitive region for cancer induction.

There seems to be no fully satisfactory way to reconcile all the results from the LSS, miner and Mayak worker studies with what one would expect from the dosimetry and experimental determinations of α -particle RBE, even taking into account the sampling errors in the various epidemiological studies. The Mayak study is ongoing, with possible improvements in the dosimetry still to be made; the LSS risk estimates are also somewhat suspect, especially their dependence on gender and age at exposure (see Section 3.2). In particular, it is odd that the risk is higher in females than males among the A-bomb survivors, despite the much lower lung cancer incidence among Japanese women than men. Also, the BEIR VII lung cancer model reflects the negative trend with age at exposure obtained from the analysis of *all solid tumors*, but there are still very little data to directly support a higher *lung cancer* risk for childhood exposures.

5.1.3 Nominal Risk Estimates for Alpha Radiation

Information on alpha-particle RBE_M (relative to γ -irradiation) for induction of cancer is sketchy, especially in humans. Laboratory studies are mostly indicative of a value of about 20, but with likely variability depending on cancer site and animal species or strain. There is also evidence in both animals and humans that the RBE_M is much lower for induction of leukemia. Comparisons of data on lung cancer induction by inhaled radon progeny or plutonium with data on the A-bomb survivors yields somewhat conflicting results, suggesting possible errors in the data or in underlying assumptions regarding the form of the models, internal dosimetry, or the sensitivity of different parts of the lung. At this point, comparisons between the radon data and the LSS data suggest an RBE much lower than 20 for lung cancer induction, but the Mayak results so far fail to substantiate this. Further follow-up of the LSS cohort and additional information on the Mayak workers may help to resolve this issue.

EPA's site-specific α -particle risk estimates will be obtained by applying an RBE of 20 to our γ -ray risk estimates, with three exceptions: 1) an RBE = 2 for leukemia, 2) an RBE = 40 for liver cancer, and 3) continued use of models derived from BEIR VI to estimate lung cancer risk from inhaled radon progeny (NAS 1999, EPA 2002). The low dose, γ -ray risk estimate for bone cancer is obtained by dividing the risk per Gy for α -particles – estimated from patients injected with ^{224}Ra – by an RBE of 10.

Aside from those revisions pertaining to leukemia, liver cancer, and bone cancer described above, this approach is consistent with previous EPA practice except in the case of breast cancer, where previously an RBE of 10 was employed rather than 20 (EPA 1994). The justification for the lower RBE was that the estimated (γ ray) DDREF was 1 for breast cancer but 2 for other solid tumors. The evidence for such a difference in DDREF appears weaker now, and, for simplicity, we are now applying the same nominal DDREF (1.5) and RBE (20) for most solid tumors, including breast.

5.1.4 Uncertainties in Risk Estimates for Alpha Radiation

For most cancer sites, the uncertainty in α -particle risk can be calculated from the combined uncertainties in γ -ray risk, as presented in Section 4, and in α -particle RBE. For solid cancers, EPA previously assigned a lognormal uncertainty distribution to the alpha-particle RBE, with a 90% CI from 5 to 40. The median value is thus ≈ 14.1 and the GSD ≈ 1.88 (EPA 1999a). This distribution still appears reasonable for solid tumors other than liver and bone cancers. The uncertainty distribution for leukemia induced by alpha-emitters deposited in the bone was previously taken to be uniform over the interval [0,1] (EPA 1999a). Based on the more current information discussed above, a lognormal distribution is now assumed, with GM=2 and GSD=1.4.

In the case of α -particle induced liver cancer, EPA is basing its 95% upper confidence limit on the risk estimate derived from the modeling approach of Leenhouts et al. ($4 \times 10^{-1} \text{ Gy}^{-1}$). This upper bound value is consistent with a lognormal distribution with a GM equal to EPA's nominal central estimate of $8 \times 10^{-2} \text{ Gy}^{-1}$ and a GSD of 2.66. The lower 95% confidence limit on the distribution is then $1.6 \times 10^{-2} / \text{Gy}$, which corresponds to what would be inferred from the LSS liver cancer risk estimate in conjunction with an assumed α -particle RBE of 8.

Risk projections for bone cancer are only important when considering internally deposited "bone-seekers." Given the difficulties in estimating the dose to target cells in bone, EPA is deferring the quantification of uncertainty in bone cancer risks until the Agency reevaluates the risks from specific internal emitters.

5.2 Lower Energy Beta Particles and Photons

As energetic electrons lose energy in passing through matter, they become more densely ionizing: i.e., the average distance between ionization events shrinks, and more energy is deposited in ionization clusters. As discussed earlier, such clusters produce DSBs and complex DNA damage that are more difficult for the cell to repair. Indeed it has been suggested that a large fraction of the residual damage caused by low-LET radiation may stem from such clusters produced at the ends of electron tracks (Nikjoo and Goodhead 1991). For this reason, it might also be expected that lower energy beta particles would be more biologically damaging than higher energy betas. Furthermore, since the energy distribution of secondary (Compton) electrons is shifted downward as incident photon energy is reduced, the biological effectiveness of photons might also be expected to rise with decreasing energy, implying that lower energy photons, including medical x rays, which typically have energies below 250 keV, might be more damaging than the gamma rays to which the LSS cohort was exposed.

Results from many studies tend to confirm these predictions for low-LET radiations, including measurements of chromosome aberrations, mutations, cell transformation and cancer induction. The most direct source of data on the subject consists of comparative studies of x- and gamma-ray induction of dicentrics in human lymphocytes. In these studies, 220-250 kVp x rays, which are often used for diagnostic purposes in medicine, generally produced 2-3 times as many dicentrics as ^{60}Co gamma rays (NCRP 1990). The relevance of such findings for cancer induction is unclear, however, since a dicentric will render a cell incapable of cell division. Other laboratory studies directed at ascertaining the RBE for various types of radiation relative to x rays or gamma rays provide additional indirect information, suggesting again that orthovoltage x rays may be a factor of 2-3 times more hazardous than gamma rays with energies above about 250 keV (Kocher et al. 2005, NCRP 1990, NRC 2006). Kocher et al.

further conclude that x rays below 30 keV, such as those used in mammography may have a slightly higher RBE than those in the range 30-250 keV.

Kocher et al. also consider what RBEs should be applied to beta particles. Noting that the average energy of a Compton electron produced by an incident 250 keV photon is 60 keV, they conclude that beta particles above about 60 keV should have about the same RBE as those [photons??] above 250 keV – i.e., ≈ 1.0 . One important radionuclide that emits a substantial fraction of its decay energy in the form of a lower energy beta is ^3H , for which the mean beta energy is 5.7 keV and the maximum is 18.6 keV. For ^3H and other betas with average energy below 15 keV, the authors recommend a lognormal uncertainty distribution with $\text{GM}=2.4$ and a $\text{GSD}=1.4$, corresponding to a 95% CI of (1.2, 5.0). The reference radiation is again chronic gamma rays. In addition, they assign the same probability distribution to the RBE for internal conversion or Auger electrons with energy < 15 keV as for ^3H . This uncertainty range is comparable to what was recommended for <30 keV photons and is generally consistent with experiments in which investigators compared ^3H with gamma rays in the induction of various end-points.

Kocher et al. also state that electrons of energy 15-60 keV would be expected to have about the same RBE as 30-250 keV photons but that direct biological data are lacking.

A review of tritium risks has recently been conducted by an independent advisory group for the Health Protection Agency of the UK (HPA 2007). The authors found that, in a wide variety of cellular and genetic studies, the RBE values for tritiated water were 1-2 when compared with low dose-rate orthovoltage x rays and 2-3 when compared with chronic gamma rays. It was concluded that “an RBE of two compared with high energy gamma radiation would be a sensible value to assume”. Although much of the experimental evidence suggested a value between two and three, fractional values were “not considered appropriate.”

The conclusions of the HPA report were supported by experimental and theoretical evidence (Nikjoo and Goodhead 1991, Goodhead 2006) that the biological effects of low-dose, low-LET radiation predominantly reflect complex DNA damage generated by ionization and excitation events produced by low energy electrons near the ends of their tracks with energies above 100 eV but no more than about 5 keV. Figure 5-1 shows a plot, for various incident radiations, of F , the cumulative fraction of the total dose deposited in an aqueous medium by electrons of energy T (>100 eV). These fractions were estimated by Nikjoo & Goodhead (1991) using track-structure simulation codes and results were found to be similar to those of a numerical approximation method developed by Burch (1957). Assuming that the amount of critical damage is proportional to $F(5 \text{ keV})$, the estimated RBE is ≈ 2.3 for ^3H beta particles and ≈ 1.4 for 220 kV x rays, both relative to ^{60}Co gamma rays or 1 MeV electrons. Alternatively, if the critical

damage is taken to be proportional to $F(1 \text{ keV})$, the estimated RBEs would be ≈ 1.6 for ^3H and ≈ 1.2 for the x rays.

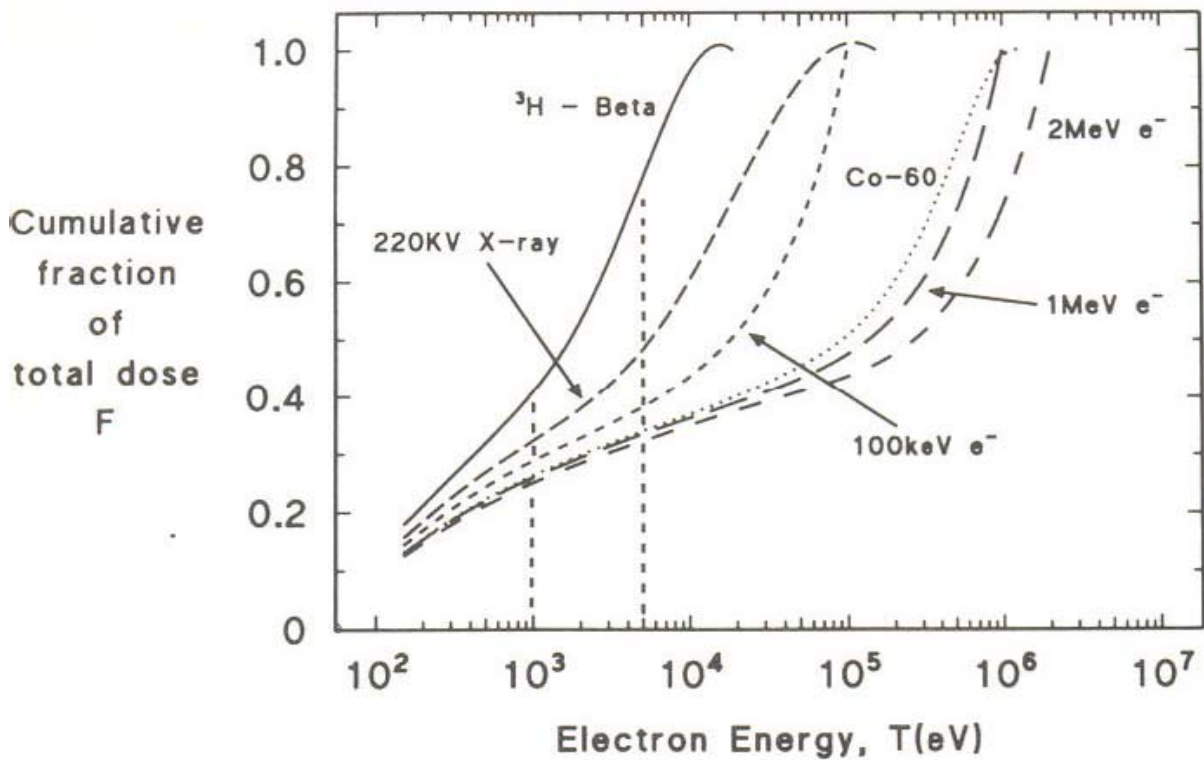


Figure 5-1: Cumulative fraction of the total dose, F , plotted against secondary electron kinetic energies, T , for a variety of low-LET radiations calculated by Nikjoo & Goodhead (1991) using the method of Burch (1957).

By means of a more accurate Monte Carlo procedure, Nikjoo and Goodhead calculated, for each of several initial electron energies, the cumulative fraction of the total dose deposited by electrons with energies between 100 eV and a specified energy. Those results are shown in Figure 5-2. From the figure, it is estimated that the contribution of low-energy (0.1 to 5 keV) electrons to the total dose from an electron with initial energy 10 keV would be $\approx 63\%$, compared to $\approx 51\%$ for an incident 100 keV electron. The authors did not calculate the distribution for higher energy incident electrons, but assuming that the fractional increase in F obtained in applying the Monte Carlo method in place of the Burch approximation is about the same as for 100 keV electrons ($\approx 10\%$), the result would be $\approx 37\%$ for the higher energy electrons or ^{60}Co gamma rays. Using this approach, it should be possible to estimate average RBEs for a whole range of low-energy beta emitters. Furthermore, from spectral information on the secondary electrons produced by a photon source of a given energy, RBEs could also be estimated for photon emitters.

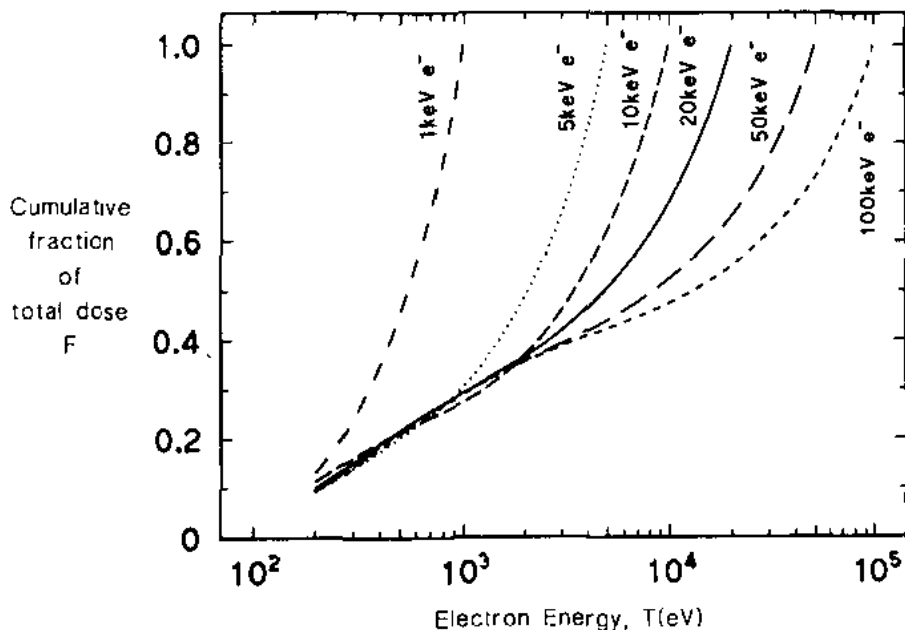


Figure 5-2: Cumulative fraction of total dose, F , plotted against secondary electron kinetic energies, T , for a variety of slow and fast initial electron energies calculated by the Monte Carlo track structure method (Nikjoo and Goodhead, 1991).

No firm conclusions can be drawn from human epidemiological data on the RBE for lower energy photons and electrons. Risk coefficients derived from studies of cohorts medically irradiated with x rays are in some cases lower than what has been observed for the A-bomb survivors. Nevertheless, given the various uncertainties, such as those relating to dosimetry, sampling error, population differences, and possible confounders, it is still possible that medical x rays are significantly more carcinogenic, per unit dose, than gamma rays. This issue can only be resolved through experiment and a better understanding of the dependence of DNA damage and carcinogenesis on microdosimetric parameters.

6. Risks from Prenatal Exposures

First carried out by Stewart and coworkers (Stewart et al. 1958, Bithell and Stewart 1975), case-control studies of childhood cancer have shown about a 40% increase in risk associated with exposure to diagnostic x rays *in utero*. Typically, the x rays employed in Stewart's "Oxford series" were 80 kVp and the mean dose was 6-10 mGy; this corresponds to about 1 photon per cell nucleus. Hence this finding argues against the likelihood of a threshold for radiation carcinogenesis.

The estimate of risk for childhood cancer derived from the Oxford survey is about 0.06 per Gy (95% CI 0.01-0.126) for all cancers and about 0.025 per Gy for leukemia (Mole 1990, Doll and Wakeford 1997). Although numerous other case-control studies have shown a similar radiation-related risk as the Oxford survey (Doll and Wakeford 1997), the evidence from cohort studies is equivocal (Boice and Miller 1999). Children exposed *in utero* to radiation from the atomic bomb explosions have not experienced any detectable increase in cancer, and the derived upper bound is lower than the estimate derived from the case-control studies (Doll and Wakeford 1997). Results from a large cohort study did show an increase in leukemia of about the same magnitude as the Oxford series, but the observed increase in childhood solid tumors was much lower and not statistically significant (Monson and MacMahon 1984). Another question regarding the risk of solid tumors has been that the excess relative risk seen in the case-control studies is about the same, regardless of the type of tumor. This may suggest that the increase is due to some unaccounted for source of confounding (Boice and Miller 1999).

On balance, the evidence from the epidemiological studies indicates that the fetus is at risk of childhood cancer from ionizing radiation (Doll and Wakeford 1997). Following the recommendations of Doll and Wakeford (1997) and the ICRP (2000), EPA adopts the estimate of 0.06 Gy^{-1} for prenatal exposures to diagnostic x rays. Survival rates for childhood cancer are approximately 70-80% for childhood cancer for both leukemia and solid tumors (SEER 2006c, Tables XXVIII-1- and XXIX-6), but this does not include any delayed mortality due to second cancers resulting from the treatment. NCRP cites a value of $5 \times 10^{-2} \text{ Sv}^{-1}$ for fetal exposure to internally deposited radionuclides (NCRP 1998). However, as discussed in Section 5.2, an RBE of about 1.4 for cancer induction should perhaps be assigned to x rays commonly used in medicine. Therefore, in the case of most internally deposited β/γ -emitters or external gamma radiation, a lower risk estimate of $\approx 4 \times 10^{-2} \text{ Gy}^{-1}$ should be applied for childhood cancer incidence.

The studies of medically irradiated fetuses only address the induction of childhood cancers. Epidemiological follow-up of the A-bomb survivors has indicated that individuals irradiated *in utero* may have a lower risk of adult cancers than those irradiated as young children, but the difference is not

statistically significant (Preston et al. 2008). Based on this finding, we adopt the same set of models employed for calculating risk for exposure to young children to assess the risk of adult cancers caused by *in utero* exposure. More specifically, we directly applied the risk models of Section 3 with age-at-exposure set to 0. The sex-averaged projected risk for adult cancers (attained age > 15) is 0.29 per Gy for incidence and 0.12 per Gy for mortality. This risk is a factor of 2-3 times higher than that for the general U.S. population. It is also about a factor of 5 times the estimated risk of a radiogenic childhood cancer from prenatal exposures. Nevertheless it constitutes only a small fraction (<3%) of the risk from a uniform whole-body exposure to the U.S. population.

7. Radionuclide Risk Coefficients

Subsequent to publication of this report, EPA will use its revised radiation risk models and ICRP's latest dosimetric models to update the radionuclide risk coefficients in Federal Guidance Report 13 (EPA 1999b). Radionuclide risk coefficients are EPA's best estimates of the lifetime excess mortality or morbidity risk per unit intake of a given radionuclide by ingestion or inhalation, or per unit exposure for external irradiation. The current version of FGR 13 contains risk coefficients for environmental exposure to over 800 radionuclides.

Based on the values in Table 3-12, EPA expects that updated mortality risk coefficients for those radionuclides that irradiate the body uniformly will be similar to currently published values, whereas corresponding morbidity risk coefficients will likely increase by about 20%. For radionuclides irradiating the body nonuniformly, EPA anticipates both increases and decreases, depending on the target organ. For example, updated risk coefficients for inhaled radionuclides retained in the lung may be larger than present estimates because the population-averaged lung cancer risk has increased substantially over time. Conversely, updated risk coefficients for radionuclides that are poorly absorbed from the intestines into the bloodstream and that emit short-range radiation, especially alpha particles, should be smaller than current values because of reduction in colon cancer risk and adoption of new ICRP alimentary tract models (ICRP 2009) that place the location of target cells in the intestinal wall out of range of alpha particles emitted from the contents of the colon.

REFERENCES

- Andersson M, M Vyberg, J Visfeldt, B Carstensen and HH Storm. 1994. Primary liver tumours among Danish patients exposed to Thorotrast. *Radiat Res* **137**: 262-273.
- Arias E, LR Curtin, RW Wei, RN Anderson. 2008. *U.S. Decennial Life Tables for 1999-2001, United States Life Tables. National Vital Statistics Reports, Vol 57 No 1*. Hyattsville, Maryland: National Center for Health Statistics. Accessed 10/31/08 at CDC web-site:
http://www.cdc.gov/nchs/data/nvsr/nvsr57/nvsr57_01.pdf
- Azzam EI, SM de Toledo, GP Raaphorst, REJ Mitchel. 1996. Low-dose ionizing radiation decreases the frequency of neoplastic transformation to a level below the spontaneous rate in C3H 10T1/2 cells. *Radiat Res* **146**: 369-373.
- Azzam EI, SM de Toledo, T Gooding, JB Little. 1998. Intercellular communication is involved in the bystander regulation of gene expression in human cells exposed to very low fluences of alpha particles. *Radiat Res* **150**: 497-504.
- Bauer S, BI Gusev, LM Pivina, KN Apsalikov, B Grösche. 2005. Radiation exposure to local fallout from Soviet atmospheric nuclear weapons testing in Kazakhstan: solid cancer mortality in the Semipalatinsk historical cohort, 1960-1999. *Radiat Res* **164**: 409-419.
- Bijwaard H, MJP Brugmans, HP Leenhouts. 2004. Two-mutation model for bone cancer due to radium, strontium and plutonium. *Radiat Res* **162**: 171-184.
- Bland KI, HR Menck, CEH Scott-Conner, M Morrow, DJ Winchester, and DP Winchester. 1998. The national cancer data base 10-year survey of breast carcinoma treatment at hospitals in the United States. *Cancer* **83**: 1262-1273.
- Boice JD, Jr., G Engholm, RA Kleinerman, M Blettner, M Stovall, H Lisco, et al. 1988. Radiation dose and second cancer risk in patients treated for cancer of the cervix. *Radiat Res* **116**: 3-55.
- Boice JD, Jr., D Preston, FG Davis, RR Monson. 1988. Frequent chest X-ray fluoroscopy and breast cancer incidence among tuberculosis patients in Massachusetts. *Radiat Res* **125**: 214-222.
- Boice JD, Jr., RW Miller. 1999. Childhood and adult cancer after intrauterine exposure to ionizing radiation. *Teratol* **59**: 227-233.

Brenner DJ, R Doll, DT Goodhead, EJ Hall, CE Land, JB Little, et al. 2003. Cancer risks attributable to low doses of ionizing radiation: Assessing what we really know. PNAS **100**: 13761-13766.

Brenner DJ, RK Sachs. 2003. Domestic radon risks may be dominated by bystander effects—but the risks are unlikely to be greater than we thought. Health Phys **85**: 103-108.

Brenner DJ, RK Sachs. 2006. Estimating radiation-induced cancer risks at very low doses: rationale for using the linear no-threshold approach. Radiat Environ Biophys **44**: 253-256.

Breslow NE, NE Day. 1987. Statistical Methods in Cancer Research. Volume II: The Design and Analysis of Cohort Studies. International Agency for Research on Cancer. Lyon.

Burch PRJ. 1957. Some physical aspects of relative biological efficiency. Br J Radiol **30**: 524-529.

Cardis E, M Vrijheid, M Blettner, E Gilbert, M Hakama, C Hill, et al. 2005. Risk of cancer after low doses of ionising radiation: retrospective cohort study in 15 countries. BMJ **331**: 77 doi:10.1136/bmj.38499.599861.E0 (published 29 June 2005).

Cardis E, M Vrijheid, M Blettner, E Gilbert, M Hakama, C Hill, et al. 2007. The 15-country collaborative study of cancer risk among radiation workers in the nuclear industry: Estimates of radiation-related cancer risks. Radiat Res **167**: 396-416.

CDC (Centers for Disease Control) and NCI (National Cancer Institute). U.S. Cancer Statistics Working Group. 2005. *United States Cancer Statistics: 2002 Incidence and Mortality*. Atlanta: U.S. Department of Health and Human Services, Centers for Disease Control and Prevention and National Cancer Institute. Accessed 7/24/06 at CDC web-site: http://www.cdc.gov/cancer/npcr/uscs/pdf/2002_uscs.pdf

Coates PJ, SA Lorimore, EG Wright. 2004. Damaging and protective cell signalling in the untargeted effects of ionizing radiation. Mutat Res **568**: 5-20.

Cornforth MN, SM Bailey, EH Goodwin. 2002. dose responses for chromosome aberrations produced in noncycling primary human fibroblasts by alpha particles, and gamma rays delivered at sublimiting low dose rates. Radiat Res **158**: 43-53.

Cronin K, E Feuer, M Wesley, A Mariotto, S Scoppa, D Green. 2003. Current Estimates for 5 and 10 Year Relative Survival. Statistical Research and Applications Branch, National Cancer Institute; Technical Report #2003-04. Accessed 10/17/08 at NCI website: <http://srab.cancer.gov/reports/tech2003.04.pdf>

Darby S, D Hill, A Auvinen, JM Barros-Dios, H Baysson, F Bochicchio, H Deo, et al. 2005. Radon in homes and risk of lung cancer: collaborative analysis of individual data from 13 European case-control studies. *BMJ* **330**: 223.

Delongchamp RR, K Mabuchi, Y Yoshimoto, DL Preston. 1997. Cancer mortality among atomic bomb survivors exposed to *in utero* or as young children, October 1950-May 1992. *Radiat Res* **147**: 385-395.

Doll R, R Wakeford. 1997. Risk of childhood cancer from fetal irradiation. *Brit J Radiol* **70**: 130-139.

Doody MM, JE Lonstein, M Stovall, DG Hacker, N Luckyanov, CE Land. 2000. Breast cancer mortality after diagnostic radiography: Findings from the U.S. Scoliosis Cohort Study. *Spine* **25**: 2052-2063.

Edwards AA. 1999. Neutron RBE values and their relationship to judgements in radiological protection. *J Radiol Prot* **19**: 93-105.

Elkind MM. 1994. Radon-induced cancer: a cell-based model of tumorigenesis due to protracted exposures. *Int J Radiat Biol* **66**: 649-653.

Elmore E, X-Y Lao, R Kapadia, E Gedzinski, C Limoli, JL Redpath. 2008. Low doses of very low-dose-rate low-LET radiation suppress radiation-induced neoplastic transformation *in vitro* and induce an adaptive response. *Radiat Res* **169**: 311-318.

EPA (Environmental Protection Agency). 1994. Estimating Radiogenic Cancer Risks. EPA Report 402-R-93-076, Washington, DC: U.S. EPA.

EPA (Environmental Protection Agency). 1999a. Estimating Radiogenic Cancer Risks. Addendum: Uncertainty Analysis. EPA Report 402-R-99-003, Washington, DC: U.S. EPA.

EPA (Environmental Protection Agency). 1999b. Cancer Risk Coefficients for Environmental Exposure to Radionuclides. EPA Report 402-R-99-001, Washington, DC: U.S. EPA.

EPA (Environmental Protection Agency). 2003. EPA Assessment of Risks from Radon in Homes. EPA Report 402-R-03-003, Washington, DC: U.S. EPA.

Gilbert ES. 1991. Chapter 3: Late somatic effects. In: S Abrahamson, MA Bender, BB Boecker et al. *Health Effects Models for Nuclear Power Plant Accident Consequence Analysis. Modifications of Models Resulting from Recent Reports on Health Effects of Ionizing Radiation, Low LET Radiation, Part II*:

Scientific Bases for Health Effects Models. NUREG/CR-4214, Rev. 1, Part II, Addendum 1, LMF-132, U.S. Nuclear Regulatory Commission, Washington, DC.

Gilbert ES, NA Koshurnikova, ME Sokolnikov, et al. 2000. Liver cancers in Mayak workers. *Radiat Res* **154**: 246-252.

Gilbert ES, NA Koshurnikova, ME Sokolnikov, et al. 2004. Lung cancer in Mayak workers. *Radiat Res* **162**: 505-516.

Goodhead DT. 2006. Energy deposition stochastics and track structure: What about the target? *Radiat Prot Dosim* **122**: 3-15.

Grogan HA, WK Sinclair, PG Voillequé. 2001. Risks of fatal cancer from inhalation of 239,240 plutonium by humans: a combined four-method approach with uncertainty evaluation. *Health Phys* **80**: 447-461.

Hahn FF, BA Muggenburg, RA Guilmette, BB Boecker. 1999. Comparative stochastic effects of inhaled alpha- and beta-particle-emitting radionuclides in beagle dogs. *Radiat Res* **152**: S19-S22.

Harrison JD, CR Muirhead. 2003. Quantitative comparisons of induction in humans by internally deposited radionuclides and external radiation. *Int J Radiat Biol* **79**:1-13.

Hatch M, E Ron, A Bouville, L Zablotska, G Howe. 2005. The Chernobyl disaster: Cancer following the accident at the Chernobyl Nuclear Power Plant. *Epidemiol Rev* **27**: 56-66.

Hildreth NG, RE Shore and PM Dvoretzky. 1989. The risk of breast cancer after irradiation of the thymus in infancy. *N Engl J Med* **321**: 1281-1284.

Howe GR, J McLaughlin. 1996. Breast cancer mortality between 1950 and 1987 after exposure to fractionated moderate-dose-rate ionizing radiation in the Canadian fluoroscopy cohort study and a comparison with breast cancer mortality in the atomic bomb survivors study. *Radiat Res* **145**: 694-707.

HPA (Health Protection Agency) (UK). 2007. *Review of Risks from Tritium*. Report of the Independent Advisory Group on Ionising Radiation. Available at: www.hpa.org.uk/publications/2007/tritium_advice/RCE_Advice_on_tritium.pdf

Hwang S-L, J-S Hwang, Y-T Yang, WA Hsieh, T-C Chang, H-R Guo, M-H Tsai, J-L Tang, I-F Lin, WP Chang. 2008. Estimates of relative risks for cancers in a population after prolonged low-dose-rate radiation exposure: A follow-up assessment from 1983 to 2005. *Radiat Res* **170**: 143-148.

ICRP (International Commission on Radiological Protection). 1991. 1990 Recommendations of the International Commission on Radiological Protection. ICRP Publication 60. Ann ICRP **21**(1-3).

ICRP (International Commission on Radiological Protection). 1991. The Biological Basis for Dose Limitation in the Skin. ICRP Publication 59. Ann ICRP **22**(2).

ICRP (International Commission on Radiological Protection). 1993. Age-dependent Doses to Members of the Public from Intake of Radionuclides: Part 2. Ingestion Dose Coefficients. ICRP Publication 67. Ann ICRP **23**(3/4).

ICRP (International Commission on Radiological Protection). 2000. Pregnancy and Medical Radiation. ICRP Publication 84. Ann ICRP **30**(1).

ICRP (International Commission on Radiological Protection). 2003. Relative Biological Effectiveness (RBE), Quality Factor (Q), and Radiation Weighting Factor (w_R). ICRP Publication 92. Ann ICRP **33**(4).

Ishikawa Y, JAH Humphreys, CG Collier, ND Priest, Y Kato, T Mori, R Machinami. 1999. Revised organ partition of thorium-232 in Thorotrast patients. Radiat Res **152**: S102-S106.

James AC, A Birchall, G Akabani. 2004. Comparative dosimetry of BEIR VI revisited. Radiat Prot Dosimetry **108**: 3-26.

Kadhim MA, DA MacDonald, DT Goodhead, SA Lorimore, SJ Marsden, EG Wright. 1992. Transmission of chromosomal instability after plutonium alpha-particle irradiation. Nature **355**: 738-740.

Kadhim MA, SR Moore, EH Goodwin. 2004. Interrelationships amongst radiation-induced genomic instability, bystander effects, and the adaptive response. Mutat Res **568**: 21-32.

Karagas MR, ER Greenberg, SK Spencer, TA Stukel, LA Mott. 1999. The New Hampshire Skin Cancer Study Group. Increase in incidence rates of basal cell and squamous cell skin cancer in New Hampshire, USA. *Int J Cancer* **81**: 555-559.

Kocher, DC, AI Apostoaei, FO Hoffman. 2005. Radiation effectiveness factors for use in calculating probability of causation of radiogenic cancers. Health Phys **89**:3-32.

Kocher DC, AI Apostoaei, RW Henshaw, FO Hoffman, MK Schubauer-Berigan, DO Stancescu, BA Thomas, JR Trabalka, ES Gilbert, CE Land. 2008. Interactive Radioepidemiological Program (IREP): A Web-based tool for estimating

probability of causation/assigned share of radiogenic cancers. *Health Phys* **95**: 119-147.

Koshurnikova, NA, ES Gilbert, M Sokolnikov, VF Khokhryakov, S Miller, DL Preston, SA Romanov, NS Shilnikova, KG Suslova, VV Vostrotin. 2000. Bone cancers in Mayak workers. *Radiat Res* **154**: 237-245.

Krestinina LY, DL Preston, EV Ostroumova, MO Degteva, E Ron, OV Vyushkova, et al. 2005. Protracted radiation exposure and cancer mortality in the Techa River Cohort. *Radiat Res* **164**: 602-611.

Krewski D, JH Lubin, JM Zielinski, M Alavanja, VS Catalan, RW Field, JB Klotz et al. 2005. Residential radon and the risk of lung cancer: A combined analysis of 7 North American case-control studies. *Epidemiol* **16**: 137-145.

Land CE. 1980. Estimating cancer risks from low doses of ionizing radiation. *Science* **209**:1197-1203.

Land CE, WK Sinclair. 1991. The relative contributions of different organ sites to the total cancer mortality associated with low-dose radiation exposure. In: *Risks Associated with Ionising Radiations*, *Annals of the ICRP* **22 (1)**.

Leenhouts HP, MJP Brugmans, M Andersson, HH Storm. 2002. A reanalysis of liver cancer incidence in Danish patients administered Thorotrast using a two-mutation carcinogenesis model. *Radiat Res* **158**: 597-606.

Lehnert BE, EH Goodwin, A Deshpande. 1997. Extracellular factor(s) following exposure to alpha particles can cause sister chromatid exchanges in normal human cells. *Cancer Res* **57**: 2164-2171.

Lewis EB. 1963. Leukemia, multiple myeloma, and aplastic anemia in American radiologists. *Science* **142**: 1492-1494.

Lewis KG, MA Weinstock. 2004. Nonmelanoma skin cancer mortality (1988-2000). The Rhode Island follow-back study. *Arch Dermatol* **140**: 837-842.

Little JB, H Nagasawa, T Pfenning, H Vetrovs. 1997. Radiation-induced genomic instability: delayed mutagenic and cytogenetic effects of X-rays and α -particles. *Radiat Res* **148**: 299-307.

Little MP, DG Hoel, J Molitor, JD Boice Jr., R Wakeford, CR Muirhead. 2008. New models for evaluation of radiation-induced lifetime cancer risk and its uncertainty employed in the UNSCEAR 2006 report. *Radiat Res* **169**: 660-676.

Löbrich M, N Rief, M Kühne, M Heckmann, J Fleckenstein, C Rübe, M Uder. 2005. *In vivo* formation and repair of DNA double-strand breaks after computed tomography examinations. *PNAS* **102**: 8984-8989.

Loucas BD, R Eberle, SM Bailey, MN Cornforth. 2004. Influence of dose rate on the induction of simple and complex chromosome exchanges by gamma rays. *Radiat Res* **162**: 339-349.

Lunn DJ, A Thomas, N Best, D Spiegelhalter. 2000. WinBUGS – a Bayesian modeling framework: concepts, structure, and extensibility. *Stat Comput* **10**: 325-337.

Lyng FM, CB Seymour, C Mothersill. 2000. Production of a signal by irradiated cells which leads to a response in unirradiated cells characteristic of initiation of apoptosis. *Brit J Cancer* **83**: 1223-1230.

Marková E, N Schultz, IY Belyaev. 2007. Kinetics and dose-response of residual 53BP1/ γ -H2AX foci: Co-localization, relationship with DSB repair and clonogenic survival. *Internat J Radiat Biol* **83**: 319-329.

Marples B, MC Joiner. 1993. The response of Chinese hamster V79 cells to low radiation doses: Evidence of enhanced sensitivity of the whole cell population. *Radiat Res* **133**: 41-51.

Mays CW, H Speiss. 1972. Bone sarcoma incidence vs. alpha particle dose. Pp. 409-430 in *Radiobiology of Plutonium*, BJ Stover and WSS Jee, eds. Salt Lake City: The J.W. Press.

Mays CW, RE Rowland, AF Stehney. 1985. Cancer risk from lifetime intake of Ra and U isotopes. *Health Phys* **48**: 635-647.

Mitchell SA, G Randers-Pehrson, DJ Brenner, EJ Hall. 2004. The bystander response in C3H 10T $\frac{1}{2}$ cells: the influence of cell-to-cell contact. *Radiat Res* **161**: 397-401.

Mole RH. 1990. Childhood cancer after prenatal exposure to diagnostic X-ray examinations in Britain. *Br J Cancer* **62**: 152-168.

Morgan WF, JP Day, MI Kaplan, EM McGhee, CL Limoli. 1996. Genomic instability induced by ionizing radiation. *Radiat Res* **146**: 247-258.

Mothersill C, CB Seymour. 1998. Cell-cell contact during gamma irradiation is not required to induce a bystander effect in normal human keratinocytes: evidence for release during irradiation of a signal controlling survival into the medium. *Radiat Res* **149**: 256-262.

NCHS (National Center for Health Statistics). 2004. Bridged-Race Population Estimates, United States, 1990 - 2004, By Age Groups. Compiled from the April 1, 2000 resident population developed by the Bureau of the Census in collaboration with the NCHS – accessed from the CDC WONDER On-line Database on June 3, 2006.

NCRP (National Council on Radiation Protection and Measurements). 1980. *Influence of Dose and Its Distribution in Time on Dose-Response Relationships for Low-LET Radiations. NCRP Report No. 64.* Bethesda, MD: National Council on Radiation Protection and Measurements.

NCRP (National Council on Radiation Protection and Measurements). 1985. *Induction of Thyroid Cancer by Ionizing Radiation. NCRP Report No. 80.* Bethesda, MD: National Council on Radiation Protection and Measurements.

NCRP (National Council on Radiation Protection and Measurements). 1990. *The Relative Effectiveness of Radiations of Different Quality. NCRP Report No. 104.* Bethesda, MD: National Council on Radiation Protection and Measurements.

NCRP (National Council on Radiation Protection and Measurements). 1998. *Radionuclide Exposure of the Embryo/Fetus. NCRP Report No. 128.* Bethesda, MD: National Council on Radiation Protection and Measurements.

NCRP (National Council on Radiation Protection and Measurements). 2001. *Evaluation of the Linear-Nonthreshold Dose-Response Model for Ionizing Radiation. NCRP Report No. 136.* Bethesda, MD: National Council on Radiation Protection and Measurements.

Nekolla EA, M Kreisheimer, AM Kellerer, M Kuse-Isingschulte, W Gössner, H Speiss. 2000. Induction of malignant bone cancers in radium-224 patients: risk estimates based on improved dosimetry. *Radiat Res* **153**: 93-103.

Nikjoo H and DT Goodhead. 1991. Track structure analysis illustrating the prominent role of low-energy electrons in radiobiological effects of low-LET radiations. *Phys Med Biol* **36**: 229-238.

Nikjoo H, S Uehara, WE Wilson, M Hoshi and DT Goodhead. 1998. Track structure in radiation biology: theory and applications. *Int J Radiat Biol* **73**: 355-364.

NIOSH (National Institute for Occupational Safety and Health). 2002. NIOSH-Interactive RadioEpidemiological Program (NIOSH-IREP), Technical Documentation. Cincinnati, OH: National Institute for Occupational Safety and Health. Available at: <http://www.cdc.gov/niosh/ocas/pfs/irep/irepfnl.pdf>. Accessed 6/06.

NRC (National Research Council). 1988. *Health Effects of Radon and Other Internally Deposited Alpha-Emitters (BEIR IV)*. Washington, DC: National Academy Press.

NRC (National Research Council). 1990. *Health Effects of Exposure to Low Levels of Ionizing Radiation. (BEIR V)*. Washington, DC: National Academy Press.

NRC (National Research Council). 1999. *Health Effects of Exposure to Radon. BEIR VI*. Washington, DC: National Academy Press.

NRC (National Research Council). 2006. *Health Risks from Exposure to Low Levels of Ionizing Radiation. BEIR VII Phase 2*. Washington, DC: National Academy Press.

Ostroumova E, B Gagnière, D Laurier, N Gudkova, L Krestinina, P Verger, et al. 2006. Risk analysis of leukemia incidence among people living along the Techa River: a nested case-control study. *J Radiol Prot* **26**: 17-32.

Pierce DA, GB Sharp and K Mabuchi. 2003. Joint effects of radiation and smoking on lung cancer risk among atomic bomb survivors. *Radiat Res* **159**: 511-520.

Pierce DA, M Vaeth, and Y Shimizu. 2007. Selection bias in cancer risk estimation from A-bomb survivors. *Radiat Res* **167**: 735-741.

Pierce DA, M Vaeth, and JB Cologne. 2008. Allowance for random dose estimation errors in atomic bomb survivor studies: a revision. *Radiat Res* **170**: 118-126.

Portess, DI, G Bauer, MA Hill, P O'Neill. 2007. Low-dose irradiation of nontransformed cells stimulates the selective removal of precancerous cells via intercellular induction of apoptosis. *Cancer Res* **67**: 1246-1253.

Pottern LM, MM Kaplan, PR Larsen, JE Silva, RJ Koenig, JH Lubin, et al. 1990. Thyroid nodularity after irradiation for lymphoid hyperplasia: A comparison of questionnaire and clinical findings. *J Clin Epidemiol* **43**: 449-460.

Preston DL, H Cullings, A Suyama, S Funamoto, N Nishi, M Soda, K Mabuchi, K Kodama, F Kasagi, RE Shore. 2008. Solid cancer incidence in atomic bomb survivors exposed in utero or as young children. *JNCI*, in press.

Preston DL, A Mattsson, E Holmberg, R Shore, NG Hildreth, JD Boice Jr. 2002. Radiation effects on breast cancer risk: a pooled analysis of eight cohorts. *Radiat Res* **158**: 220-235.

Preston DL, DA Pierce, Y Shimizu, HM Cullings, S Fujita, S Funamoto, K Kodama. 2004. Effects of recent changes in atomic bomb survivor dosimetry on cancer mortality risk estimates. *Radiat Res* **162**: 377-389.

Preston, DL, E Ron, S Tokuoka, S Funamoto, N Nishi, M Soda, K Mabuchi, K Kodama. 2007. Solid cancer incidence in atomic bomb survivors: 1958-1998. *Radiat Res* **168**:1-64.

Priest ND, DG Hoel, PN Brooks. 2006. Relative toxicity of chronic irradiation by ⁴⁵Ca beta particles and ²⁴²Cm alpha particles with respect to the production of lung tumors in CBA/Ca mice. *Radiat Res* **166**: 782-793.

Puskin JS. 2008. What can epidemiology tell us about risks at low doses? *Radiat Res* **169**: 122-124.

Raabe O, SA Book, NJ Parks. 1983. Lifetime bone cancer dose-response relationships in beagles and people from skeletal burdens of ²²⁶Ra and ⁹⁰Sr. *Health Phys.* **44**: 33-48.

Ramsey ML. 2006. Basal Cell Carcinoma. eMedicine web-site, www.emedicine.com/derm/topic47.htm, last updated May 9, 2006.

Redpath JL, RJ Antoniono. Induction of an adaptive response against spontaneous neoplastic transformation *in vitro* by low-dose gamma radiation. 1998. *Radiat Res* **149**: 517-520.

Ries LAG, D Harkins, M Krapcho, A Mariotto et al. (eds). 2006. *SEER Cancer Statistics Review, 1975-2003*, National Cancer Institute. Bethesda, MD, http://seer.cancer.gov/csr/1975_2003/, based on November 2005 SEER data submission, posted to the SEER web site, 2006.

Ries LAG, Young JL, Keel GE, Eisner MP, Lin YD, Horner M-J (editors). SEER Survival Monograph: Cancer Survival Among Adults: U.S. SEER Program, 1988-2001, Patient and Tumor Characteristics. National Cancer Institute, SEER Program, NIH Pub. No. 07-6215, Bethesda, MD, 2007.

Ries LAG, Melbert D, Krapcho M, Stinchcomb DG, Howlader N, Horner MJ, Mariotto A, Miller BA, Feuer EJ, Altekruse SF, Lewis DR, Clegg L, Eisner MP, Reichman M, Edwards BK (eds). *SEER Cancer Statistics Review, 1975-2005*, National Cancer Institute. Bethesda, MD, http://seer.cancer.gov/csr/1975_2005/, based on November 2007 SEER data submission, posted to the SEER web site, 2008.

Roesch WC. 1987. Radiation Effects Research Foundation and the National Academy of Sciences (U.S.). US-Japan joint reassessment of atomic bomb

radiation dosimetry in Hiroshima and Nagasaki. Minami-ku, Hiroshima: Radiation Effects Research Foundation.

Ron E, B Modan, D Preston, E Alfandary, M Stovall, JD Boice Jr. 1989. Thyroid neoplasia following low-dose radiation in childhood. *Radiat Res* **120**: 516-531.

Ron E, JH Lubin, RE Shore, K Mabuchi, B Modan, L Pottern, AB Schneider, MA Tucker, JD Boice. 1995. Thyroid cancer after exposure to external radiation: a pooled analysis of seven studies. *Radiat Res* **141**: 259-277.

Ron E, B Modan, DL Preston, E Alfandary, M Stovall, JD Boice. 1989. Thyroid neoplasia following low-dose radiation in childhood. *Radiat Res* **120**: 516-531.

Ron E, DL Preston, M Kishikawa, T Kobuke, M Iseki, S Tokuoka, M Tokunaga, K Mabuchi. 1998. Skin tumor risk among atomic-bomb survivors in Japan. *Cancer Causes and Control* **9**, 393-401.

Rossi HH, AM Kellerer. 1986. The dose rate dependence of oncogenic transformation by neutrons may be due to variation of response during the cell cycle (Letter to the Editor). *Int J Radiat Biol* **47**: 731-734.

Rothkamm K, M Löbrich. 2003. Evidence for a lack of DNA double-strand break repair in human cells exposed to very low x-ray doses. *PNAS* **100**: 5057-5062.

Sasaki MS, T Nomura, Y Ejima, H Utsumi, S Endo, I Saito, T Itoh, M Hoshi. 2008. Experimental derivation of relative biological effectiveness of A-bomb neutrons in Hiroshima and Nagasaki and implications for risk assessment. *Radiat Res* **170**: 101-117.

Schneider AB, E Ron, J Lubin, M Stovall, TC Gierlowski. 1993. Dose-response relationships for radiation-induced thyroid cancer and thyroid nodules: Evidence for the prolonged effects of radiation on the thyroid. *J Clin Endocrinol Metab* **77**: 362-369.

(SEER 2007a). Surveillance, Epidemiology, and End Results (SEER) Program (www.seer.cancer.gov) SEER*Stat Database: Incidence and Mortality – SEER 13 Regs Public-Use, Nov 2007 Sub (1992-2005), National Cancer Institute, DCCPS, Surveillance Research Program, Cancer Statistics Branch, released April 2008, based on the November 2007 submission.

(SEER 2007b). Surveillance, Epidemiology, and End Results (SEER) Program (www.seer.cancer.gov) SEER*Stat Database: Incidence – SEER 17 Regs Public-Use, Nov 2007 Sub (2000-2005), National Cancer Institute, DCCPS, Surveillance Research Program, Cancer Statistics Branch, released April 2008, based on the November 2007 submission.

Shilnikova NS, DL Preston, E Ron, ES Gilbert, EK Vassilenko, SA Romanov, et al. 2003. Cancer mortality risk among workers at the Mayak Nuclear Complex. *Radiat. Res.* **159**: 787-798.

Shore RE. 1990. Overview of radiation-induced skin cancer in humans. *Int J Radiat Biol* **57**:809-827.

Shore RE, N Hildreth, E Woodard, P Dvoretzky. 1986. Breast cancer among women given x-ray therapy for acute postpartum mastitis. *J Natl Cancer Inst* **77**: 689-696.

Shore RE, N Hildreth, P Dvoretzky, E Andresen, M Moscsos, and B Pasternak. 1993. Thyroid cancer among persons given x-ray treatment in infancy for an enlarged thymus gland. *Am J Epidemiol* **137**:1068-1080.

Shore RE. 2001. Radiation-induced skin cancer in humans. *Med Pediat Oncol* **36**:549-554.

Smith PG, R Doll. 1981. Mortality from cancer and all causes among British radiologists. *Br J Radiol* **49**: 187-194.

Sokolnikov ME, ES Gilbert, DL Preston, NS Shilnikova, VV Khokhryakov, EK Vasilenko, NA Koshurnikova. 2008. Lung, liver, and bone cancer mortality in Mayak workers. *Int J Cancer* **123**: 905-911.

Stewart A, J Webb, D Hewitt. 1958. A survey of childhood malignancies. *Br Med J* **1**: 1495-1508.

Tapio S, V Jacob. 2007. Radioadaptive response revisited. *Radiat Environ Biophys* **46**: 1-12.

Thompson DE, K Mabuchi, E Ron, M Soda, S Tokunaga, S Ochikubo et al. 1994. Cancer incidence in atomic bomb survivors. Part II: Solid tumors, 1958-1987. *Radiat Res* **137 (Suppl.)**: S17-S67.

Tucker MA, PH Morris, J Jones, D Boice, Jr., LL Robison, BJ Stone, M Stovall et al. 1991. Therapeutic radiation at a young age is linked to secondary thyroid cancer. *Cancer Res* **51**: 2885-2888.

Tubiana M, A Aurengo, D Averbeck, A Bonnin, B Le Guen, R Masse, et al. 2005. Dose-effect relationships and the estimation of the carcinogenic effects of low doses of ionizing radiation. Institut de France Académie des Sciences, Paris. (www.academie-sciences.fr/publications/rapports/pdf/dose_effet_07_04_05_gb.pdf)

Ullrich RL, RJ Preston. 1987. Myeloid leukemia in male RFM mice following irradiation with fission spectrum neutrons or gamma-rays. *Radiat Res* **109**:165-170.

UNSCEAR. 1993. United Nations Scientific Committee on the Effects of Atomic Radiation. UNSCEAR 1993 Report to the General Assembly with Scientific Annexes. United Nations, New York.

UNSCEAR. 2000a. United Nations Scientific Committee on the Effects of Atomic Radiation. UNSCEAR 2000 Report to the General Assembly with Scientific Annexes. Volume I: Sources. United Nations, New York.

UNSCEAR. 2000b. United Nations Scientific Committee on the Effects of Atomic Radiation. UNSCEAR 2000 Report to the General Assembly with Scientific Annexes. Volume II: Effects. United Nations, New York.

Van Kaick G, A Dalheimer, S Hornik, A Kaul, D Liebermann, H Luhrs, et al. 1999. The German Thorotrast study: recent results and assessment of risks. *Radiat Res* **152**: S64-S71.

Wang J-X, JD Boice Jr, B-X Li, J-Y Zhang, JF Fraumeni Jr. 1988. Cancer among medical diagnostic x-ray workers in China. *J Natl Cancer Inst* **80**: 344-350.

Weinstock MA. 1994. Epidemiologic investigation of nonmelanoma skin cancer mortality: the Rhode Island follow-back study. *J Invest Dermatol* **102**:65-95.

Wick RR, EA Nekolla, W Gössner, AM Kellerer. 1999. Late effects in ankylosing spondylitis patients treated with ²²⁴Ra. *Radiat Res* **152**: S8-S11.

Wick RR, EA Nekolla, M Gaubitz, TL Schulte. 2008. Increased risk of myeloid leukaemia in patients with ankylosing spondylitis following treatment with radium-224. *Rheumatology* **47**: 855-859.

Young RW and GW Kerr, Eds. Reassessment of the Atomic Bomb Radiation Dosimetry for Hiroshima and Nagasaki: Dosimetry System 2002. Radiation Effects Research Foundation. Hiroshima, 2005.

GLOSSARY

Absorbed dose: The energy deposited by ionizing radiation per unit mass of tissue irradiated. It can be expressed in units of gray (Gy) or milligray (mGy) where 1 Gy = 1000 mGy.

Adaptive response: A reduced response to IR radiation induced by a prior dose.

Alpha particle: A particle consisting of two protons and two neutrons emitted from a decay of certain heavy atomic nuclei. A type of high-LET IR.

Apoptosis: Programmed cell death.

BCC: Basal cell carcinoma.

Baseline cancer rate: The cancer mortality or incidence rate in a population in the absence of the specific exposure being studied.

Bayesian: A statistical approach in which probability reflects the state of knowledge about a variable, often incorporating subjective judgment.

BEIR VII: A National Research Council Report, *Health Risks from Exposure to Low Levels of Ionizing Radiation. BEIR VII. Phase 2.*

Beta particle: An electron emitted from a decay of an atomic nucleus. A type of low-LET IR.

Bystander effect: A change in a cell due to irradiation of a nearby cell.

Confidence Interval (CI): A range of values calculated from sample observations that are believed, with a particular probability to contain the true parameter value. Upper and lower values of a CI are called confidence limits. A 90% CI implies that if the estimation process were repeated many times, about 90% of the intervals would contain the true value. The 90% probability refers to the properties of the interval and not the parameter itself.

Confounder: In an epidemiological study, a factor that is associated with both the exposure and outcome of interest and thereby distorts or masks the true effect of the exposure.

Dose and dose-rate effectiveness factor (DDREF): A factor used to account for an apparent decrease in the effectiveness of low-LET radiation in causing a biological end-point (e.g., cancer) at low doses and dose rates compared with observations made at high, acutely delivered doses.

Dose effectiveness factor (DEF): A factor estimated from the LQ model to account for a decrease in the effectiveness of low-LET radiation in causing a biological end-point (e.g., cancer) at low doses compared with that at high acute doses.

Dose equivalent: A weighted sum of absorbed doses of different types of IR, measured in units of sieverts (Sv). The ICRP recommended values for the weighting factors w_r are: 1.0 for photons and electrons, 10 for fission neutrons, and 20 for alpha particles. Thus, for low-LET radiation, the dose equivalent in Sv is numerically equal to the absorbed dose in Gy, whereas for alpha-particles an absorbed dose of 1 Gy corresponds to 20 Sv.

Dose rate effectiveness factor (DREF): A factor used to account for an apparent decrease in the effectiveness of low-LET radiation in causing a biological end-point (e.g., cancer) at low dose rates compared with high dose rates.

Double strand break (DSB): DNA damage in which a break extends over both strands of the double helix.

Electron volt (eV): The customary unit of energy for all *ionizing radiations*: 1 eV is equivalent to the energy gained by an electron passing through a potential difference of 1 volt. 1 keV = 1000 eV; 1 MeV = 1,000,000 eV.

EPA: Environmental Protection Agency.

Excess absolute risk (EAR): The rate of disease in an exposed population minus that in an unexposed population. Also termed “attributable risk.”

Excess relative risk (ERR): The rate of disease in an exposed population divided by that in an unexposed population minus 1.

Gamma rays (or gamma radiation): Photons of nuclear origin similar to x rays but usually of higher energy. A type of low-LET IR.

Genomic instability: An enhanced rate of spontaneous genetic change in a cell population..

Geometric mean (GM): The GM of a set of positive numbers is the exponential of the arithmetic mean of their logarithms.

Geometric standard deviation (GSD): The GSD of a lognormal distribution is the exponential of the standard deviation of the associated normal distribution.

Gray (Gy): Unit of absorbed dose.

High-LET radiation: IR such as neutrons or alpha particles that produce ionizing events densely spaced on a molecular scale (e.g., LET > 10 keV/μm).

HPA: Health Protection Agency of the United Kingdom

ICRP: International Commission on Radiological Protection. An independent international organization that provides recommendations and guidance on radiation protection against ionizing radiation.

Ionizing Radiation (IR): Any radiation capable of removing electrons from atoms or molecules as it passes through matter, thereby producing ions.

kVp (kV): Kilovolt potential – refers to the potential difference between the electrodes of an x ray tube. For example, the output of a 200 kVp x-ray tube will consist of photons with a range of energies up to 200 keV.

LET: Average amount of energy lost per unit track length of an ionizing charged particle.

Life table: A table showing the number of persons who, of a given number born or living at a specified age, live to attain successively higher ages, together with the number who die in each interval.

Linear no-threshold (LNT) model: Dose-response for which any dose greater than zero has a positive probability of producing an effect. The probability is calculated from the slope of a linear (L) model or from the limiting slope, as the dose approaches zero, of a linear-quadratic (LQ) model.

Linear (L) model: A model in which the probability of an effect (e.g., cancer) is expressed as being proportional to the dose.

Linear-quadratic (LQ) model: A model in which the probability of an effect (e.g., cancer) is expressed as the sum of two terms – one proportional to the dose, the other to the square of the dose. In the limit of low doses and low dose rates, the quadratic term can be ignored.

Low-LET radiation: IR such as x rays, gamma rays, or electrons that produce sparse ionizing events on a molecular scale (e.g., LET < 10 keV/μm).

Lognormal distribution: A distribution in which the logarithm of a randomly distributed quantity has a normal distribution.

Life Span Study (LSS): Long term study of health effects in the Hiroshima and Nagasaki atomic bomb survivors.

Mortality (rate): the frequency at which people die from a specific cause (e.g., lung cancer), often expressed as the number of deaths per 100,000 population per year.

NCRP: National Council on Radiation Protection and Measurements. A Council commissioned to formulate and disseminate information, guidance, and recommendations on radiation protection and measurements.

NIOSH: National institute for Occupational Safety and Health.

Photon: A quantum of electromagnetic energy. Energetic photons in the form of x rays or gamma rays can ionize atoms or molecules in a medium upon which they are incident.

Radiation Effectiveness Factor (REF): An estimate of the RBE for estimating human cancer risk. The estimated value at low doses is denoted as REF_L .

Relative Biological Effectiveness (RBE): The relative effectiveness of a given type of radiation in producing a specified biological effect compared to some reference radiation. For purposes of this document, the reference radiation is generally taken to be low dose gamma rays.

RBE_M: The maximal limiting value of the RBE for a high-LET radiation attained in the limit of low doses.

Relative Risk (RR): The rate of disease in an exposed population divided by that in an unexposed population.

Risk coefficient: the increase in the annual incidence or mortality rate per unit dose: (1) absolute risk coefficient is the increase in the incidence or mortality rate per unit dose; (2) relative risk coefficient is the fractional increase above the baseline incidence or mortality rate per unit dose.

SCC: Squamous cell carcinoma.

SEER: Surveillance, Epidemiology, and End Results.

Sievert (Sv): Unit of dose equivalent. In the BEIR VII analysis of the A-bomb survivor data, the dose equivalent was calculated from the absorbed gamma ray and neutron doses, assuming a radiation weighting factor of 10 for neutrons.

Stationary population: A hypothetical population in which the relative number of people of a given age and gender is proportional to the probability of

surviving to that age. At age 0, the number of males is taken to be 1.051 times the number of females to reflect males' higher birth rate.

Uncertainty: A term used to describe the lack of precision and accuracy of a given estimate.

Uncertainty distribution: A mathematical expression defining the relative probabilities of different values for an estimated quantity.

UNSCEAR: United Nations Scientific Committee on the Effects of Atomic Radiation. A UN committee that publishes reports on sources and effects of ionizing radiation.

WLM: Working level months, a measure of radon decay product exposure.

X radiation or x rays: Energetic photons usually produced by bombarding a metallic target with fast electrons in a high vacuum.